Methylglyoxal induces chromosomal instability under normal and folic acid deficient conditions

Leigh Donnellan

Bachelor of Nutrition and Food Science

Bachelor of Biomedical Research (Honours)

This thesis is submitted in the fulfilment for the degree of

Doctor of Philosophy

Clinical and Health Sciences

University of South Australia

On this day

13/10/2022



Acknowledgements

First, I would like to thank my principal supervisor Permal Deo. You have been a big support throughout my entire research career and have allowed me a lot of independence, even if that meant making mistakes. It is because of your guidance and support that I have made it to this point. Next, to the first of my co-supervisors Bradley Simpson, who was always available to catch up and go over my data or just catch up just for a chat and to check in. You always managed to squeeze me into your busy schedule and for that I am grateful. I would also like to thank my other co-supervisors, Maurizio Costabile and Varinderpal Dhillon for your support throughout my PhD. You have both been a tremendous help. The last of my supervisors, Michael Fenech, who's knowledge in the field of DNA damage is something to be admired. Your support and encouragement throughout my PhD have meant a lot.

I would like to make a special mention to the technical staff of UniSA. In particular Andrew Beck who introduced myself and another lab member to the Nanozoom, which saved us countless hours looking through a microscope and help accelerate my PhD. Also, Amanda Kenyon and Lora Bowes who always made themselves available to help and answer what crazy questions I had on any particular day. Lastly I would like to thank Maulik Ghetia who helped tech me the ins and outs of mass spectrometry.

I would also like to thank my fellow lab members Emma Jaunay and Brock Peake. Whether it was helping with specific experiments or catching up to complain, the PhD process would have been a very boring experience without the two of you.

I would like to acknowledge the financial support received through an Australian Government Research Training Program Scholarship.

Lastly, I would like to thank my wife Jana Hildebrandt, who while trying to complete her own PhD listened to me rattle on day and night about anything and everything. Your support throughout my PhD has meant so much and I hope I can make it up to you one day. I cannot wait for the next stage of our lives with our beautiful little boy Charlie.

Executive Summary

Methylglyoxal (MGO) is a reactive metabolite formed as a by-product of glycolysis, which can react with proteins and DNA to form a class of compounds referred to as Advanced Glycation Endproducts (AGEs). These compounds are elevated in various disease states, such as Type 2 Diabetes (T2D) and have been shown to correlate with levels of DNA damage. Furthermore, recent studies have shown folic acid deficiency can increase the genotoxicity of glucose. The overall aim of this project was to investigate the mechanisms underlying MGO-related DNA damage.

Elevated MGO concentrations were shown to increase the frequency of DNA damage biomarkers, in particular micronuclei (MNi) in WIL2-NS B-lymphoblastoid cell line, using both exogenous MGO and inhibition of Glyoxalase 1, its major detoxifying enzyme. MGO increased DNA damage biomarkers in peripheral blood lymphocytes (PBL) isolated from healthy donors, validating the former result. We found that DNA damage biomarkers were more closely associated with the formation of protein AGEs, rather than DNA AGEs, measured using liquid chromatography tandem mass spectrometry (LC-MS/MS). As MNi were the major form of DNA damage to be observed in cells treated with MGO, we used fluorescent *in situ* hybridization (FISH) with pan-centromeric probes to identify the origin of MNi. This analysis revealed that the majority of MNi formed by MGO were centromeric positive, concordant with chromosome malsegregation events.

The relationship between folic acid, glucose and MGO on chromosomal instability in WIL2-NS cells was also investigated. High glucose concentrations and MGO were shown to be more genotoxic in folic acid-deficient cells, with respect to the formation of MNi. Aminoguanidine, a well-validated MGO and free radical scavenger was able to prevent further MNi formation in cells under the same conditions, which may be due to a reduction in MGO-induced oxidative stress. Therefore, folic acid deficiency appears to increase cellular susceptibility to glucose and MGO-induced DNA damage.

Shot-gun proteomics was used to identify target proteins harboring AGE modifications to explore the potential underlying mechanisms of MGO-induced chromosome malsegregation events. From this analysis, various mitotic proteins were identified with these modifications, including those involved in the separation and cohesion of sister chromatids. Furthermore, label free quantitation showed elevation

in Securin, an inhibitor of sister protein separation, after exposure to MGO. Cytological examination of chromosome spreads revealed MGO does impair sister chromatid separation and induce various nuclear anomolies associated with failed sister chromatid separation. The same proteomics data generated in the previous study was probed to identify pathways and processes over-represented with these modifications. Most notably, enzymes of the glycolytic pathway were enriched with MGO modifications suggesting sensitivity to MGO. Moreover, these modifications were present on various residues known to regulate protein function.

The studies presented in this thesis clearly demonstrate the genotoxic properties of MGO, under normal and folic acid deficient conditions. Furthermore, proteomics data suggest this is the result of failed sister chromatid separation. These results further the understanding of the pathophysiological consequences of elevated MGO and may provide insight into why individuals with T2D experience elevated levels of DNA damage.

Declaration

I declare that:

This thesis presents work carried out by myself and does not incorporate without acknowledgement any material previously submitted for a degree or diploma in any university; to the best of my knowledge it does not contain any materials previously published or written by another person except where due reference is made in the text; and all substantive contributions by others to the work presented, including jointly authored publications, is clearly acknowledged.

Leigh Donnellan

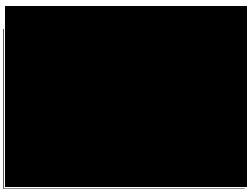

University of South Australia

Clinical and Health Sciences, Health and Biomedical Innovation

Playford Building. City East Campus,

Adelaide, SA, 5000

Thesis Publications

Publications generated from this thesis are listed below.

Aim 1

Donnellan, L., Simpson, B., Dhillon, V.S., Costabile, M., Fenech, M., and Deo, P. (2021) Methylglyoxal induces chromosomal instability and mitotic dysfunction in lymphocytes. *Mutagenesis*, **36**, 339-348.

Aim 2

Donnellan, L., Simpson, B.S., Dhillon, V.S., Costabile, M., Fenech, M., and Deo, P. (2022) Folic acid deficiency increases sensitivity to DNA damage by glucose and methylglyoxal. *Mutagenesis*, 37, 24-33. *(Editor's choice)*

Aim 3

Donnellan, L., Young, C., Simpson, B.S., Dhillon, V.S., Costabile, M., Hoffmann, P., Fenech, M., and Deo, P. (2022) Methylglyoxal Impairs Sister Chromatid Separation in Lymphocytes. *International Journal of Molecular Sciences*, **23**.

Aim 4

Donnellan, L., Young, C., Simpson, B.S., Acland, M., Dhillon, V.S., Costabile, M., Fenech, M., Hoffmann, P., and Deo, P. (2022) Proteomic Analysis of Methylglyoxal Modifications Reveals Susceptibility of Glycolytic Enzymes to Dicarbonyl Stress. *International Journal of Molecular Sciences*, 23, 3689.

Other published work during candidature

Deo, P., McCullough, C.L., Almond, T., Jaunay, E.L., **Donnellan, L**., Dhillon, V.S., and Fenech, M. (2020) Dietary sugars and related endogenous advanced glycation end-products increase chromosomal DNA damage in WIL2-NS cells, measured using cytokinesis-block micronucleus cytome assay. *Mutagenesis*, **35**, 169-177.

Deo, P., Dhillon, V.S., Lim, W.M., Jaunay, E.L., **Donnellan, L**., Peake, B., McCullough, C., and Fenech, M. (2020) Advanced glycation end-products accelerate telomere attrition and increase pro-inflammatory mediators in human WIL2-NS cells. *Mutagenesis*, **35**, 291-297.

Forbes, J.M., Le Bagge, S., Righi, S., Fotheringham, A.K., Gallo, L.A., McCarthy, D.A., Leung, S., Baskerville, T., Nisbett, J., Morton, A., Teasdale, S., D'Silva, N., Barrett, H., Jones, T., Couper, J., Donaghue, K., Isbel, N., Johnson, D.W., **Donnellan, L.**, Deo, P., Akison, L.K., Moritz, K.M., and O'Moore-Sullivan, T. (2021) Advanced glycation end products as predictors of renal function in youth with type 1 diabetes. *Scientific Reports*, **11**, 9422.

Snelson, M., S. M. Tan, R. E. Clarke, C. de Pasquale, V. Thallas-Bonke, T.-V. Nguyen, S. A. Penfold, B. E. Harcourt, K. C. Sourris, R. S. Lindblom, M. Ziemann, D. Steer, A. El-Osta, M. J. Davies, **L. Donnellan**, P. Deo, N. J. Kellow, M. E. Cooper, T. M. Woodruff, C. R. Mackay, J. M. Forbes and M. T. Coughlan (2021). "Processed foods drive intestinal barrier permeability and microvascular diseases." *Science advances* **7**(14)

Author statement

This dissertation is submitted as a thesis containing peer-reviewed publications presented as typescript (Thesis Containing Published Research in accordance with the UniSA Academic Regulations for Higher Degrees).

The format of this Thesis is presented in a conventional chapter format. **Chapters 2, 3, 4 and 5** are accepted publications. The reader is advised that some aspects of the respective chapters may appear repetitive, however due to the nature of the investigations and experiments conducted this was unavoidable. Furthermore, the format of some chapters may differ slightly due to variations in formatting required for each journal that the corresponding chapter was published.

As first authored peer-reviewed journal articles presented in this thesis, I undertook all experiments and analysis of data. Ideas and concepts were guided by the supervisory team, as was drafting and proofing of the submitted manuscripts.

Abbreviations

10-fTHF	10-formyltetrahydrofolate
2-dG	2-deoxyguanosine
5,10-meTHF	5,10-methylenetetrahydrofolate
5-meTHF	5-methyltetrahydrofolate
8oxodG	8-oxo-2′-deoxyguanosine
ACTB	Beta-actin
AGEs	Advanced glycation endproducts
ALDOA/C	Fructose bisphosphate aldolase A/C
alkMGO	Alkyne-labelled methylglyoxal analogue
ANOVA	Analysis of variance
APC/C	Anaphase promoting complex/ cyclosome
ARNT	Aryl hydrocarbon receptor nuclear translocator
BBGC	S-p-Bromobenzylglutathione cyclopentyl diester
BCA	Bicinchoninic acid
BN	Binucleated
CBMNcyt	Cytokinesis block micronucleus cytome
CBP	CREB-binding protein
CBPR	Chemoresistance to the chemotherapeutic drug carboplatin
CDC20	Cell division cycle protein 20 homolog
CEA	Carboxyethylarginine
CEdG	N^2-(1,R/S-carboxyethyl)-deoxyguanosine
CEL	N^{ϵ}-(carboxyethyl)lysine
Cent	Centromere
cGAS	Cyclic 2’-3’-GMP-AMP synthase
CID	Collision-induced dissociation
CIN	Chromosomal Instability
CML	N^{ϵ}-(carboxymethyl)lysine
Cyt-b	Cytochalasin-b
DAVID	Database for Annotation, Visualization and Integrated Discovery
DHAP	Dihydroxyacetone phosphate
DHF	Dihydrofolate
DJ-1	Protein Deglycase DJ-1
DOI	Digital Object Identifier
DSB	Double stranded break
dTTP	Deoxythymidine triphosphate
dUMP	Deoxyuridine monophosphate
ENO1/3	Enolase 1/3
ESPL1	Separase
FDR	False discovery rate
FISH	Fluorescent *in situ* hybridization
FUS	Fused
GA3P	Glyceraldehyde-3 phosphate
GLO	Glyoxalase
GPI	Glucose-6-phosphate isomerase
HBSS	Hanks Balanced Salt Solution
HCD	Higher-energy C-trap dissociation
HIF-1α	Hypoxia inducible factor-1α

HMEC-1	Human microvascular endothelial cells
HPLC	High performance liquid chromatography
HRE	Hypoxia Response Element
KEAP1	Kelch-like ECH associated protein 1
k-MT	Kinetochore-microtubule
LC-MS	Liquid chromatography - mass spectrometry
LC-MS/MS	Liquid chromatography tandem mass spectrometry
LFQ	Label free quantitation
MGdG	3-(2'eoxyribosyl)-6,7-dihydro-6,7-dihydroxy-6/7-methylimidazo-[2, deoxyguanosine]
MG-H1	N^{δ}-(5-hydro-5-methyl-4-imidazolon2-yl)ornithine
MGO	Methylglyoxal
MICA	Methylimidazole crosslink between proximal cysteine and arginine residues
MNi	Micronuclei
MODIC	2-ammonio-6-((2-[(4ammonio-5-oxido-5-oxopentyl)amino]-4-methyl-4,5dihydro-1H-imidazol-5-ylidene)amino)hexanoate
MOLD	1,3-di(N^{ϵ}-lysino)-4-methyl-imidazolium
MRM	Multiple reaction monitoring
NBUD/ Nbud	Nuclear bud
NDI	Nuclear division index
NMR	Nuclear magnetic resonance
NPB	Nucleoplasmic bridge
NRF2	Nuclear factor erythroid 2 (NF-E2)-related factor 2
PAD4	Protein arginine deaminase-4
PBL	Peripheral blood lymphocyte
PDB	Protein Data Bank
PDLF	Periodontal ligament fibroblasts
PGK	Phosphoglycerate kinase
PGM	Phosphoglucomutase
PHA	Phytohemagglutinin
PKM	Pyruvate kinase M
PPI	Protein-protein interaction
ProAla	Proalanase
PTM	Post translational modification
PTTG1	Securin
QqQ	Triple quadrupole
RAD21	Double-strand-break repair protein rad21 homolog
RAGE	Receptor for advanced glycation endproducts
RPM	Revolutions per minute
SAC	Spindle Assembly Checkpoint
SHMT	Serine hydroxymethyltransferase
SSAO	Semicarbazide amine oxidase
STRING	Search Tool for the Retrieval of Interacting Genes
T2D	Type 2 Diabetes
THF	Tetrahydrofolate
THP	Tetrahydropyrimidine
TPI	Triosephosphate isomerase
UBE	Ubiquitin conjugating enzyme
WCE	Whole cell extract

Table of Contents

Chapter 1 Contents

1 Chapter 1. Introduction 1

1.1 Micronuclei 2

1.1.1 Origin of MNi 3

1.1.2 Consequences of micronuclei: Chromotripsis and cGAS signaling 6

1.2 Measuring DNA damage 7

1.2.1 Cytokinesis-block micronucleus cytome (CBMNcyt) assay 7

1.2.2 Nucleoplasmic Bridges (NPBs) 8

1.2.3 Nuclear Buds (NBUDs) 9

1.3 Methylglyoxal (MGO) 10

1.3.1 Formation of MGO 10

1.3.2 MGO detoxification, the glyoxalase system 11

1.3.3 Formation of advanced glycation endproducts from MGO 11

1.3.4 Formation of advanced glycation endproducts from other metabolites. 12

1.3.5 Repair or removal of MGO-modified proteins 13

1.3.6 Consequences of MGO modification 13

1.3.7 Specific examples of MGO modification 14

1.3.8 AGE analytics 18

1.3.9 Site specific determination of AGE modifications 19

1.4 Folate 29

1.4.1 Folate mediated one carbon metabolism. 29

1.4.2 Folate deficiency and chromosomal instability 30

1.4.3 Folic acid deficiency increases sensitivity to genome damage by other genotoxins 31

1.5 Hypotheses and Research Aims 33

2 Chapter 2. Methylglyoxal induces chromosomal instability and mitotic dysfunction in lymphocytes 43

2.1 Abstract 44

2.2 Introduction 45

2.3 Methods 46

2.3.1 Materials 46

2.3.2 WIL2-NS cell culture 46

2.3.3 Volunteers, sample collection and primary lymphocyte culture 46

2.3.4 CBMNcyt assay/ multipolar assay with MGO/ Glo1 inhibitor 47

2.3.5 Fluorescent *in situ* hybridization (FISH) 47

2.3.6 Synthesis of CEdG and $13C_3$-CEdG 48

2.3.7 Quantification of dicarbonyl stress biomarkers by LC-MS/MS 49

2.3.8 Statistical analysis 49

2.4 Results 50

2.4.1 Dicarbonyl stress parameters are increased upon exposure to exogenous MGO 50

2.4.2 MGO increases DNA damage biomarkers measured by the CBMNcyt assay. 51

2.4.3 MGO causes cells to undergo multipolar mitosis. 53

2.4.4 Inhibition of GLO1 in WIL2-NS with BBGC increases MGO and DNA damage. 54

2.4.5 MGO induces DNA damage in peripheral blood lymphocytes (PBL) 57

2.4.6 MGO causes whole chromosome loss in WIL2-NS 59

2.5 Discussion 60

2.6 Conclusion 63

3 Chapter 3. Folic acid deficiency increases sensitivity to DNA damage by glucose and methylglyoxal 67

3.1 Abstract 68

3.2 Introduction 69

3.3 Methods 71

3.3.1 Materials 71

3.3.2 Media preparation 71

3.3.3 WIL2-NS cell culture 71

3.3.4 CBMNcyt assay 73

3.3.5 Quantification of MGO in cells and media 74

3.3.6 Quantification of protein-bound MG-H1, CEL and Lysine 74

3.3.7 Quantification of free MG-H1 and CEL 75

3.3.8 Quantification of media 8-Oxo-2'-deoxyguanosine (8-oxodG) 76

3.3.9 Statistical Analysis 76

3.4 Results 76

3.4.1 Folic acid deficient cells are sensitive to glucose-induced DNA damage 76

3.4.2 Folic acid deficient cells are sensitive to MGO 79

3.4.3 Aminoguanidine rescues high glucose-induced DNA damage in folic acid deficient cells 81

3.4.4 Folic acid deficiency increases dicarbonyl stress biomarkers 83

3.5 Discussion 85

4 Chapter 4. Methylglyoxal impairs sister chromatid separation in Lymphocytes 91

4.1 Abstract 92

4.2 Introduction 92

4.3 Methods 93

4.3.1 Materials 93
4.3.2 WIL2-NS cell culture 94
4.3.3 Identification of DNA damage biomarkers 94
4.3.4 Quantification of MG-H1 and CEL in whole cell extracts 94
4.3.5 Sister chromatid resolution assay 95
4.3.6 Proteomic analysis of WIL2-NS 96
4.3.7 Data analysis 97
4.4 Results 97
4.4.1 MGO induced micronuclei formation is associated with increased AGEs 97
4.4.2 MGO modifies various components of the mitotic machinery 98
4.4.3 Methylglyoxal impairs sister chromatid separation 101
4.5 Discussion 103
5 Chapter 5. Proteomic analysis of methylglyoxal modifications reveals susceptibility of glycolytic enzymes to dicarbonyl stress 108
5.1 Abstract 109
5.2 Introduction 109
5.3 Methods 111
5.3.1 Materials 111
5.3.2 WIL2-NS cell culture 111
5.3.3 Whole cell quantification of MG-H1 and CEL 111
5.3.4 Isolation and purification of peripheral blood lymphocytes 112
5.3.5 Proteomic analysis of WIL2-NS and PBL 113
5.3.6 High resolution orbitrap mass spectrometry 114
5.3.7 Data analysis 114
5.4 Results 115

5.4.1 Characterization of MGO modified proteins 115

5.4.2 Enrichment analysis of MGO modified proteins 118

5.4.3 Modification of glycolytic enzymes 121

5.5 Discussion 124

6 Chapter 6. Conclusion and future directions 132

6.1 MGO induced DNA damage 132

6.2 Folic acid deficiency increases susceptibility to MGO induced DNA damage 133

6.3 MGO impairs sister chromatid separation 134

6.4 Future Directions 135

6.5 Conclusion 135

7 Appendix 139

7.1 Appendix A. Statement of Authorship Aim 1 139

7.2 Appendix B. Statement of Authorship Aim 2 141

7.3 Appendix C. Statement of Authorship Aim 3 143

7.4 Appendix D. Statement of Authorship Aim 4 145

7.5 Appendix E. Copyright License for Chapter 2 148

7.6 Appendix F. Copyright License for Chapter 3 151

List of Figures

Figure 1.1. Schematic diagram describing the origin of lagging chromosomes 4

Figure 1.2. A diagrammatic outline of the process of chromotripsis and chromoanagenesis in micronucleated cells and activation of cGAS-STING signaling following MNi disruption. 7

Figure 1.3. Formation of MNi and NPB in cells undergoing nuclear division. 8

Figure 1.4: Examples of common advanced glycation endproducts.....12

Figure 1.5: Examples of MGO modifications on specific proteins and resulting functional consequences. 17

Figure 1.6. Schematic representing a standard workflow for shot-gun proteomics.....21

Figure 1.7: Formation of DNA advanced glycation endproducts derived from MGO. 27

Figure 1.8. Diagram depicting the different forms of folate. 30

Figure 1.9. A diagrammatic outline of folate mediated one carbon metabolism and its role in various cellular processes. 30

Figure 2.1. Methylglyoxal increases DNA damage biomarkers in WIL2-NS. 52

Figure 2.2. Methylglyoxal induces mitotic dysfunction. 54

Figure 2.3. Inhibition of Glyoxalase 1 by BBGC increases DNA damage in WIL2-NS cells. 57

Figure 2.4. Methylglyoxal induces DNA damage in peripheral blood lymphocytes.....59

Figure 2.5. MGO induces whole chromosome loss in WIL2-NS cells.....60

Figure 3.1. Culturing procedure for experiments 1-3.....73

Figure 3.2. Folic acid deficient WIL2-NS cells are sensitive to glucose induced DNA damage.....78

Figure 3.3. Folic acid deficient WIL2-NS cells are sensitive to MGO induced DNA damage. 80

Figure 3.4. Aminoguanidine prevents glucose-induced DNA damage in folic acid-deficient cells. 82

Figure 3.5. Folic acid deficiency increases concentration of dicarbonyl stress biomarkers. 84

Figure 4.1. Time and dose dependent MG-H1, CEL and MNi formation. 98

Figure 4.2: Enrichment analysis.....100

Figure 4.3: MGO impairs sister chromatid separation.....102

Figure 5.1. Proteomic analysis of MGO modifications. 117

Figure 5.2. Protein-protein interaction network of MGO modified proteins 119

Figure 5.3. MGO modifies critical residues of glycolytic enzymes.....123

Figure 5.4. Modification of glycolytic enzymes by MGO is present across various cell lines.....124

List of Tables

Table 1.1.Studies on reactions of MGO with dG or DNA 26

Table 2.1. Dicarbonyl stress biomarkers measured in WIL2-NS cells treated with MGO 51

Table 2.2. Dicarbonyl stress biomarkers measured in WIL2-NS cells treated with the GLO1 inhibitor 56

Table 3.1. Two-way ANOVA of CBMNcyt assay biomarkers to determine effect of folic acid, glucose and their interaction. 79

Table 3.2. Two-way ANOVA of CBMNcyt assay biomarkers to determine effect of folic acid, MGO and their interaction. 81

Table 3.3. Dicarbonyl stress biomarkers measured in WIL2-NS cells cultured under folic acid deficient conditions (23 nmol/L) in LG or HG, with or without aminoguanidine. 83

Table 4.1: Pearson correlation for relationship between AGE biomarkers and MNi 98

Table 5.1 Enrichment analysis for biological processes enriched with MGO modifications. 120

1 Chapter 1. Introduction

DNA damage caused by environmental, dietary and lifestyle factors gives rise to chromosomal instability (CIN), an initiating step in carcinogenesis (3). A continuous cycle of DNA damage and repair occurs in every cell of the body, and it is estimated that up to 70,000 DNA lesions occur per cell each day (4). When the frequency of damage begins to outweigh the cell's DNA repair capacity, chromosomal aberrations and gene mutations can give rise to malignant transformation. Various endogenous and exogenous agents, including ultraviolet radiation, ionizing radiation, free radicals produced by activated immune cells and anti-cancer drugs can induce DNA damage (3). It has been well established that an increased level of DNA damage is a predictive marker of cancer onset in humans (5). Moreover, people with neurodegenerative disease, cardiovascular disorders and nutrient deficiencies have also been shown to present with a higher frequency of DNA damage compared with healthy individuals (6). Therefore, identifying previously unknown genotoxins is critical to further our understanding of disease progressions.

Type 2 Diabetes (T2D) is characterized by decreased insulin production, resulting in hyperglyceamia. Two recent meta-analyses have shown that individuals with T2D have higher micronucleus frequency (a biomarker of CIN) with a meta-MR (mean ratio) of 1.99 ($P < 0.01$) and 1.74 ($P < 0.001$), when compared with healthy individuals (7,8). Despite this association of DNA damage in individuals with T2D, few studies have investigated the underlying mechanisms. Several studies have suggested that higher levels of oxidative stress observed in T2D is responsible for elevated levels of DNA damage (9-12). Elevated levels of oxidative stress can cause oxidation of deoxyguanosine producing the adduct 8-oxo-2′-deoxyguanosine (8-oxodG), which has been associated with double stranded DNA breaks (DSBs). Indeed, the plasma and urine concentration of 8-oxodG is significantly increased in T2D individuals and, similar to MNi, is further increased in those with diabetic nephropathy (13,14). Interestingly, a recent meta-analysis showed that advanced glycation endproducts (AGEs) and glycated haemoglobin ($HbA1_C$) were associated with the frequency of MNi with a meta-MR of 1.62 (AGEs; $P<0.0001$), 2.13 ($HbA1_C$; $P = 0.002$) and 1.83 (combined; $P=0.01$) (7)

AGEs are a heterogenous group of compounds, formed by spontaneous reactions of reducing sugars and reactive dicarbonyl species with proteins and nucleic acids (15). Because these modifications are

primarily formed by glucose, and glucose metabolic byproducts, they are known to be elevated in individuals with T2D (13,16). Therefore, in individuals with T2D, the formation of AGEs on DNA or proteins with a role in DNA repair, DNA replication or cell division may be in part responsible for the DNA damage observed in these individuals. The following sections will discuss mechanisms resulting in DNA damage, with particular focus on MNi. Following this, an introduction and review is provided of the current literature relating to AGEs and their impact on genomic integrity with a focus on the quantitatively important methylglyoxal (MGO) derived AGEs will be presented. Finally, an overview of folate metabolism and the impact of folate deficiency on genomic integrity and susceptibility to genotoxins will be discussed,

1.1 Micronuclei

Micronuclei (MNi) are small nuclear bodies that are formed from either lagging whole chromosomes or chromatid fragments that fail to incorporate into the main nuclei during the late stages of mitosis (6). MNi have frequently been used as a marker of genotoxic stress and CIN in various disease states. A significant increase in the incidence of all cancers was reported in a prospective study of cohorts with medium (1.84-fold increase in relative risk) and high MNi frequency (1.53-fold increase in relative risk) (5). Other prospective studies in Italy confirmed the association of high MNi frequency with cancer and cardiovascular disease and a prospective study in Australia reported that higher MNi at 18 weeks gestation predicted a higher risk of pregnancy complications such as pre-eclampsia and intra-uterine growth restriction of the fetus (17-20). The two main mechanisms of MNi formation are (i) lagging chromosomes that do not properly segregate during mitosis and (ii) acentric chromatid fragments formed by unrepaired or mis-repaired double-stranded DNA breaks (DSBs). However, other mechanisms such as defects in the mitotic spindle apparatus, inefficient or defective mitotic checkpoints, and improper coordination of nuclear envelope assembly have also been reported to result in MNi formation (21,22).

1.1.1 Origin of MNi

1.1.1.1 Kinetochore defects

Formation of MNi from lagging chromosomes can result from malfunctional centromeres and kinetochores, abnormal kinetochore-microtubule (k-MT) attachments and defects in various aspects of the mitotic spindle assembly machinery, amongst others (23). To ensure correct segregation of chromosomes during mitosis, the cell must ensure spindles involved in k-MT attachments originate from opposite spindle poles and have an even number of attachments on both sister chromatids. These attachments between spindles and kinetochore occur randomly, therefore, erroneous attachments can occur (Figure 1.1) (24). These are referred to as (i) Amphitelic; an even k-MT attachments between sister chromatid, (ii) Monotelic; only one sister chromatid has k-MT attachments, (iii) Syntelic; both sister chromatids only have k-MT attachments originating from the same spindle pole and (iv) Merotelic; k-MT attachments between sister chromatid are uneven (2). In normal cases, the spindle assembly checkpoints (SAC) prevents mitotic progression in the event of incorrect k-MT attachments, however, in the event of SAC deficiency, cells with erroneous k-MT attachments can progress through anaphase, resulting in mal-segregated chromosomes and MNi (Figure 1.1) (2,25).

Given the complexity and number of proteins involved in k-MT attachments, particularly kinetochore formation which comprises >150 proteins, it is no surprise that loss of proteins or protein interactions from this complex can result in compromised chromosome segregation and MNi formation (26). For example, depletion of histone H3 variant CENP-A, which is critical for determining kinetochore position on each chromosome results in MNi formation during mitotic anaphase/telophase (27). Loss of CENP-A prior to kinetochore assembly prevents recruitment of CENP-N and CENP-C, both of which are critical for recruitment of constitutive centromere associated network (CCAN) proteins to the kinetochore (26-28). Unsurprisingly, defects in other kinetochore protein networks, such as the KMN (comprised of three multi-protein complexes Knl-1, Mis12 and Ndc80) found in the outer kinetochore and interacts with spindle microtubules can also result in chromosome mal-segregation (29,30). Interestingly, a recent study revealed that mis-expression of centromeric and kinetochore genes (including CENP-A and several genes involved in the CCAN and KMN networks) was associated with

genomic instability, adverse tumor properties, poor patient survival for breast and lung cancer and was useful in predicting patient response to radiotherapy and chemotherapy (31).

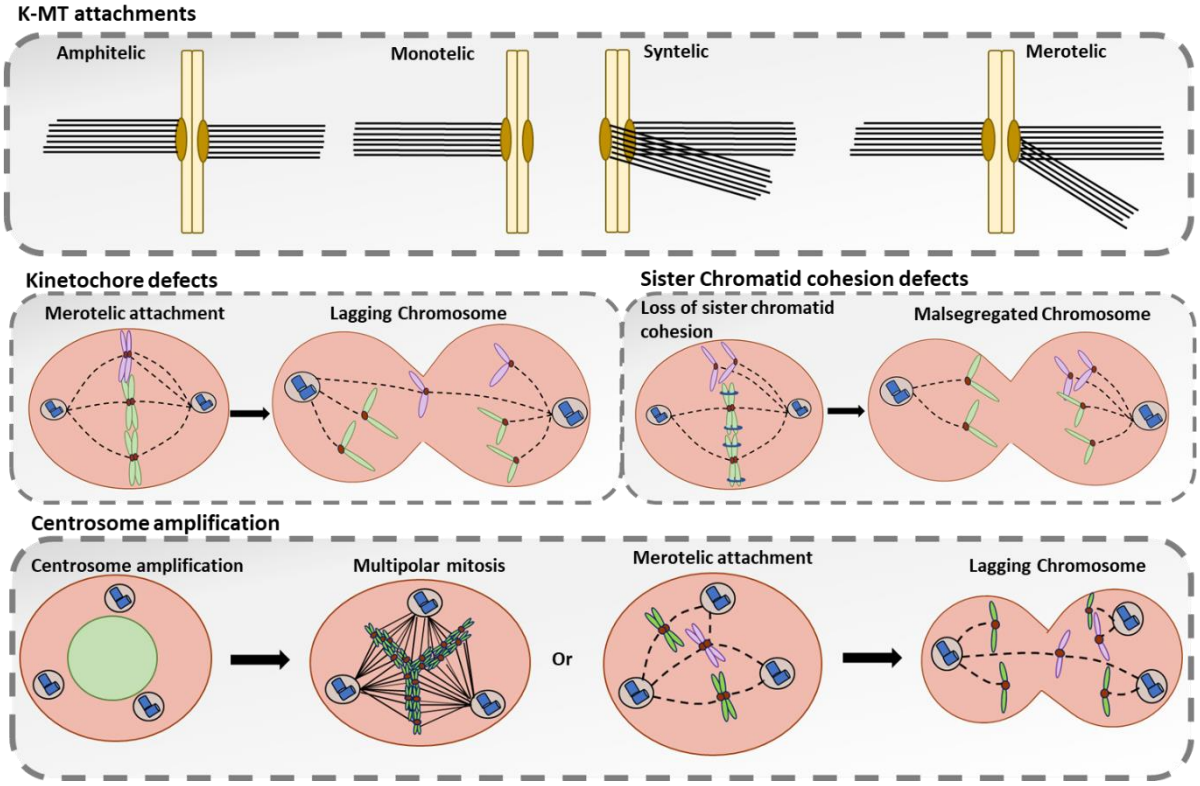

Figure 1.1. Schematic diagram describing the origin of lagging chromosomes or chromatid forming from erroneous K-MT defects and those how those attachments occur, defects in sister chromatid cohesion and centrosome amplification. This figure was adapted from (2).

1.1.1.2 Centrosome amplification

Centrosomes are major microtubule organizing centers in eukaryotic cells which organize spindle poles during mitosis. In the initial stages of mitosis, centrosomes migrate to opposite poles and begin assembling the mitotic spindle (32). The centrosome cycle ensures that centrosome duplication occurs only once per cell cycle. However, defects in any number of core proteins can result in excessive centrosome amplification (more than one round of duplication) (32). A cell with more than 2 centrosomes is at risk of becoming multipolar. However, this event is rare in cells with functioning cell cycle checkpoint proteins (e.g. p53) and because clustering of centrosomes means bipolar spindle formation can occur in the presence of multiple (>2) centrosomes (Figure 1.1) (33). However, it is common for cancer cells to have deficiencies in cell cycle check point proteins which means centrosome amplification can occur and is shown to correlate with mutations in p53 (34). Furthermore, bipolar

spindle formation in the presence of multiple (>2) centrosomes does increase the presence of merotelic attachments, which in turn leads to lagging chromosomes and malsegregation events (Figure 1.1) (33).

1.1.1.3 Sister chromatid cohesion

For accurate and even segregation of sister chromatids into daughter cells during mitosis, it is critical to establish a physical connection between them and maintain this until they are required to separate in early anaphase (35). Cohesion of sister chromatids is maintained by several proteins which form the cohesin protein complex. Removal of cohesion is regulated by various kinases which ultimately allow sister chromatid separation (35). Loss of structural maintenance of chromosome protein 3 (SMC3) protein activity, amongst other cohesin complex proteins, can cause both loss of arm cohesion and complete loss of cohesion between sister chromatid (36). Premature loss of cohesion between sister chromatids affects their biorientation at the metaphase plate, and results in misaligned and scattered chromosomes, causing them to missegregate eventually leading to the formation of MNi (Figure 1.1) (36). Moreover, failure of sister chromatids to separate can also result in CIN. Cleavage of the cohesin complex is executed by Separase, a cysteine-protease which is inhibited by Securin until the onset of anaphase. Increased expression of Securin, and/or non-cleavable cohesin prevent sister chromatid separation resulting in the formation of various nuclear anomolies associated with CIN (37-39).

1.1.1.4 Double stranded DNA breaks

MNi can also form from acentric chromosome/chromatid fragments that fail to incorporate into daughter nuclei during mitosis (1). Acentric fragments can form by, (i) direct induction of DNA strand breaks and/or simultaneous excision of damaged DNA bases within proximity on opposite DNA strands resulting in DSBs (40). For example, the removal of two closely spaced uracil bases that have been incorrectly inserted into DNA can result in DSBs and formation of MNi (40). This process has been shown to occur under folic acid deficient conditions (which results in uracil misincorporation in DNA; explained in 1.4) but is likely to occur following base modification that requires removal of damaged base by base or nucleotide excision repair pathways (40). (ii) Chemicals such as cytosine arabinoside which blocks the gap-filling step of DNA repair can inhibit or alter DNA repair pathways (41), and (iii)

Dysfunctional homologous recombination or non-homologous end-joining repair pathways which may either leave DSBs unrepaired or result in mis-repair of DNA strand breaks leading to the incorrect joining of broken ends of chromosomes resulting in the formation of either dicentric chromosomes or acentric chromosome fragments (21).

1.1.2 Consequences of micronuclei: Chromotripsis and cGAS signaling

For a long time, it was thought that MNi were only biomarkers of induced chromosomal instability without any further pathological consequences. However, recent studies have shown that MNi themselves can amplify chromosomal instability in just one or two cell cycles (42). This phenomenon results from chromotripsis (also referred to as fragmentation, shattering and pulverization) described as complex genomic rearrangements acquired in a single catastrophic event (Figure 1.2) (42). The cause of chromotripsis in MNi may be either due to a defective nuclear envelope, which prevents transport of DNA repair proteins, or a porous MNi membrane which allows access to DNAse enzymes (43). Alternatively, DNA replication in the MNi may be lagging behind the main nucleus. If DNA in MNi is still replicating when the main nucleus enters mitosis, ligation of newly synthesized DNA patches (also known as Okazaki fragments) will not be completed and incompletely replicated DNA will be prematurely condensed resulting in the formation of a severely fragmented chromatid (44). These catastrophic events highlight that MNi themselves are a major mechanism by which chromosomes are hypermutated.

Interestingly, loss of nuclear envelope integrity and exposure of MNi DNA to the cytoplasm has also been shown to stimulate the innate immune system (45). A cellular surveillance system exists to detect foreign DNA in the cytoplasm by the enzyme cyclic 2'-3'-GMP-AMP synthase (cGAS) (Figure 1.2) (46). cGAS binds to cytoplasmic DNA and in turn generates the cyclic dinucleotide cyclic GMP-AMP (cGAMP) which binds to the central scaffold of the innate immune response called STING (46). Activation of STING induces a type 1 interferon response resulting in interferon-stimulated gene expression ultimately leading to an inflammatory response (45). Therefore, by physical chromosomal rearrangement events and activation of the innate immune system, MNi themselves can have distinct

pathophysiological outcomes, which extend beyond the chromosomal loss or DSB event from which they originated.

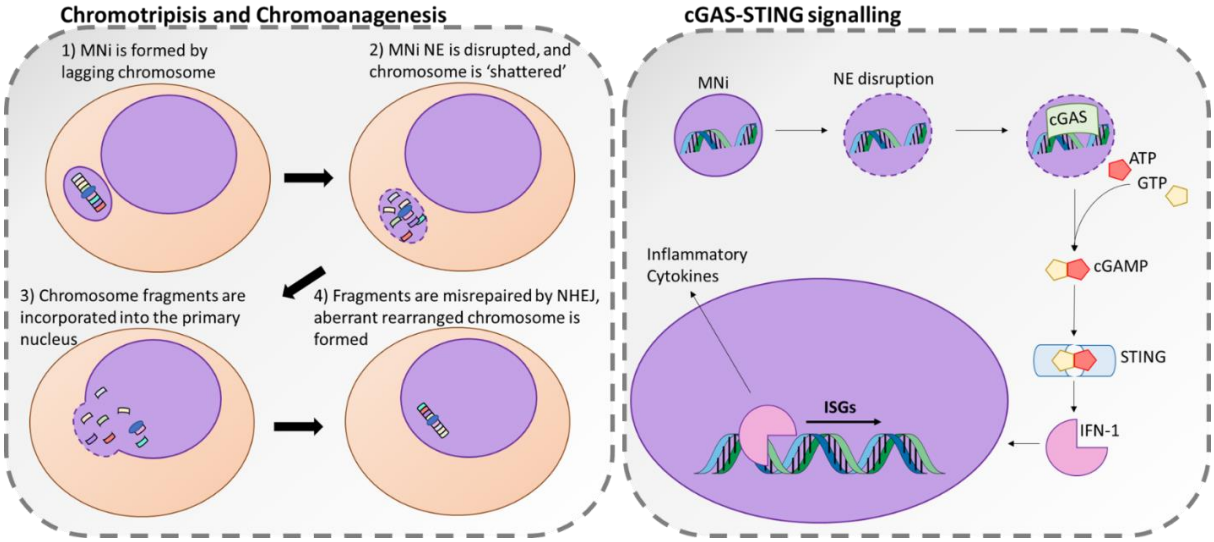

Figure 1.2. A diagrammatic outline of the process of chromotripsis and chromoanagenesis in micronucleated cells and activation of cGAS-STING signaling following MNi disruption. This figure was adapted from (47).

1.2 Measuring DNA damage

1.2.1 Cytokinesis-block micronucleus cytome (CBMNcyt) assay

The cytokinesis-block micronucleus cytome (CBMNcyt) assay is a standard method for measuring MNi formation and other DNA damage biomarkers induced by radiation, chemical carcinogens, nutritional deficiency and other genotoxic lifestyle factors or for assessing the levels of chromosomal integrity within a cohort in epidemiological and public health studies (48). The assay allows for the simultaneous measurement of (i) DNA damage; measured by the frequency of MNi, nucleoplasmic bridges (NPBs) and nuclear buds (NBUDs) in binucleated cells (Figure 1.3), (ii) Cytostasis; a measure of the nuclear division index is determined by the proportion of mononucleated, binucleated and multinucleated cells and iii) Cytotoxicity; determined by the frequency of necrotic and apoptotic cells (48). Formation of MNi, NPBs and NBUDs occurs during the mitotic cycle and therefore they can only be accurately scored in cells that have just completed mitosis i.e. at the binucleated stage in telophase, prior to cytokinesis.

Therefore, to accurately quantify DNA damage in the CBMNcyt assay, cells are treated with cytochalasin-B (cyt-B), which prevents cells from completing cytokinesis and results in the formation of binucleated cells (after one round of mitosis) or multinucleated cells (after >two rounds of replication). This allows for the easy identification and scoring of cells which have undergone one round of mitosis (binucleated cells), which is necessary for cells to express their DNA damage as MNi, NPBs or NBUDs (48).

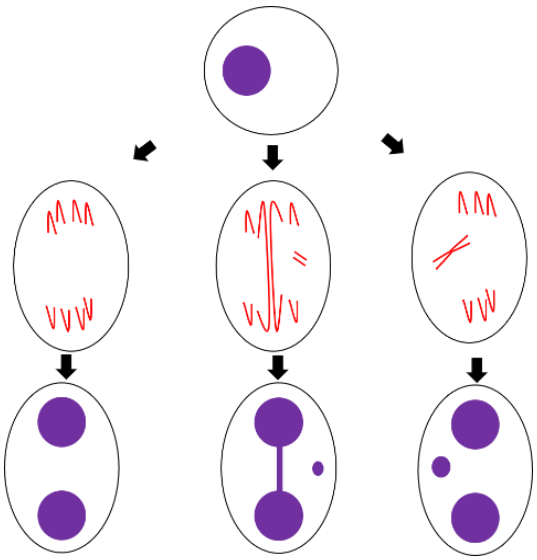

Figure 1.3. Formation of MNi and NPB in cells undergoing nuclear division. MNi originate from either acentric fragments (middle) in which dicentric chromosome formation may also be present resulting in a NPB. MNi also form from lagging whole chromosomes (right). This figure was adapted from (1).

1.2.2 Nucleoplasmic Bridges (NPBs)

NPBs are a measure of dicentric chromosome formation due to the misrepair of DNA breaks or telomere end fusions. NPBs are a product of anaphase bridges which form during anaphase when centromeres of dicentric chromosomes are pulled to opposite poles (49). Following cytokinesis block, the bridge remains intact and nuclear membrane forms around the stretched strand of DNA allowing for identification of a NPB (Figure 1.3). Therefore, NPB scoring is restricted to cytokinesis blocked binucleated cells, as the NPB will break if cytokinesis is allowed to continue (48). Dicentric chromosomes can form by misrepair of DSBs, in which two damaged chromosomes are joined with each other, rather than their respective fragments. In this scenario, a MNi containing the acentric

fragments will likely accompany the NPB (49). Telomere end fusion can also lead to the formation of dicentric chromosomes, and is caused by inappropriate assembly of telosome proteins that encapsulate and protect the telomere, excessive telomere shortening, telomere loss due to terminal chromosome deletion and also as a result of base damage within the telomere sequence (1).

1.2.3 Nuclear Buds (NBUDs)

NBUDs are a measure of gene amplification because amplified DNA is localized to the periphery of the nucleus and extruded during the S phase of the cell cycle (50). They have similar morphology as MNi with the exception that they are still connected to the nucleus by a thin stalk of nuclear material (1). To determine the formation of NBUDs, Lindberg et.al (2007) used fluorescent *in situ* hybridization (FISH) techniques with DNA probes that either specifically detected all centromeres (pancentromeric) or specifically detected all telomeres (pan-telomeric) (50). Of the 116 nuclear buds studied in normal cells, 52.6% were positive for only telomeric DNA, suggesting the presence of chromatid fragments. Only 5.1% contained a centromeric DNA, with or without a telomeric DNA suggesting the NBUD contained whole chromosomes and lastly, 42.3% contained no signal suggesting the presence of interstitial DNA (50). Therefore, it appears that NBUDs can form via chromatid fragments and elimination of excess chromosomes in aneuploid cells (1,50). Moreover, NBUDs containing interstitial fragments (without pancentromeric or pan-telomeric DNA) may form from broken chromatid bridges, elimination of unresolved DNA/DNA repair protein complexes or removal of amplified DNA from chromosomes by recombination between homologous sequences generated during breakage-fusion-bridge cycles (51).

1.3 Methylglyoxal (MGO)

1.3.1 Formation of MGO

Methylglyoxal (MGO) is primarily formed as a by-product of glycolysis, in which intermediate triosephosphates glyceraldehyde-3 phosphate (GA3P) and dihydroxyacetone phosphate (DHAP) spontaneously degrade forming MGO (52). Studies in red blood cells and endothelial cells has shown spontaneous degradation of triosephosphates and formation of MGO accounts for ~0.05-0.1% of their fate. Total whole body cellular formation of MGO by triosephosphate degradation equates to ~3 mmol/ day (or 3 mg/kg of body weight/day) and is an unavoidable by-product of glycolysis (53). Formation of MGO by triosephosphate degradation is elevated with increased glucose metabolism, as seen in hyperglycaemia in insulin independent cells (e.g. endothelial cells) and in cancer cells following metabolic reprogramming from oxidative phosphorylation as their primary energy source to glycolysis (known as the Warburg effect) (53-55). Moreover, pathological specific increases in MGO have also been observed. For example, in diabetic nephropathy, sulfenylation of the glycolytic enzyme pyruvate kinase M2 causes decreased tetramer formation which is crucial for its activity. This results in a build-up of glycolytic intermediates, which ultimately increases MGO precursor abundance (GA3P and DHAP) and thus its formation (56).

Other minor pathways of MGO formation include threonine catabolism, which produces an unstable intermediate 2-amino-3-ketobutyrate that spontaneously decarboxylates to aminoacetone. Semicarbazide amine oxidase (SSAO) enzymatically convert aminoacetone to MGO (57,58). Formation of MGO by SSAO under normal physiological conditions is estimated to be 0.1 mmol of MGO per day which equates to approximately 3% of total MGO formation (59). Due to the low abundance of SSAO in tissue it is unlikely this pathway is a major source of MGO synthesis. However, in the vascular compartment where it is more abundant, its contribution to MGO synthesis may be more pronounced (60). MGO can also be formed during catabolism of ketone bodies, by which cytochrome P450 2E1 facilitates the oxidation of acetone to MGO (61). However, this pathway of MGO formation is relatively low except in certain circumstances such as diabetic ketoacidosis or prolonged periods of fasting (62,63).

1.3.2 MGO detoxification, the glyoxalase system

As the formation of MGO is an unavoidable consequence of glucose metabolism, the cell needs to prevent concentrations reaching toxic levels. The glyoxalase system is an enzymatic pathway present in the cytosol of human cells, responsible for metabolism of MGO (and other dicarbonyl species) to the non-toxic D-Lactate (15). This system in combination with other minor defense systems, such as aldo-keto reductases and aldehyde dehydrogenase is responsible for the majority of MGO detoxification (64). The glyoxalase pathway consists of two enzymes; glyoxalase 1 (GLO1), which catalyzes the isomerization of the hemithioacetal formed spontaneously from MGO and reduced glutathione (GSH) to S-D-lactoylglutathione, and glyoxalase 2 (GLO2) which catalyzes the hydrolysis of S-D-lactoylglutathione to GSH and D-Lactate (65,66). *In situ* activity of GLO1 is directly proportional to the cellular concentration of GSH, thus oxidative or non-oxidative depletion of GSH can impact MGO concentration (67).

1.3.3 Formation of advanced glycation endproducts from MGO

Modification of protein or DNA by MGO forms a class of post translational modification (PTM) collectively referred to as advanced glycation endproducts (AGEs). It is also important to note that while MGO is the major glycating agent *in vivo*, other dicarbonyl species (glyoxal and 3-deoxyglucosone) and reducing sugars (glucose, fructose and pentose) can also form AGEs. MGO primarily reacts with the guanidino group of arginine residues yielding three cyclic MGO-derived hydroimidazolone isomers (MG-H1, MG-H2 and MG-H3) (Figure 1.4). MG-H1 is the predominant MG-H isomer formed *in vivo*, while no formation of MG-H2 is observed in physiological systems (68). MG-H3 is found *in vivo*, however high pH or when it is in close proximity to basic residues, it has been shown to convert to carboxyethylarginine (CEA), which is present at similar levels to MG-H1 (Figure 1.4) (69). MGO modification of arginine residues can also yield N^{δ}-(5-hydroxy-4,6-dimethylpyramidine-2-yl)-L-ornithine argpyrimidine (70) and N^{δ}-(4-carboxy-4,6-dimethyl-5,6-dihydroxy-1,4,5,6-tetrahydropyrimidine-2-yl)-L-ornithine tetrahydropyrimidine (THP), however, to a lesser extent than hydroimidazolone modifications. MGO can also react with lysine residues forming N^{ε}-carboxyethyllysine or the lysine dimer 1,3-di(N^{ε}-lysino)-4-methyl-imidazolium (MOLD) (Figure 1.4).

Lastly, MGO can form a methylimidazole crosslink between proximal cysteine and arginine residues (MICA) and 2-ammonio-6-((2-[(4ammonio-5-oxido-5-oxopentyl)amino]-4-methyl-4,5dihydro-1H-imidazol-5-ylidene)amino)hexanoate (MODIC) between arginine and lysine residues (Figure 1.4) (71,72). Although it is suggested that non-hydroimidazolone and crosslink modifications on arginine residues are less abundant, quantitative data for these is relatively scarce. Furthermore, certain cellular microenvironments may favour formation of these less abundant AGEs and thus, they may still regulate pathophysiological or non-pathophysiological effects.

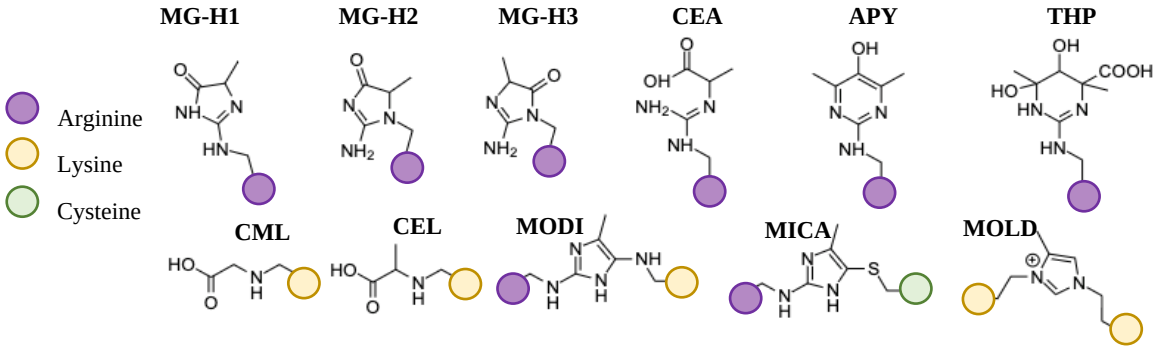

Figure 1.4: Examples of common advanced glycation endproducts.

1.3.4 Formation of advanced glycation endproducts from other metabolites.

As mentioned in the previous section, other metabolites such as glyoxal, 3-deoxyglucosone and reducing sugars (e.g. glucose, fructose and pentose) can also form AGEs. Glycation by glucose is directed toward lysine residues and results in both early and advanced stage of AGEs. Reactions of glucose with lysine forms an initial Schiff base product which undergoes Amadori rearrangement to form *N*-(1-deoxy-D-fructos-1-yl)amino acid or fructosamine, an early stage glycation adduct (73). Fructosamine can undergo further rearrangement or oxidative processes to form various AGEs such as the well characterised N^{ε}-carboxymethyllysine (CML) (Figure 1.4). In addition, CML can be formed directly by modification of lysine residues by glyoxal (74) Moreover, glyoxal and 3-deoxyglucosone can modify arginine residues forming the hydroimidazolone modifications G-H1/3 and 3-DG-H1/3, respectively, amongst others (74).

1.3.5 Repair or removal of MGO-modified proteins

Two recent examples of MGO-modified 'repair' proteins, Protein Deglycase DJ-1 (DJ-1/ PARK7) and protein arginine deaminase-4 (PAD4) have recently been described (75-77). The exact mechanism of repair by DJ-1 is still under debate, specifically whether it acts as a deglycase (removing MGO modification) or by direct conversion of MGO to D-Lactate (78). Experimental evidence suggests that DJ-1 acts by repairing early stage aminocarbonyl formation by MGO, which is hydrolyzed to form D-Lactate (75,76,79). Nevertheless, cells studies have shown that DJ-1 knock-out cells display higher levels of protein glycation (80). PAD4 is another protein which has recently been shown to display deglycase activity. However, unlike DJ-1, PAD4 does not return the arginine residue back to its original state but rather catalyses deamination of modified arginine residue to produce citrulline (77). However, the deglycase activity of PAD4 has only been shown to occur on histone proteins, thus it is unclear how far its protective properties extend to the rest of the cell (77).

1.3.6 Consequences of MGO modification

Proteins susceptible to modification, and resulting functional impairment are referred to as the dicarbonyl proteome (81). Modification of arginine residues by MGO produces a loss of charge and loss of electrostatic interactions involved in neighboring groups and ligand-ligand interactions of the modified protein (82). Loss of arginine positive charge is likely to affect thermodynamic stability of protein folding and intramolecular bonding at protein-protein interfaces by disrupting arginine salt bridge interactions and cation-π interactions of the guanidinium sidechain cations with the aromatic π-electron distribution of tyrosine sidechains, respectively (83,84). Modification of arginine residues creates a hydrophobic shift, which differs from native proteins in which hydrophobic residues are often found in globular or shielded protein domains (84). Moreover, surface hydrophobic residues are a signature of misfolded proteins, targeting them for degradation by the ubiquitin proteasome system (85). Thus, modification of protein arginine residues is likely to result in misfolding, which will affect protein activity and decrease protein abundance. It is still unclear why certain arginine or lysine residues are more susceptible to modification than others. It has been suggested that arginine residues with low *p*Ka are more susceptible to modification by MGO (83). However, recent studies have suggested this is not

the case, but rather glycation is governed by the chemical microenvironment such as neighboring amino acids. By employing a combinatorial peptide library, it was revealed that nearby polar and ionizable groups govern both hydroimidazolone formation and the specific MG-H isomer formed (86). These results suggest formation of MG-H1, and other MG-H isomers are influenced by both long and medium-range cooperative interactions of neighboring residues and highlights the potential of MGO mediated glycation as a functional PTM (86).

1.3.7 Specific examples of MGO modification

While MGO has been shown to covalently modify numerous proteins, many of these studies rely on *in vitro* procedures with reagent conditions not reflecting those found physiologically. Therefore, the site, function and molecular characteristics of these modifications are poorly characterized. Nevertheless, several recent studies have identified specific protein targets for MGO with robust biological and chemical detail describing their functional consequences. A few examples of these proteins are described below.

1.3.7.1 Hypoxia Response Element-1α

Under normoxic conditions, HIF-1α is hydroxylated, making it a target for the Von Hippel-Lindau tumor suppressor protein, which ubiquitinates HIF-1α, making it a target for proteasomal degradation. (Figure 1.5) Under hypoxic conditions, HIF-1α is stabilized and is translocated to the nucleus where it dimerizes with HIF-1β and forms heterodimers with aryl hydrocarbon receptor nuclear translocator (ARNT-1) and recruits coactivators CREB-binding protein (CBP)/p300. This complex binds to genes containing hypoxia response elements and activates expression of genes required for adaptive cellular response to hypoxia. However, under hyperglycemic, or conditions of dicarbonyl stress, HIF-1α is modified by MGO at arginine 17 and 23 of the basic helix-loop-helix binding domain (87). These modifications lead to a rapid proteasome-dependent degradation of HIF-1α, regardless of oxygen concentrations (normoxic or hypoxic), decreased heterodimer formation with ARNT and heterodimer binding with hypoxia response elements (Figure 1.5) (87,88).

1.3.7.2 Kelch-like ECH associated protein 1

The nuclear factor erythroid 2 (NF-E2)-related factor 2 (NRF2) - Kelch-like ECH associated protein 1 (KEAP1) pathway is a major regulator of antioxidant responses to endogenous and exogenously caused oxidative stress (89). NRF2 is a key signaling protein within this transcriptional axis that together with Maf proteins, binds antioxidant response elements regulatory region of target genes (89). KEAP1 repressor protein binds NRF2, promoting its degradation via the ubiquitin proteasome system. A recent report identified a compound (CBR-470-1) was able to increase NRF2 signaling (71). It was determined that this compound was a potent inhibitor of phosphor-glycerate kinase 1 (PGK1) which is responsible for the conversion of 1,3-bisphosphoglycerate to 3-phosphoglycerate in glycolysis. Inhibition of this process resulted in an accumulation of triosephosphate GA3P (71). The authors identified a high molecular weight KEAP1 at twice the molecular mass of monomeric KEAP1. This response was also observed following knockdown of PGK1 and treatment with various glycolytic intermediates with reactive functionalities, however, the greatest increase in high molecular weight-KEAP1 was observed following treatment with MGO (Figure 1.5). Using mass spectrometry and nuclear magnetic resonance (NMR) spectroscopy, the authors were able to deduce this dimerization of KEAP1 was caused by crosslinking of cysteine 152 and arginine 135, resulting in the novel methylimidazole crosslink between proximal cysteine and arginine residues (MICA) (71). Crosslinking of KEAP1 decreased NRF2 degradation and caused accumulation of NRF2 and an increase in various genes containing antioxidant response elements (71). This study demonstrated a clear connection between a site specific MGO modification and cellular response. Furthermore, the results are of particular interest regarding dicarbonyl stress as NRF2 is a transcriptional regulator of GLO1 and enzymes involved in glutathione synthesis, both of which are critical in the detoxification of MGO and may suggest the presence of a positive feedback loop (90).

1.3.7.3 Histone proteins

Genomic DNA in eukaryotic cells is packaged into chromatin, the structure of which fundamentally controls all nuclear processes involving DNA, such as DNA replication/ repair and transcription (91). Packaging of DNA is regulated by a family of small proteins called histones, which interact with anionic

phosphodiester backbone of DNA with their cationic, lysine and arginine rich tails. Modulation of this interaction between histones and DNA is regulated through PTMs which ultimately controls gene accessibility. Histone PTMs can be derived through either enzymatic process (methylation, ubiquitination etc) which are controlled by proteins called enzyme 'writers' or 'erasers'. Moreover, various PTMs can be derived from non-enzymatic covalent modifications caused by electrophilic metabolites which react with nucleophilic residues of arginine and lysine.(92). Modification of histone proteins by reactive electrophiles causes 4 key issues for chromatin: i) induction of crosslinks between histone proteins or histone and DNA. ii) loss of electrostatic interactions between DNA and histones caused by a loss of lysine or arginine positive charge following modification. iii) Alteration of 3D structure and surface topology. iv) competition with other enzymatic derived PTMs (92) .

Recent studies have shown that histone proteins do indeed contain various MGO induced PTMs such as MG-H1, CEA and CEL. These modifications occur at similar frequencies to other PTMs, such as asymmetric dimethylarginine which has a role in transcriptional regulation, and succinylation of Lys (69,93). However, their concentration was lower than acetylation and trimethylation of lysine (69). Increased modification of histones by MGO has been shown to reduce the level of other PTMs such as H3K9me3, H3K4me3, H3R8me2, H2BK120Ub and overall acetylation (80). Whether this reduction in other PTMs was a result of direct competition for lysine and arginine residues or by modification of neighbouring residues impairing enzyme (writer) access remains to be shown, however, it does highlight the potential importance of MGO modifications in regulating the histone code (Figure 1.5). Modification of histones by MGO has also been shown to affect chromatin compaction (Figure 1.5) (80). At low concentrations of MGO chromatin relaxes, likely due to a loss of arginine and lysine positive charges weakening electrostatic interactions with negatively charged DNA (80). In contrast, high concentrations of MGO resulted in increased chromatin compaction, which was suggested to be caused by histone-histone and/or histone-DNA crosslinks (Figure 1.5) (80). Chromatin compaction is critical in regulating gene accessibility, which is consistent with observations that MGO causes global changes in gene expression (69,94). Unfortunately, site specific identification of MGO adducts has only been determined in cells which experienced a ~200-fold excess of intracellular MGO, thus, it is still unclear which sites are most susceptible and most relevant (95).

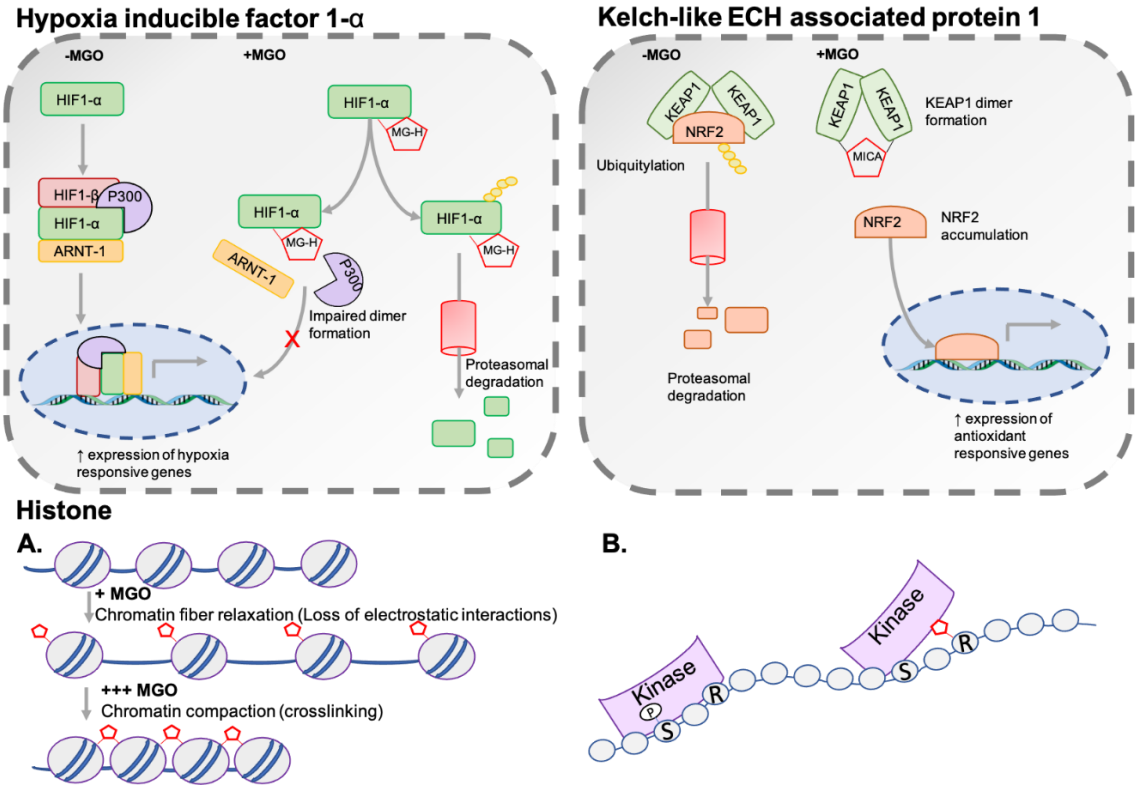

Figure 1.5: Examples of MGO modifications on specific proteins and resulting functional consequences. Top left; A schematic showing the various effects of MGO modification of HIF-1α. Top right; A schematic showing increased NRF2 activation following MGO crosslinking of KEAP1. Bottom; Graphical representation of changes in histone topology following MGO modification (A) and interference with Kinase (B).

1.3.8 AGE analytics

1.3.8.1 Absolute quantification of AGEs

Early methods to quantify AGE species utilized techniques such as measuring total AGE fluorescence with excitation and emission wavelengths of 350 nm and 450 nm, respectively. Unfortunately, most quantitatively important AGE species are non-fluorescent and therefore not quantified with this method and interference from other fluorophores can interfere with this assay (96). Chromatographic techniques utilizing HPLC coupled to UV or fluorescence detectors have also been utilized (97). While these methods can measure all quantitively important AGEs, for adequate sensitivity and chromatographic resolution they do require pre-column derivatization and gradients exceeding 90 minutes limiting their high-throughput capabilities (97). The current 'gold standard' method for quantification of AGEs is liquid chromatography tandem mass spectrometry (LC-MS/MS) utilizing triple quadrupole (QqQ) mass spectrometers. However, ion trap, quadrupole-time of flight and quadrupole-orbitrap mass spectrometers can also be utilized (98), Electrospray ionization avoids the need for pre-column derivatization and multiple reaction monitoring (MRM) data acquisition mode gives high selectivity and sensitivity allowing for shorter gradients and higher throughput. Stable isotopic dilution analysis allows for the accurate quantification of all AGE species present in a sample. These methods have been applied to a wide range of matrices including plasma, urine, tissue, plants, beverages and food systems (16,90,99-101).

Pre sample processing for quantification of protein-bound AGEs requires complete hydrolysis of protein samples to release the AGE as a free species. Various methods have been described to accomplish this. The most widely used approach is acid-hydrolysis which relies on incubating the protein sample in 6M HCl at 100-110°C for 20-24 hours to completely hydrolyze the protein. Although this is the most commonly used method, it is not suitable for acid labile AGEs, including the quantitatively major MG-H1. Degradation of MG-H1 during the acid hydrolysis procedure has been reported between 30 and 90% (97,102). An alternative method is exhaustive enzymatic hydrolysis with sequential addition of several protease enzymes (103). Digestion is initiated with pepsin under acidic conditions. After 24 hours, the pH is adjusted to 7.4 and Pronase E is added for another 24 hours. Lastly, aminopeptidase and prolidase are added for 48 hours (103). This method is limited to minimally modified proteins as

enzymatic digestion is impaired in highly modified samples, such as heat-treated foods or *in vitro* glycated proteins (104). However, most biological sample, such as plasma and intracellular proteins are suitable for this approach. Similar methods have been described utilizing an initial digestion with TPCK treated trypsin, followed by incubation with aminopeptidase. This method has been employed to study lysine and arginine modifications in mammalian cells and tissues (105).

Absolute quantification of AGE species is an incredibly useful tool, particularly when investigating their association with specific disease states. However, as absolute quantification methods require complete hydrolysis of proteins, these methods don't reveal which proteins were initially modified which is critical for elucidating under lying mechanisms associated with protein modification by MGO and other AGE precursors. To study this, proteomic techniques, primarily utilizing high resolution orbitrap mass spectrometry is the gold standard approach. The following section will discuss the application of proteomic techniques to the study of MGO modifications, as well as other AGE species.

1.3.9 Site specific determination of AGE modifications

1.3.9.1 Standard Proteomics Workflow

A typical mass spectrometry-based proteomics experiment consists of 5 steps (Figure 1.6) (106). (1) Protein is isolated from sample (cell lysate, tissue, plant etc.). (2) Proteins are digested, typically by trypsin or Lys/ C, however various other protease enzymes exist and their suitability is largely application dependent (107). Trypsin cleaves at the C-terminus of arginine or lysine residues leading to peptides which are protonated at the C-terminus, an advantage for subsequent peptide analysis. (3) Peptides are partially resolved by nanoflow liquid chromatography and eluted into an electrospray ionization source where they are nebulized into small, highly charged droplets. (4) Protonated peptides enter the mass spectrometer where a mass spectrum (MS) is taken. A prioritized list of peptides is generated for fragmentation. (5) Prioritized peptides enter a collision cell where they are collided with a gas by collision-induced dissociation (CID) or higher-energy C-trap dissociation (HCD) to create fragments. Fragments masses are collected in what is known as tandem or MS/MS spectra. MS and MS/MS are matched against a protein sequence database (106).

1.3.9.2 Previous studies

Analysis of MGO modifications follows the same procedure as described for a typical MS-based proteomics approach, except that peptide mass shift of +54 Da and +72 Da, corresponding to MG-H and CEL/ CEA modification, respectively, are searched against the database (104). Although proteomics offers unparalleled potential for the study of MGO modifications, only a few studies have utilized this technology. The biggest challenge facing proteomic studies of MGO modifications, as well as other AGEs is their low abundance, low stoichiometry compared to their unmodified counterpart (20-100 fold more abundant) and heterogeneity at each residue (104). Studies which have tried to investigate MGO modifications under basal conditions have resulted in low number of identifications. For example, in human aortic endothelial cells, only 10 proteins were identified with MG-H modifications. Similarly in periodontal ligament fibroblasts only 5 proteins were identified under normal conditions (108). In both these studies, to increase the concentration of MGO modifications, exogenous MGO was added to proteins extracted from the cell lysate to increase their abundance to 10-20-fold (54,108). Similarly, in a study investigating MGO histone modifications, no modifications were identified under normal conditions despite HPLC enrichment of individual histone proteins. To overcome this, the author's treated GLO1 knockout cells with 1 mM of MGO, allowing for the identification of 21 modification sites across the 4 canonical histone proteins (69). More recently, MG-H modifications were investigated in HEK293T cells treated with 131 µM of MGO and further a subcellular fractionation was employed to decrease sample complexity which led to the identification of >600 MGO modified proteins showing over-representation on spliceosome proteins (109). While this approach is effective at increasing the concentration of MGO modifications, care needs to be taken to ensure that levels do not exceed what would be expected physiologically. Failure to do so will result in modification of proteins unlikely to be modified under normal, or pathological conditions, in which MGO modifications rarely exceed > 3-fold increase.

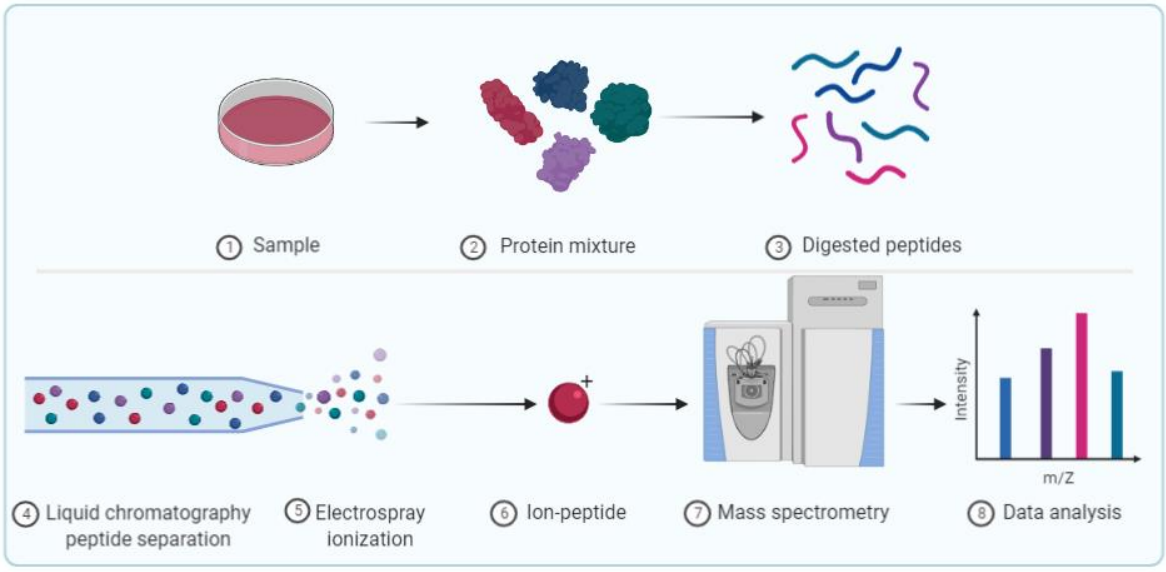

Figure 1.6. Schematic representing a standard workflow for shot-gun proteomics.

1.3.9.3 Enrichment strategies.

Only a handful of enrichment strategies, or strategies to increase identification of AGE modified proteins have been described. For example, a recent study used antibody-based enrichment strategy to enrich CML-modified peptides from various cell lines and tissue samples (110). This technique was effective at increasing the number of peptide spectrum matches containing a CML modification by ~10-fold in treated samples but was less effective under control conditions (110). Furthermore, CML modified peptides never reached above 5% of total peptide spectrum matches, likely due to cross reactivity of CML antibodies with other AGE species such as CEL and other acyl modifications. Use of immobilized antibodies for the enrichment of MGO modified peptides has only been reported once by Galligan et.al (2018) in order to enrich MGO modified histone peptides using antibodies specific to each MG-H isomer and CEA, however, no enrichment was achieved (69). Several commercial MG-H antibodies are available and may be suitable for this approach. Interestingly, enrichment of AGEs and advanced lipoxidation endproducts was recently described using magnetic beads functionalized with the receptor for advanced glycation endproducts (RAGE) VC1 domain, allowing for the selective enrichment of glycated proteins (111). Because true enrichment strategies for AGE species are scarce, other techniques such as pre-column fractionation and subcellular fractionation are effective at reducing sample complexity and increasing the number of modifications identified. The latter was recently utilized to investigate MG-H modifications in HEK293T cells, in which 120 and 68 MGO modified proteins were

identified in the nucleus and mitochondria, respectively (109). Pre column fractionation is another suitable technique to reduce sample complexity. Standard pre column fractionation is done under high pH, however, several MGO modifications, including MG-H1 are labile under these conditions making it unsuitable. Therefore, other pre fractionation strategies, including hydrophilic like interaction chromatography have been employed to investigate AGE modifications in *Arabidopsis thaliana* (112). Recent technological advancements have also been made which allow for gas phase separation with ion mobility mass spectrometry. These include trapped ion mobility spectrometer (TIMS) in which ions are trapped in an electrodynamic tunnel by opposing forces of a gas flow in one direction (toward exit of tunnel) and an analytical direct current in the opposing direction (toward entrance of tunnel). Ions are separated in the TIMS tunnel based on their size and shape and come to rest at what is known as their collisional cross section, and can be eluted sequentially by decreasing the electrical field (113). TIMS was recently used to differentiate between the isobaric lysine PTMs acrolein and propionyl, which can be indistinguishable by traditional MS, but are separable by their collisional cross section (114). High field asymmetric waveform ion mobility spectrometry is another ion mobility technique that separates ions in the gas phase based on their behavior in strong and weak electrical fields (115). Both of these ion mobility techniques are effective at separating interfering species, allowing detection of peptides that would otherwise be missed, including low intensity peptides and co-eluting species of similar *m/z*. Given the low abundance of MGO modifications, ion mobility techniques would likely be effective at reducing interference from higher abundance peptides. Furthermore, they may be effective at differentiating between isomeric modifications, such as hydroimidazolone isomers (MG-H1,2 or 3), or between CEL and the recently identified lact(o)yllysine which share the same mass shift (95).

1.3.9.4 Confirmation of methylglyoxal modifications

MGO modifications can be detected on peptides with mass increments of 54+ and 72+ for MG-H and carboxyethyl modifications. Confirmation of MGO modifications, as with most modifications is best achieved by characteristic mass shifts of *b* or *y* ions in the MS/MS spectra relating to the modification of the lysine or arginine residue. This is commonly the case with high abundant proteins in which modified peptides create a complete, or near complete set of *b* or *y* ion series. However, as the

concentrations of some modifications is low, this is not always the case. Trypsin cleavage after a modified arginine or lysine residue is impaired, producing peptides with a characteristic missed cleavage (82). Presence of a missed cleavage due to MGO modified residue can also provide information on the site of modification. Previous studies have also reported peptide free side chain fragment ions with an immonium ion structure for each MGO modification which can be further applied to improve confidence on the presence of the modification (104). For example, analysis of plasma digests by nanoflow-LTQ orbitrap XL ETD mass spectrometry, scanning of tryptic peptides for 152.1 (glyoxal modified arginine) and 166.1 (MG-H) led to the identification of 44 hydroimidazolone and dihydroxy imidazolidine-derived peptides (116).

1.3.9.5 MGO modified DNA

It is commonly stated in the literature that MGO can react with DNA to form a class of DNA AGEs. Despite this, only a handful of studies have investigated their formation or cellular impact. Given the stability, uniform cellular distribution and longer half-life of DNA molecules compared to that of protein, its modification may comprise a large level of cellular glycation. The following section will discuss the formation of DNA AGEs, as well as their pathophysiological consequences in the context of mammalian systems.

1.3.9.6 Formation of glycated DNA adducts

Various DNA AGEs have been identified upon reactions of deoxyguanosine (dG) with MGO or other dicarbonyl compounds and glucose. Despite the discovery of numerous adducts, there is still debate in the literature regarding primary product formed and relative abundance in physiological conditions (Table 1.1). Early studies showed conflicting results with the products formed by reactions of MGO and dG (summarized in Table 1.1). For example, Shapiro et.al (1969) showed that 3-(20-deoxyribosyl)-6,7-dihydro-6,7-dihydroxy-6/7methylimidazo-[2,3-b]purine-9(8)one (MGdG) was the only adduct observed after an 18 hour incubation time with ~ 30:1 ratio of MGO:dG (Figure 1.7) (117). This is in agreement with both Frischman et.al (2005) and Shuck et.al (2018) which showed MGdG was the primary adduct formed during the first 24 hours, but rapidly degraded thereafter to undetectable limits (118,119). Studies with an incubation time beyond 24 hours show N2-(1,R/S-carboxyethyl)-deoxyguanosine (CEdG) and a bis adduct corresponding to the addition of two MGO equivalents MG-CEdG to be the primary adducts formed (Figure 1.7) (118-121). A recent study by Shuck et al (2018) aimed to resolve these discrepancies. The authors showed that stoichiometry of MGO:dG and water activity were important experimental parameters in the formation of different adducts. Formation of MGdG and MG-CEdG were favored when concentrations of MGO exceeded dG (2:1), however, consistent with previous reports, the former rapidly degraded after 24 hours. On the other hand, CEdG was favored when MGO concentrations were less than that of dG (0.1:1), which is a condition more likely to reflect the cellular microenvironment. Formation of MG-CEdG was shown to be a result of MGO addition to N7 of CEdG, as no product with only the addition of MGO to N7 of dG has been

reported. Therefore, assuming under physiological conditions where the stoichiometry of MGO:dG is much lower than *in vitro* studies, MG-CEdG is unlikely to form. This is also consistent with the fact that it has not been observed in cellular DNA.

Water activity, which affects hydration equilibria of MGO is another reaction condition which likely accounts for discrepancies in the literature. The unhydrated and monohydrated forms of MGO are the main reactive forms, whereas the dihydrated is expected to be unreactive. Reactions of MGO with dG in 90% DMSO, which should favor the unhydrated form of MGO showed the almost exclusive formation MGdG for up to 96 hours (119). The importance of water activity in the formation of dG adducts is reflected by the fact that nuclear and mitochondrial compartments are rich with solutes, accounting for ≥ 20% of the activity of water (122). Therefore, MGO hydration may be skewed toward the unhydrated form, accounting for the high levels of MGdG that has been detected in mammalian DNA compared to that of CEdG (13,123). Results from various studies have shown levels of MGdG and CEdG to be approximately 6 and 0.7-10 adducts/ 10^6 dG, respectively, depending on cell, tissue or species DNA was isolated from (123-125). Although both MGdG and CEdG may serve as biomarkers for MGO derived metabolites, the chemical stability of CEdG may make it more robust. CEdG has been shown to be elevated in the urine and tissue of db/db mice and the urine of individuals with diabetic nephropathy (13,124). Furthermore, urinary CEdG was shown to correlate with urinary albumin excretion, an already established biomarker of diabetic nephropathy (13).

Table 1.1.Studies on reactions of MGO with dG or DNA

Study	MGO	dG	DNA	Time	Temp	Products	Ref
[1]	52 mmol	1.65 mmol	-	18 hours	65	dG-MG	(117)
[2]	a. 10 mM	5 mM	-	2 weeks	37	MG-CEdG $CEdG_{A/B}$	(118)
	b. 100 µM	5 mM	-	2 weeks	37	dG-MG* $CEdG_{A/B}$	
	c. 100 mM	-	Un	1 week	37	MG-CEdG $CEdG_{A/B}$	
	d. 10 µM	-	Un	1 week	37	$CEdG_{A/B}$	
[3]	400 µmol	20 µmol		48 hours	37	MG-CEdG	(120)
[4]	6 mmol (DL-glyceraldehyde)[#]	2 mmol		2 weeks	40	$CEdG_{A/B}$	(121)
[5]	a. 2*	1*	-	96 hours	25	MG-CEdG	(119)
	b. 1*	1*	-	96 hours	25	dG-MG	
	c. 0.1	0.1*	-	96 hours	25	$CEdG_{A/B}$	
	d. 10 mM	-	10 nM	24 hours	25	MG-CEdG $CEdG_{A/B}$	
[6]	0.01-100 mM	-	1 mg/mL	15 hours	37	dG-MG $CEdG_{A/B}$	(123)

*Indicates ratio between MGO:dG. [#]DL-Glyceraldehyde was used which forms MGO *in situ* by dehydration and enol-keto tautomerization. Un; Unspecified.

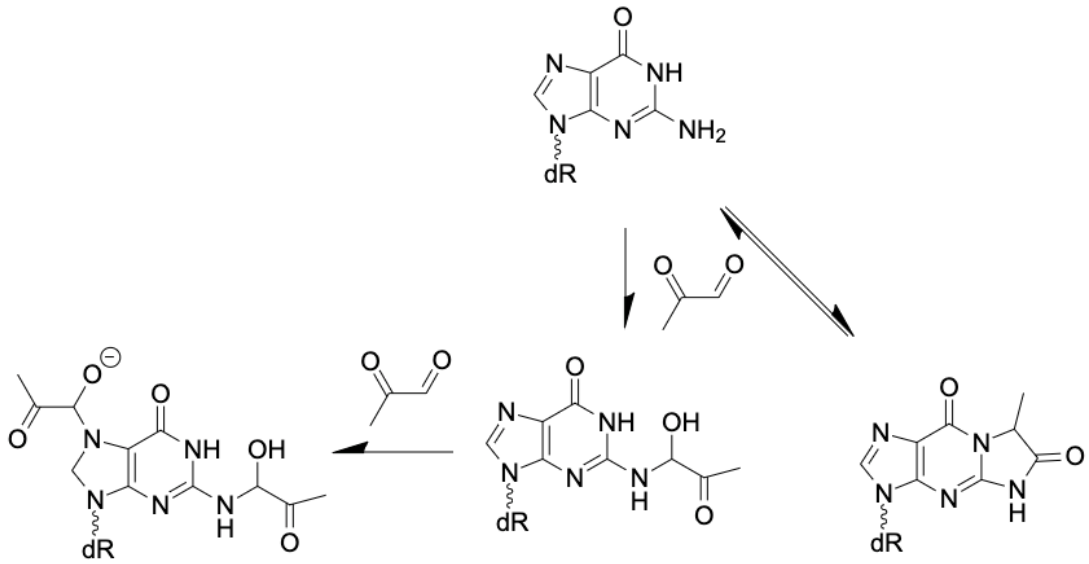

Figure 1.7: Formation of DNA advanced glycation endproducts derived from MGO.

1.3.9.7 Consequences of DNA Glycation

Although the biological consequences of nucleotide glycation have not been well established, they have been shown to cause DSBs, DNA-DNA and DNA-protein crosslinks and have low mutagenic activity in cells with functioning nucleotide excision repair capacity (123,126-129). DNA strand breaking effects of CEdG were first described >20 years ago by Pischetsrieder et.al (1999). In this study, plasmid DNA treated with dihydroxyacetone to increase CEdG content to ~1.5 CEdG/10^5 dG was shown to decrease the presence of supercoiled DNA, and subsequently increase the presence of linearized DNA by gel electrophoresis (126). This study confirmed that the effects seen were not the result of oxidative DNA damage and that the carbonyl group of dihydroxyacetone was necessary for the DNA strand breaks to occur. Subsequent studies, using mammalian cells have supported these results. For example, HL-60 cells treated with MGO (524 µM) or Glo1 inhibitor (BBGD; 10 µM) for 2 hours were shown to increase MGdG content by 2 and 5-fold, respectively, with no increase in other MGO adducts or 8-oxodG (123). This increase in MGdG corresponded to a 7- and 27- fold increase in DNA strand breaks, measured by terminal deoxynucleotidyl transferase-mediated dUTP-FITC nick-end labeling (TUNEL) method. More

recently, a decrease in GLO1 activity, achieved by exchange of threonine 107 residue with alanine to prevent phosphorylation increased the MGdG content of DNA (130). Elevated MGdG was associated with DNA damage, determined by measuring tail length using the COMET assay and increased protein abundance of p53 and γH2Ax (130).

Currently, only modification of DNA has been investigated into the genotoxicity of MGO. However, as discussed in Section 1.1.1 loss and/ or changes in the activity in numerous proteins involved in various aspects of mitosis can cause genomic instability. Furthermore, as we know that MGO can cause changes in protein activity, it is conceivable that modification in such proteins may result in genomic instability. Therefore, the genotoxicity of MGO may stem beyond its ability to modify DNA, and modification of proteins involved in mitosis may also be implicated and therefore contribute to increased numerical chromosome abnormalities (aneuploidy) systemically.

1.4 Folate

1.4.1 Folate mediated one carbon metabolism.

One-carbon metabolism comprises a series of biosynthetic reactions required to regenerate the various forms of methylated folate needed in several critical reactions such as the synthesis of methionine from homocysteine, which may also be converted to cysteine via the transsulfuration pathway (131). This complex network of biochemical reactions facilitates the transfer of one-carbon units for various cellular processes including molecular biosynthesis (nucleotide, polyamines, amino acids, creatine and phospholipids), DNA synthesis, epigenetic regulation via maintenance of DNA methylation patterns and redox defense (131). B vitamins such as folates (B9), pyridoxal-phosphate (B6), cobalamin (B12) and riboflavin (B2) mediate one-carbon metabolic processes by acting as substrates or cofactors.

Folates are a class of compounds that consist of the following three moieties; pteroylglutamic acid, a *para* aminobenzoic acid ring and a tail containing one or more glutamic acid residues linked through a (gamma)-carboxyl group (132). Folate molecules differ in the extent of polyglutamylation, oxidation state and the type of carbon-one unit attached to R1 and R2 (Figure 1.8) (132). For example, tetrahydrofolate (THF), the most reduced form of folate, is the active form, whereas folic acid, a synthetic form of folate is completely oxidized (Figure 1.8). The folate pool of a cell or food source is a mixture of different folate molecules. In plasma and urine, the main form of folate is the methylated, reduced monoglutamate form, 5-methyltetrahydrofolate (5-meTHF), which can readily be absorbed by the cell where it becomes polyglutamated which enables its retention within the cell (132).

Folic acid, the synthetic form of folate enters the one-carbon metabolism cycle by being converted to dihydrofolate (DHF) and then to the biologically active form, THF (Figure 1.9) (131). THF is then converted to 5,10-methyleneTHF (5,10-meTHF) by the pyridoxal-phosphate dependent enzyme, serine hydroxy methyltransferase (SHMT) (Figure 1.9). 5,10-meTHF is used to convert deoxyuridine monophosphate (dUMP) to deoxythymidine triphosphate (dTTP) by the enzyme thymidylate synthase (TS) (Figure 1.9) (131). Alternatively, 5,10-meTHF can be converted to 10-formylTHF (10-fTHF) for purine synthesis or to 5-meTHF for remethylation of homocysteine to methionine and eventually S-adenosyl methionine, the common methyl donor used for epigenetic regulation (Figure 1.9) (131).

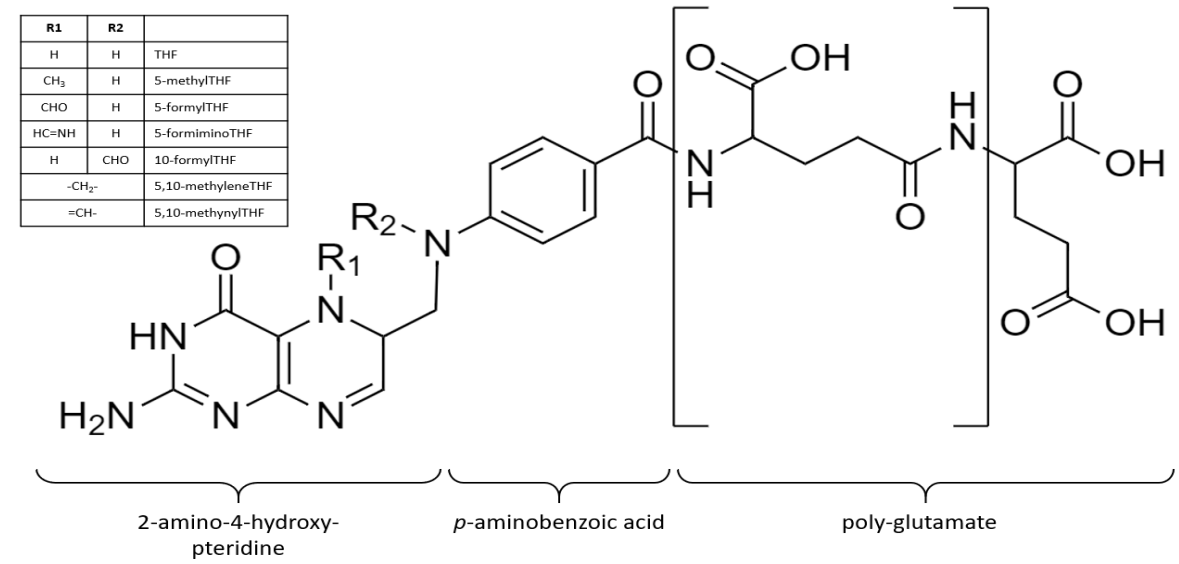

Figure 1.8. Diagram depicting the different forms of folate. This figure is adapted from (132).

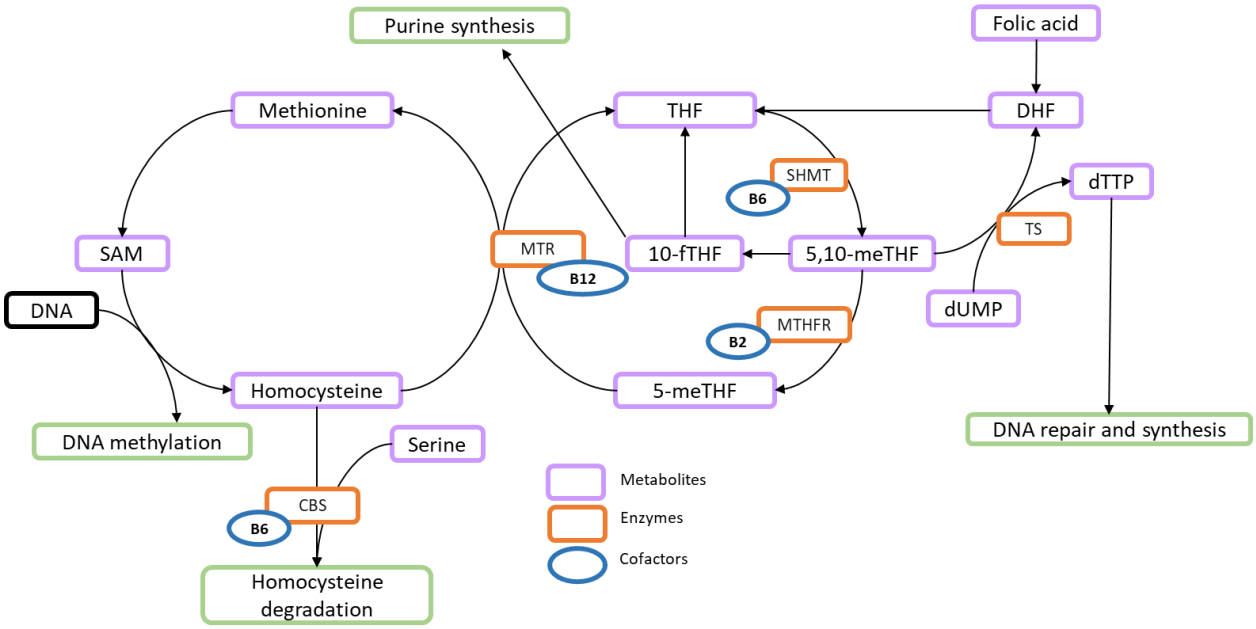

Figure 1.9. A diagrammatic outline of folate mediated one carbon metabolism and its role in various cellular processes. This figure was adapted from (131).

1.4.2 Folate deficiency and chromosomal instability

The importance of folate in regulating genomic integrity can be highlighted by comparisons showing that human peripheral blood lymphocytes (PBL) cultured in folic acid deficient media (12 nmol/L) or exposed to 0.2 Gy equivalent ionizing radiation (10 times the annual safe exposure limit) experienced

similar levels of DNA damage (133,134). Furthermore, numerous *in vitro* and *in vivo* studies in both rodents and humans have shown an association between folic acid deficiency and elevated frequency of MNi and other DNA damage biomarkers (135-137). Folate deficiency causes uracil misincorporation into DNA because it is required (in the form of 5-10-meTHF) as a methyl donor to convert dUMP to dTMP (131). When folate is deficient, dUMP accumulates and uracil is incorporated into DNA instead of thymidine (138). The simultaneous excision of two closely spaced uracil bases (<12 base pairs) can lead to DNA strand break formation which subsequently can be measured as MNi (40). Peripheral blood lymphocytes (PBL) grown in folic acid deficient media have been shown to contain elevated frequencies of MNi, NPBs and NBUDs, all of which can result from DSBs (51). Interestingly, folic acid deficiency has also been shown to produce other types of DNA damage, which do not originate from DSB events (136). A small percentage of MNi (16.6%) and NBUDs (10.0%) from PBL grown in folic acid deficient media (12 nmol/L) were shown to contain whole chromosomes, suggesting whole chromosome loss events are also a pathological outcome of folate deficiency (136). This is supported by recent studies showing various mitotic aberrations in folic acid deficient cells, including chromosomal misalignment, multipolar mitosis and compromised spindle assemble checkpoint (139,140). Furthermore, it has been shown that WIL2-NS B lymphoblastoid cells grown in folic acid deficient media contain both dysfunctional long and short telomeres, and NPBs with telomeric signals indicating telomeric end fusion events (141). Therefore, folate deficiency induced genomic instability may occur from processes beyond its role in one-carbon metabolism.

1.4.3 Folic acid deficiency increases sensitivity to genome damage by other genotoxins

Several studies have also shown that folic acid deficient cells are more sensitive to other genotoxic stresses. For example, WIL2-NS B lymphoblastoid cells grown in folic acid deficient RPMI (2 nmol/L) experienced ~2 fold increase in MNi and NPBs following exposure to ionizing radiation (1.5 Gy) compared to folic acid replete controls (200 nmol/L). Furthermore, high concentrations of sugars (glucose, fructose, galactose and sucrose) were shown to be genotoxic to normal human colon mucosal cell lines (NCM460, CCD841) and human liver (L02) cells grown in folic acid deficient, but not replete

media (142). Interestingly, deficiency of pyridoxamine, an important cofactor for SHMT in one-carbon metabolism has also been shown to increase sensitivity of brain cells isolated from *Drosophila melanogaster* and HeLa cells to high concentration of glucose (143). This interaction between pyridoxamine deficiency and glucose was prevented by co-administration of α-lipoic acid, a well validated scavenger of AGE precursors (143). Therefore, deficiency in metabolites required for one-carbon metabolism may leave cells sensitive to glycation derived by glucose and the glycolytic byproduct MGO. This may be due to reduced DNA damage repair capacity in folic acid and pyridoxamine deficient cells which then prevents repair of DNA damage induced by AGE formation allowing for it to accumulate and reach cytotoxic and genotoxic levels. Moreover, one-carbon metabolism is required for the transulfuration pathway which is involved in synthesis of glutathione. As previously discussed (section 1.3.2), glutathione spontaneously reacts with MGO and is then detoxified by the glyoxalase system. Therefore, deficiency in folic acid and/or pyridoxamine may prevent MGO detoxification and result in an increase in its concentration.

1.5 Hypotheses and Research Aims

Hypotheses

In this study, we proposed the following hypotheses…

1. Methylglyoxal will induce DNA damage as measured by the cytokinesis block micronucleus cytome assay
2. Folic acid deficiency will increase cellular susceptibility to glucose and methylglyoxal induced DNA damage as measured by the cytokinesis block micronucleus cytome assay
3. Modification of mitotic proteins by methylglyoxal will be associated with DNA damage caused by methylglyoxal.

Aim 1:

Currently, very few studies have investigated the genotoxicity of MGO. Moreover, studies which have assessed genotoxic activity have been performed using techniques such as measuring abundance of p53, γH2Ax or TUNEL assays which only measure specific types of DNA damage. Therefore, the first aim was to determine the genotoxicity of MGO, induced by exogenous addition of MGO or inhibition of GLO1 enzyme in WIL2-NS and PBL using the CBMNcyt assay. LC-MS/MS analysis of various dicarbonyl stress biomarkers were quantified to determine their association with DNA damage.

Key objectives

- Optimize LC-MS/MS methods to quantify various dicarbonyl stress biomarkers including (intra and extracellular protein AGEs, intra and extracellular MGO and the DNA glycation adduct CEdG)
- Using the CBMNcyt assay, determine the genotoxicity of MGO in WIL2-NS and PBL
- Using Fluorescent *in situ* hybridization (FISH), determine the contents of MNi induced by MGO

Aim 2:

It was recently shown that folic acid deficiency increases glucose induced genotoxicity. We hypothesized this interaction may be due to elevated levels of MGO induced by high glucose concentrations. Therefore, the second aim was to investigate the interaction between folic acid deficiency and glucose with respect to DNA damage and determine if this interaction is associated with the formation of MGO.

Key objectives

- Confirm an interaction between glucose and folic acid deficiency with respect to DNA damage as measured by CBMNcyt assay
- Determine if there is an interaction between MGO and folic acid deficiency with respect to DNA damage as measured by CBMNcyt assay
- Determine the role of MGO on the interaction between high glucose and folic acid deficiency with respect to DNA damage as measured by the CBMNcyt assay.

Aim 3:

As previously discussed, little is known about the intracellular protein targets of MGO. Therefore, using shot-gun proteomics approach, identify proteins containing. MGO modifications. Furthermore, based on these targets, investigate if modification is consistent with observed DNA damage.

Key objectives

- Identify proteins with MGO modifications using high resolution orbitrap mass spectrometry
- Based on those protein targets, investigate underlying mechanisms associated with MGO induced DNA damage.

Aim 4:

Perform bioinformatic analysis on protein targets of MGO to identify biological processes and cellular targets sensitive to modification by MGO

Key objectives

- Identify biological processes, molecular processes and/or cellular components that are over-represented with MGO modifications.

References

1. Fenech, M., Kirsch-Volders, M., Natarajan, A.T., Surralles, J., Crott, J.W., Parry, J., Norppa, H., Eastmond, D.A., Tucker, J.D., and Thomas, P. (2011) Molecular mechanisms of micronucleus, nucleoplasmic bridge and nuclear bud formation in mammalian and human cells. *Mutagenesis*, **26**, 125-132.
2. Gregan, J., Polakova, S., Zhang, L., Tolic-Norrelykke, I.M., and Cimini, D. (2011) Merotelic kinetochore attachment: causes and effects. *Trends in Cell Biology*, **21**, 374-381.
3. Roos, W.P., Thomas, A.D., and Kaina, B. (2016) DNA damage and the balance between survival and death in cancer biology. *Nature Reviews Cancer*, **16**, 20-33.
4. Tubbs, A., and Nussenzweig, A. (2017) Endogenous DNA Damage as a Source of Genomic Instability in Cancer. *Cell*, **168**, 644-656.
5. Bonassi, S., Znaor, A., Ceppi, M., Lando, C., Chang, W.P., Holland, N., Kirsch-Volders, M., Zeiger, E., Ban, S., Barale, R., Bigatti, M.P., Bolognesi, C., Cebulska-Wasilewska, A., Fabianova, E., Fucic, A., Hagmar, L., Joksic, G., Martelli, A., Migliore, L., Mirkova, E., Scarfi, M.R., Zijno, A., Norppa, H., and Fenech, M. (2007) An increased micronucleus frequency in peripheral blood lymphocytes predicts the risk of cancer in humans. *Carcinogenesis*, **28**, 625-631.
6. Guo, X., Ni, J., Liang, Z., Xue, J., Fenech, M.F., and Wang, X. (2019) The molecular origins and pathophysiological consequences of micronuclei: New insights into an age-old problem. *Mutation Research/Reviews in Mutation Research*, **779**, 1-35.
7. Deo, P., Fenech, M., and Dhillon, V.S. (2021) Association between glycation biomarkers, hyperglycemia, and micronucleus frequency: A meta -analysis. *Mutation Research/Reviews in Mutation Research*, **787**.
8. Kirsch-Volders, M., Bolognesi, C., Ceppi, M., Bruzzone, M., and Fenech, M. (2020) Micronuclei, inflammation and auto-immune disease. *Mutation Research*, **786**, 108335.
9. Shaik, N.A., Shaik, J.P., Ali, S., Imran, A., and Rao, D.K. (2010) Increased frequency of micronuclei in diabetes mellitus patients using pioglitazone and glimepiride in combination. *Food and Chemical Toxicology*, **48**, 3432-3435.
10. Shettigar, S.K., Shailaja, C., and Kulkarni, R.K. (2012) Elevated micronuclei frequency in type 2 diabetes with high glycosylated hemoglobin. *Diabetes Research and Clinical Practice*, **95**, 246-250.
11. Pereira, C.S., Molz, P., Palazzo, R.P., de Freitas, T.A., Maluf, S.W., Horta, J.A., Pra, D., and Franke, S.I. (2013) DNA damage and cytotoxicity in adult subjects with prediabetes. *Mutation Research*, **753**, 76-81.
12. Lazalde-Ramos, B.P., Zamora-Perez, A.L., Sosa-Macias, M., Guerrero-Velazquez, C., and Zuniga-Gonzalez, G.M. (2012) DNA and oxidative damages decrease after ingestion of folic acid in patients with type 2 diabetes. *Archives of Medical Research*, **43**, 476-481.
13. Waris, S., Winklhofer-Roob, B.M., Roob, J.M., Fuchs, S., Sourij, H., Rabbani, N., and Thornalley, P.J. (2015) Increased DNA dicarbonyl glycation and oxidation markers in patients with type 2 diabetes and link to diabetic nephropathy. *Journal of Diabetes Research*, **2015**, 915486.
14. Salimi, M., Broumand, B., and Mozdarani, H. (2016) Association of elevated frequency of micronuclei in peripheral blood lymphocytes of type 2 diabetes patients with nephropathy complications. *Mutagenesis*, **31**, 627-633.
15. Schalkwijk, C.G., and Stehouwer, C.D.A. (2020) Methylglyoxal, a Highly Reactive Dicarbonyl Compound, in Diabetes, Its Vascular Complications, and Other Age-Related Diseases. *Physiological Reviews*, **100**, 407-461.
16. Thornalley, P.J., Battah, S., Ahmed, N., Karachalias, N., Agalou, S., Babaei-Jadidi, R., and Dawnay, A. (2003) Quantitative screening of advanced glycation endproducts in cellular and extracellular proteins by tandem mass spectrometry. *Biochemical Journal*, **375**, 581-592.
17. Murgia, E., Ballardin, M., Bonassi, S., Rossi, A.M., and Barale, R. (2008) Validation of micronuclei frequency in peripheral blood lymphocytes as early cancer risk biomarker in a nested case-control study. *Mutation Research*, **639**, 27-34.
18. Murgia, E., Maggini, V., Barale, R., and Rossi, A.M. (2007) Micronuclei, genetic polymorphisms and cardiovascular disease mortality in a nested case-control study in Italy. *Mutation Research*, **621**, 113-118.

19. Federici, C., Botto, N., Manfredi, S., Rizza, A., Del Fiandra, M., and Andreassi, M.G. (2008) Relation of increased chromosomal damage to future adverse cardiac events in patients with known coronary artery disease. *The American Journal of Cardiology*, **102**, 1296-1300.
20. Furness, D.L., Dekker, G.A., Hague, W.M., Khong, T.Y., and Fenech, M.F. (2010) Increased lymphocyte micronucleus frequency in early pregnancy is associated prospectively with pre-eclampsia and/or intrauterine growth restriction. *Mutagenesis*, **25**, 489-498.
21. Fenech, M., Knasmueller, S., Bolognesi, C., Bonassi, S., Holland, N., Migliore, L., Palitti, F., Natarajan, A.T., and Kirsch-Volders, M. (2016) Molecular mechanisms by which in vivo exposure to exogenous chemical genotoxic agents can lead to micronucleus formation in lymphocytes in vivo and ex vivo in humans. *Mutation Research*, **770**, 12-25.
22. Liu, S., and Pellman, D. (2020) The coordination of nuclear envelope assembly and chromosome segregation in metazoans. *Nucleus*, **11**, 35-52.
23. Krupina, K., Goginashvili, A., and Cleveland, D.W. (2021) Causes and consequences of micronuclei. *Current Opinions in Cell Biology*, **70**, 91-99.
24. Thompson, S.L., and Compton, D.A. (2011) Chromosome missegregation in human cells arises through specific types of kinetochore-microtubule attachment errors. *Proceedings of the National Academy of Sciences*, **108**, 17974-17978.
25. Kops, G.J., Foltz, D.R., and Cleveland, D.W. (2004) Lethality to human cancer cells through massive chromosome loss by inhibition of the mitotic checkpoint. *Proceedings of the National Academy of Sciences*, **101**, 8699-8704.
26. McAinsh, A.D. (2014) How Kinetochores CCAN resist force. *Developmental Cell*, **30**, 637-638.
27. Hoffmann, S., Dumont, M., Barra, V., Ly, P., Nechemia-Arbely, Y., McMahon, M.A., Herve, S., Cleveland, D.W., and Fachinetti, D. (2016) CENP-A Is Dispensable for Mitotic Centromere Function after Initial Centromere/Kinetochore Assembly. *Cell Reports*, **17**, 2394-2404.
28. Westhorpe, F.G., and Straight, A.F. (2013) Functions of the centromere and kinetochore in chromosome segregation. *Current Opinion in Cell Biology*, **25**, 334-340.
29. DeLuca, J.G., Moree, B., Hickey, J.M., Kilmartin, J.V., and Salmon, E.D. (2002) hNuf2 inhibition blocks stable kinetochore-microtubule attachment and induces mitotic cell death in HeLa cells. *Journal of Cell Biology*, **159**, 549-555.
30. DeLuca, J.G., Dong, Y., Hergert, P., Strauss, J., Hickey, J.M., Salmon, E., and McEwen, B.F. (2005) Hec1 and nuf2 are core components of the kinetochore outer plate essential for organizing microtubule attachment sites. *Molecular biology of the cell*, **16**, 519-531.
31. Zhang, W., Mao, J.H., Zhu, W., Jain, A.K., Liu, K., Brown, J.B., and Karpen, G.H. (2016) Centromere and kinetochore gene misexpression predicts cancer patient survival and response to radiotherapy and chemotherapy. *Nature Communications*, **7**, 12619.
32. Thompson, S.L., Bakhoum, S.F., and Compton, D.A. (2010) Mechanisms of chromosomal instability. *Current Biology*, **20**, R285-295.
33. Quintyne, N.J., Reing, J.E., Hoffelder, D.R., Gollin, S.M., and Saunders, W.S. (2005) Spindle multipolarity is prevented by centrosomal clustering. *Science*, **307**, 127-129.
34. Ouyang, X., Wang, X., Xu, K., Jin, D.-Y., Cheung, A.L.M., Tsao, S.W., and Wong, Y.C. (2001) Effect of p53 on centrosome amplification in prostate cancer cells. *Biochimica et Biophysica Acta (BBA) - Molecular Cell Research*, **1541**, 212-220.
35. Mehta, G.D., Kumar, R., Srivastava, S., and Ghosh, S.K. (2013) Cohesin: functions beyond sister chromatid cohesion. *FEBS Letters*, **587**, 2299-2312.
36. Zhang, J., Shi, X., Li, Y., Kim, B.J., Jia, J., Huang, Z., Yang, T., Fu, X., Jung, S.Y., Wang, Y., Zhang, P., Kim, S.T., Pan, X., and Qin, J. (2008) Acetylation of Smc3 by Eco1 is required for S phase sister chromatid cohesion in both human and yeast. *Molecular Cell*, **31**, 143-151.
37. Hauf, S., Waizenegger, I.C., and Peters, J.M. (2001) Cohesin cleavage by separase required for anaphase and cytokinesis in human cells. *Science*, **293**, 1320-1323.
38. Jallepalli, P.V., Waizenegger, I.C., Bunz, F., Langer, S., Speicher, M.R., Peters, J.-M., Kinzler, K.W., Vogelstein, B., and Lengauer, C. (2001) Securin Is Required for Chromosomal Stability in Human Cells. *Cell*, **105**, 445-457.
39. Zur, A., and Brandeis, M. (2001) Securin degradation is mediated by fzy and fzr, and is required for complete chromatid separation but not for cytokinesis. *The EMBO journal*, **20**, 792-801.
40. Dianov, G.L., Timehenko, T.V., Sinitsina, O.I., Kuzminov, A.V., Medvedev, O.A., and Salganik, R.I. (1991) Repair of uracil residues closely spaced on the opposite strands of plasmid

DNA results in double-strand break and deletion formation. *Molecular General Genetics* **225**, 448-452.
41. Fenech, M., and Neville, S. (1992) Conversion of excision-repairable DNA lesions to micronuclei within one cell cycle in human lymphocytes. *Environmental Molecular Mutagenesis*, **19**, 27-36.
42. Zhang, C.Z., Spektor, A., Cornils, H., Francis, J.M., Jackson, E.K., Liu, S., Meyerson, M., and Pellman, D. (2015) Chromothripsis from DNA damage in micronuclei. *Nature*, **522**, 179-184.
43. Liu, S., Kwon, M., Mannino, M., Yang, N., Renda, F., Khodjakov, A., and Pellman, D. (2018) Nuclear envelope assembly defects link mitotic errors to chromothripsis. *Nature*, **561**, 551-555.
44. Pantelias, A., Karachristou, I., Georgakilas, A.G., and Terzoudi, G.I. (2019) Interphase Cytogenetic Analysis of Micronucleated and Multinucleated Cells Supports the Premature Chromosome Condensation Hypothesis as the Mechanistic Origin of Chromothripsis. *Cancers (Basel)*, **11**.
45. Mackenzie, K.J., Carroll, P., Martin, C.A., Murina, O., Fluteau, A., Simpson, D.J., Olova, N., Sutcliffe, H., Rainger, J.K., Leitch, A., Osborn, R.T., Wheeler, A.P., Nowotny, M., Gilbert, N., Chandra, T., Reijns, M.A.M., and Jackson, A.P. (2017) cGAS surveillance of micronuclei links genome instability to innate immunity. *Nature*, **548**, 461-465.
46. Sun, L., Wu, J., Du, F., Chen, X., and Chen, Z.J. (2013) Cyclic GMP-AMP Synthase Is a Cytosolic DNA Sensor That Activates the Type I Interferon Pathway. *Science*, **339**, 786-791.
47. Fenech, M., Knasmueller, S., Bolognesi, C., Holland, N., Bonassi, S., and Kirsch-Volders, M. (2020) Micronuclei as biomarkers of DNA damage, aneuploidy, inducers of chromosomal hypermutation and as sources of pro-inflammatory DNA in humans. *Mutation Research/Reviews in Mutation Research*, **786**.
48. Fenech, M. (2007) Cytokinesis-block micronucleus cytome assay. *Nature Protocols*, **2**, 1084-1104.
49. Thomas, P., Umegaki, K., and Fenech, M. (2003) Nucleoplasmic bridges are a sensitive measure of chromosome rearrangement in the cytokinesis-block micronucleus assay. *Mutagenesis*, **18**, 187-194.
50. Lindberg, H.K., Wang, X., Jarventaus, H., Falck, G.C., Norppa, H., and Fenech, M. (2007) Origin of nuclear buds and micronuclei in normal and folate-deprived human lymphocytes. *Mutation Research*, **617**, 33-45.
51. Fenech, M., and Crott, J.W. (2002) Micronuclei, nucleoplasmic bridges and nuclear buds induced in folic acid deficient human lymphocytes—evidence for breakage–fusion-bridge cycles in the cytokinesis-block micronucleus assay. *Mutation Research/Fundamental Molecular Mechanisms of Mutagenesis*, **504**, 131-136.
52. Phillips, S.A., and Thornalley, P.J. (1993) The formation of methylglyoxal from triose phosphates: investigation using a specific assay for methylglyoxal. *European Journal of Biochemistry*, **212**, 101-105.
53. Thornalley, P.J. (1988) Modification of the glyoxalase system in human red blood cells by glucose in vitro. *Biochemical Journal*, **254**, 751-755.
54. Irshad, Z., Xue, M., Ashour, A., Larkin, J.R., Thornalley, P.J., and Rabbani, N. (2019) Activation of the unfolded protein response in high glucose treated endothelial cells is mediated by methylglyoxal. *Scientific Reports*, **9**, 7889.
55. Luengo, A., Abbott, K.L., Davidson, S.M., Hosios, A.M., Faubert, B., Chan, S.H., Freinkman, E., Zacharias, L.G., Mathews, T.P., Clish, C.B., DeBerardinis, R.J., Lewis, C.A., and Vander Heiden, M.G. (2019) Reactive metabolite production is a targetable liability of glycolytic metabolism in lung cancer. *Nature Communications*, **10**, 5604.
56. Qi, W., Keenan, H.A., Li, Q., Ishikado, A., Kannt, A., Sadowski, T., Yorek, M.A., Wu, I.H., Lockhart, S., Coppey, L.J., Pfenninger, A., Liew, C.W., Qiang, G., Burkart, A.M., Hastings, S., Pober, D., Cahill, C., Niewczas, M.A., Israelsen, W.J., Tinsley, L., Stillman, I.E., Amenta, P.S., Feener, E.P., Vander Heiden, M.G., Stanton, R.C., and King, G.L. (2017) Pyruvate kinase M2 activation may protect against the progression of diabetic glomerular pathology and mitochondrial dysfunction. *Nature Medicine*, **23**, 753-762.
57. Bird, M.I., Nunn, P.B., and Lord, L.A. (1984) Formation of glycine and aminoacetone from L-threonine by rat liver mitochondria. *Biochimica et Biophysica Acta*, **802**, 229-236.
58. Lyles, G.A., and Chalmers, J. (1992) The metabolism of aminoacetone to methylglyoxal by semicarbazide-sensitive amine oxidase in human umbilical artery. *Biochemical pharmacology*, **43**, 1409-1414.

59. Kazachkov, M., and Yu, P.H. (2005) A novel HPLC procedure for detection and quantification of aminoacetone, a precursor of methylglyoxal, in biological samples. *Journal of Chromatography B*, **824**, 116-122.
60. Stolen, C.M., Yegutkin, G.G., Kurkijarvi, R., Bono, P., Alitalo, K., and Jalkanen, S. (2004) Origins of serum semicarbazide-sensitive amine oxidase. *Circulation Research*, **95**, 50-57.
61. Reichard, G.A., Skutches, C.L., Hoeldtke, R.D., and Owen, O.E. (1986) Acetone Metabolism in Humans During Diabetic Ketoacidosis. *Diabetes*, **35**, 668-674.
62. Balasse, E.O. (1979) Kinetics of ketone body metabolism in fasting humans. *Metabolism*, **28**, 41-50.
63. Magee, M.S., Knopp, R.H., and Benedetti, T.J. (1990) Metabolic Effects of 1200-kcal Diet in Obese Pregnant Women With Gestational Diabetes. *Diabetes*, **39**, 234-240.
64. Schumacher, D., Morgenstern, J., Oguchi, Y., Volk, N., Kopf, S., Groener, J.B., Nawroth, P.P., Fleming, T., and Freichel, M. (2018) Compensatory mechanisms for methylglyoxal detoxification in experimental & clinical diabetes. *Molecular Metabolism*, **18**, 143-152.
65. Racker, E. (1951) The mechanism of action of glyoxalase. *Journal of Biological Chemistry*, **190**, 685-696.
66. Rabbani, N., and Thornalley, P.J. (2015) Dicarbonyl stress in cell and tissue dysfunction contributing to ageing and disease. *Biochemical and Biophysical Research Communications*, **458**, 221-226.
67. Abordo, E.A., Minhas, H.S., and Thornalley, P.J. (1999) Accumulation of α-oxoaldehydes during oxidative stress: a role in cytotoxicity. *Biochemical Pharmacology*, **58**, 641-648.
68. Wang, T., Streeter, M.D., and Spiegel, D.A. (2015) Generation and characterization of antibodies against arginine-derived advanced glycation endproducts. *Bioorganic & Medicinal Chemistry Letters*, **25**, 4881-4886.
69. Galligan, J.J., Wepy, J.A., Streeter, M.D., Kingsley, P.J., Mitchener, M.M., Wauchope, O.R., Beavers, W.N., Rose, K.L., Wang, T., Spiegel, D.A., and Marnett, L.J. (2018) Methylglyoxal-derived posttranslational arginine modifications are abundant histone marks. *Proceedings of the National Academy of Sciences of the United States of America*, **115**, 9228-9233.
70. Shipanova, I.N., Glomb, M.A., and Nagaraj, R.H. (1997) Protein modification by methylglyoxal: chemical nature and synthetic mechanism of a major fluorescent adduct. *Archives of biochemistry and biophysics*, **344**, 29-36.
71. Bollong, M.J., Lee, G., Coukos, J.S., Yun, H., Zambaldo, C., Chang, J.W., Chin, E.N., Ahmad, I., Chatterjee, A.K., Lairson, L.L., Schultz, P.G., and Moellering, R.E. (2018) A metabolite-derived protein modification integrates glycolysis with KEAP1-NRF2 signalling. *Nature*, **562**, 600-604.
72. Sabbasani, V.R., Wang, K.P., Streeter, M.D., and Spiegel, D.A. (2019) One-Step Synthesis of 2,5-Diaminoimidazoles and Total Synthesis of Methylglyoxal-Derived Imidazolium Crosslink (MODIC). *Angewandte Chemie*, **58**, 18913-18917.
73. Hodge, J.E. (1955) The Amadori rearrangement. *Advances in carbohydrate chemistry*, **10**, 169-205.
74. Rabbani, N., and Thornalley, P.J. (2012) Glycation research in amino acids: a place to call home. *Amino Acids*, **42**, 1087-1096.
75. Richarme, G., Mihoub, M., Dairou, J., Bui, L.C., Leger, T., and Lamouri, A. (2015) Parkinsonism-associated protein DJ-1/Park7 is a major protein deglycase that repairs methylglyoxal- and glyoxal-glycated cysteine, arginine, and lysine residues. *Journal of Biological Chemistry*, **290**, 1885-1897.
76. Richarme, G., and Dairou, J. (2017) Parkinsonism-associated protein DJ-1 is a bona fide deglycase. *Biochemical and Biophysical Research Communications*, **483**, 387-391.
77. Zheng, Q., Osunsade, A., and David, Y. (2020) Protein arginine deiminase 4 antagonizes methylglyoxal-induced histone glycation. *Nature Communications*, **11**, 3241.
78. Jun, Y.W., and Kool, E.T. (2020) Small Substrate or Large? Debate Over the Mechanism of Glycation Adduct Repair by DJ-1. *Cell Chemical Biology*.
79. Richarme, G., Abdallah, J., Mathas, N., Gautier, V., and Dairou, J. (2018) Further characterization of the Maillard deglycase DJ-1 and its prokaryotic homologs, deglycase 1/Hsp31, deglycase 2/YhbO, and deglycase 3/YajL. *Biochemical and Biophysical Research Communications*, **503**, 703-709.
80. Zheng, Q., Omans, N.D., Leicher, R., Osunsade, A., Agustinus, A.S., Finkin-Groner, E., D'Ambrosio, H., Liu, B., Chandarlapaty, S., Liu, S., and David, Y. (2019) Reversible histone

glycation is associated with disease-related changes in chromatin architecture. *Nature Communications*, **10**, 1289.
81. Rabbani, N., and Thornalley, P.J. (2014) Dicarbonyl proteome and genome damage in metabolic and vascular disease. *Biochemical Society Transactions*, **42**, 425-432.
82. Ahmed, N., Dobler, D., Dean, M., and Thornalley, P.J. (2005) Peptide mapping identifies hotspot site of modification in human serum albumin by methylglyoxal involved in ligand binding and esterase activity. *Journal of Biological Chemistry*, **280**, 5724-5732.
83. Rabbani, N., Xue, M., and Thornalley, P.J. (2021) Dicarbonyl stress, protein glycation and the unfolded protein response. *Glycoconjugate Journal*, **38**, 331-340.
84. Meuzelaar, H., Vreede, J., and Woutersen, S. (2016) Influence of Glu/Arg, Asp/Arg, and Glu/Lys Salt Bridges on alpha-Helical Stability and Folding Kinetics. *Biophysical Journal*, **110**, 2328-2341.
85. Fredrickson, E.K., Rosenbaum, J.C., Locke, M.N., Milac, T.I., and Gardner, R.G. (2011) Exposed hydrophobicity is a key determinant of nuclear quality control degradation. *Molecular Biology of the Cell*, **22**, 2384-2395.
86. McEwen, J.M., Fraser, S., Guir, A.L.S., Dave, J., and Scheck, R.A. (2021) Synergistic sequence contributions bias glycation outcomes. *Nature Communications*, **12**, 3316.
87. Ceradini, D.J., Yao, D., Grogan, R.H., Callaghan, M.J., Edelstein, D., Brownlee, M., and Gurtner, G.C. (2008) Decreasing intracellular superoxide corrects defective ischemia-induced new vessel formation in diabetic mice. *Journal of Biololgical Chemistry*, **283**, 10930-10938.
88. Bento, C.F., Fernandes, R., Ramalho, J., Marques, C., Shang, F., Taylor, A., and Pereira, P. (2010) The chaperone-dependent ubiquitin ligase CHIP targets HIF-1alpha for degradation in the presence of methylglyoxal. *PLoS One*, **5**, e15062.
89. Kansanen, E., Kuosmanen, S.M., Leinonen, H., and Levonen, A.L. (2013) The Keap1-Nrf2 pathway: Mechanisms of activation and dysregulation in cancer. *Redox Biology*, **1**, 45-49.
90. Xue, M., Weickert, M.O., Qureshi, S., Kandala, N.-B., Anwar, A., Waldron, M., Shafie, A., Messenger, D., Fowler, M., Jenkins, G., Rabbani, N., and Thornalley, P.J. (2016) Improved glycemic control and vascular function in overweight and obese subjects by glyoxalase 1 inducer formulation. *Diabetes*, **65**, 2282-2294.
91. Huang, H., Lin, S., Garcia, B.A., and Zhao, Y. (2015) Quantitative proteomic analysis of histone modifications. *Chemical Reviews*, **115**, 2376-2418.
92. Maksimovic, I., and David, Y. (2021) Non-enzymatic Covalent Modifications as a New Chapter in the Histone Code. *Trends in Biochemical Sciences*, **46**, 718-730.
93. Fuhrmann, J., and Thompson, P.R. (2016) Protein Arginine Methylation and Citrullination in Epigenetic Regulation. *ACS Chemical Biology*, **11**, 654-668.
94. Lee, S.E., Yang, H., Jeong, S.I., Jin, Y.-H., Park, C.-S., and Park, Y.S. (2011) Methylglyoxal-mediated alteration of gene expression in human endothelial cells. *BioChip Journal*, **5**, 220-228.
95. Gaffney, D.O., Jennings, E.Q., Anderson, C.C., Marentette, J.O., Shi, T., Schou Oxvig, A.M., Streeter, M.D., Johannsen, M., Spiegel, D.A., Chapman, E., Roede, J.R., and Galligan, J.J. (2020) Non-enzymatic Lysine Lactoylation of Glycolytic Enzymes. *Cell Chemical Biology*, **27**, 206-213 e206.
96. Thornalley, P.J., and Rabbani, N. (2014) Detection of oxidized and glycated proteins in clinical samples using mass spectrometry--a user's perspective. *Biochimica et Biophysica Acta*, **1840**, 818-829.
97. Ahmed, N., Argirov, O.K., Minhas, H.S., Cordeiro, C.A., and Thornalley, P.J. (2002) Assay of advanced glycation endproducts (AGEs): surveying AGEs by chromatographic assay with derivatization by 6-aminoquinolyl-N-hydroxysuccinimidyl-carbamate and application to Nepsilon-carboxymethyl-lysine- and Nepsilon-(1-carboxyethyl)lysine-modified albumin. *Biochemical Journal*, **364**, 1-14.
98. Poojary, M.M., Zhang, W., Greco, I., De Gobba, C., Olsen, K., and Lund, M.N. (2020) Liquid chromatography quadrupole-Orbitrap mass spectrometry for the simultaneous analysis of advanced glycation end products and protein-derived cross-links in food and biological matrices. *Journal of Chromatography A*, **1615**, 460767.
99. Scheijen, J., Clevers, E., Engelen, L., Dagnelie, P.C., Brouns, F., Stehouwer, C.D.A., and Schalkwijk, C.G. (2016) Analysis of advanced glycation endproducts in selected food items by ultra-performance liquid chromatography tandem mass spectrometry: Presentation of a dietary AGE database. *Food Chemistry*, **190**, 1145-1150.

100. Legrand, C., Ahmed, U., Anwar, A., Rajpoot, K., Pasha, S., Lambert, C., Davidson, R.K., Clark, I.M., Thornalley, P.J., Henrotin, Y., and Rabbani, N. (2018) Glycation marker glucosepane increases with the progression of osteoarthritis and correlates with morphological and functional changes of cartilage in vivo. *Arthritis Research & Therapy*, **20**, 131.
101. Masania, J., Faustmann, G., Anwar, A., Hafner-Giessauf, H., Rajpoot, N., Grabher, J., Rajpoot, K., Tiran, B., Obermayer-Pietsch, B., Winklhofer-Roob, B.M., Roob, J.M., Rabbani, N., and Thornalley, P.J. (2019) Urinary Metabolomic Markers of Protein Glycation, Oxidation, and Nitration in Early-Stage Decline in Metabolic, Vascular, and Renal Health. *Oxidative Medicine and Cellular Longevity*, **2019**, 4851323.
102. Martens, R.J.H., Broers, N.J.H., Canaud, B., Christiaans, M.H.L., Cornelis, T., Gauly, A., Hermans, M.M.H., Konings, C., van der Sande, F.M., Scheijen, J., Stifft, F., Wirtz, J., Kooman, J.P., and Schalkwijk, C.G. (2019) Relations of advanced glycation endproducts and dicarbonyls with endothelial dysfunction and low-grade inflammation in individuals with end-stage renal disease in the transition to renal replacement therapy: A cross-sectional observational study. *PLoS One*, **14**, e0221058.
103. Rabbani, N., Shaheen, F., Anwar, A., Masania, J., and Thornalley, P.J. (2014) Assay of methylglyoxal-derived protein and nucleotide AGEs. *Biochemical Society Transactions*, **42**, 511-517.
104. Rabbani, N., Ashour, A., and Thornalley, P.J. (2016) Mass spectrometric determination of early and advanced glycation in biology. *Glycoconjugate Journal*, **33**, 553-568.
105. Galligan, J.J., Kingsley, P.J., Wauchope, O.R., Mitchener, M.M., Camarillo, J.M., Wepy, J.A., Harris, P.S., Fritz, K.S., and Marnett, L.J. (2017) Quantitative Analysis and Discovery of Lysine and Arginine Modifications. *Analytical Chemistry*, **89**, 1299-1306.
106. Aebersold, R., and Mann, M. (2003) Mass spectrometry-based proteomics. *Nature*, **422**, 198-207.
107. Giansanti, P., Tsiatsiani, L., Low, T.Y., and Heck, A.J. (2016) Six alternative proteases for mass spectrometry-based proteomics beyond trypsin. *Nature Protocols*, **11**, 993-1006.
108. Ashour, A., Xue, M., Al-Motawa, M., Thornalley, P.J., and Rabbani, N. (2020) Glycolytic overload-driven dysfunction of periodontal ligament fibroblasts in high glucose concentration, corrected by glyoxalase 1 inducer. *BMJ Open Diabetes Research & Care*, **8**.
109. Alhujaily, M., Abbas, H., Xue, M., de la Fuente, A., Rabbani, N., and Thornalley, P.J. (2021) Studies of Glyoxalase 1-Linked Multidrug Resistance Reveal Glycolysis-Derived Reactive Metabolite, Methylglyoxal, Is a Common Contributor in Cancer Chemotherapy Targeting the Spliceosome. *Frontiers in Oncology*, **11**.
110. Di Sanzo, S., Spengler, K., Leheis, A., Kirkpatrick, J.M., Randler, T.L., Baldensperger, T., Dau, T., Henning, C., Parca, L., Marx, C., Wang, Z.Q., Glomb, M.A., Ori, A., and Heller, R. (2021) Mapping protein carboxymethylation sites provides insights into their role in proteostasis and cell proliferation. *Nature Communications*, **12**, 6743.
111. Degani, G., Altomare, A.A., Colzani, M., Martino, C., Mazzolari, A., Fritz, G., Vistoli, G., Popolo, L., and Aldini, G. (2017) A capture method based on the VC1 domain reveals new binding properties of the human receptor for advanced glycation end products (RAGE). *Redox Biol*, **11**, 275-285.
112. Paudel, G., Bilova, T., Schmidt, R., Greifenhagen, U., Berger, R., Tarakhovskaya, E., Stockhardt, S., Balcke, G.U., Humbeck, K., Brandt, W., Sinz, A., Vogt, T., Birkemeyer, C., Wessjohann, L., and Frolov, A. (2016) Osmotic stress is accompanied by protein glycation in Arabidopsis thaliana. *Journal of Experimental Botany*, **67**, 6283-6295.
113. Meier, F., Park, M.A., and Mann, M. (2021) Trapped Ion Mobility Spectrometry and Parallel Accumulation-Serial Fragmentation in Proteomics. *Mol Cell Proteomics*, **20**, 100138.
114. Gomez, J.D., Ridgeway, M.E., Park, M.A., and Fritz, K.S. (2018) Utilizing Ion Mobility to Identify Isobaric Post-Translational Modifications: Resolving Acrolein and Propionyl Lysine Adducts by TIMS Mass Spectrometry. *International journal for ion mobility spectrometry*, **21**, 65-69.
115. Hebert, A.S., Prasad, S., Belford, M.W., Bailey, D.J., McAlister, G.C., Abbatiello, S.E., Huguet, R., Wouters, E.R., Dunyach, J.J., Brademan, D.R., Westphall, M.S., and Coon, J.J. (2018) Comprehensive Single-Shot Proteomics with FAIMS on a Hybrid Orbitrap Mass Spectrometer. *Analytical Chemistry*, **90**, 9529-9537.

116. Schmidt, R., Bohme, D., Singer, D., and Frolov, A. (2015) Specific tandem mass spectrometric detection of AGE-modified arginine residues in peptides. *Journal of Mass Spectrometry*, **50**, 613-624.
117. Shapiro, R., Cohen, B.I., Shiuey, S.-J., and Maurer, H. (1969) Reaction of guanine with glyoxal, pyruvaldehyde, and kethoxal, and the structure of the acylguanines. Synthesis of N2-alkylguanines. *Biochemistry*, **8**, 238-245.
118. Frischmann, M., Bidmon, C., Angerer, J., and Pischetsrieder, M. (2005) Identification of DNA adducts of methylglyoxal. *Chemical Research in Toxicology*, **18**, 1586-1592.
119. Shuck, S.C., Wuenschell, G.E., and Termini, J.S. (2018) Product Studies and Mechanistic Analysis of the Reaction of Methylglyoxal with Deoxyguanosine. *Chemical Research in Toxicolology*, **31**, 105-115.
120. Schneider, M., Quistad, G.B., and Casida, J.E. (1998) N 2, 7-Bis (1-hydroxy-2-oxopropyl)-2 '-deoxyguanosine: Identical Noncyclic Adducts with 1, 3-Dichloropropene Epoxides and Methylglyoxal. *Chemical Research in Toxicology*, **11**, 1536-1542.
121. Ochs, S., and Severin, T. (1994) Reaction of 2′-Deoxyguanosine with Glyceraldehyde. *Liebigs Annalen der Chemie*, **1994**, 851-853.
122. Minton, A.P. (2001) The influence of macromolecular crowding and macromolecular confinement on biochemical reactions in physiological media. *Journal of Biological Chemistry*, **276**, 10577-10580.
123. Thornalley, P.J., Waris, S., Fleming, T., Santarius, T., Larkin, S.J., Winklhofer-Roob, B.M., Stratton, M.R., and Rabbani, N. (2010) Imidazopurinones are markers of physiological genomic damage linked to DNA instability and glyoxalase 1-associated tumour multidrug resistance. *Nucleic Acids Research*, **38**, 5432-5442.
124. Jaramillo, R., Shuck, S.C., Chan, Y.S., Liu, X., Bates, S.E., Lim, P.P., Tamae, D., Lacoste, S., O'Connor, T.R., and Termini, J. (2017) DNA advanced glycation end products (DNA-AGEs) are elevated in urine and tissue in an animal model of type 2 diabetes. *Chemical Research in Toxicology*, **30**, 689-698.
125. Synold, T., Xi, B., Wuenschell, G.E., Tamae, D., Figarola, J.L., Rahbar, S., and Termini, J. (2008) Advanced glycation end products of DNA: quantification of N 2-(1-carboxyethyl)-2′-deoxyguanosine in biological samples by liquid chromatography electrospray ionization tandem mass spectrometry. *Chemical Research in Toxicology*, **21**, 2148-2155.
126. Pischetsrieder, M., Seidel, W., Münch, G., and Schinzel, R. (1999) N2-(1-carboxyethyl) deoxyguanosine, a nonenzymatic glycation adduct of DNA, induces single-strand breaks and increases mutation frequencies. *Biochemical and Biophysical Research Communications*, **264**, 544-549.
127. Tamae, D., Lim, P., Wuenschell, G.E., and Termini, J. (2011) Mutagenesis and repair induced by the DNA advanced glycation end product N2-1-(carboxyethyl)-2'-deoxyguanosine in human cells. *Biochemistry*, **50**, 2321-2329.
128. Wuenschell, G.E., Tamae, D., Cercillieux, A., Yamanaka, R., Yu, C., and Termini, J. (2010) Mutagenic potential of DNA glycation: miscoding by (R)- and (S)-N2-(1-carboxyethyl)-2'-deoxyguanosine. *Biochemistry*, **49**, 1814-1821.
129. Petrova, K.V., Millsap, A.D., Stec, D.F., and Rizzo, C.J. (2014) Characterization of the deoxyguanosine-lysine cross-link of methylglyoxal. *Chemical Research in Toxicolology*, **27**, 1019-1029.
130. Morgenstern, J., Katz, S., Krebs-Haupenthal, J., Chen, J., Saadatmand, A., Cortizo, F.G., Moraru, A., Zemva, J., Campos, M.C., Teleman, A., Backs, J., Nawroth, P., and Fleming, T. (2020) Phosphorylation of T107 by CamKIIδ Regulates the Detoxification Efficiency and Proteomic Integrity of Glyoxalase 1. *Cell Reports*, **32**.
131. Clare, C.E., Brassington, A.H., Kwong, W.Y., and Sinclair, K.D. (2019) One-Carbon Metabolism: Linking Nutritional Biochemistry to Epigenetic Programming of Long-Term Development. *Annual Review of Animal Biosciences*, **7**, 263-287.
132. Rébeillé, F., Ravanel, S., Jabrin, S., Douce, R., Storozhenko, S., and Van Der Straeten, D. (2006) Folates in plants: biosynthesis, distribution, and enhancement. *Physiologia Plantarum*, **126**, 330-342.
133. Courtemanche, C., Huang, A.C., Elson-Schwab, I., Kerry, N., Ng, B.Y., and Ames, B.N. (2004) Folate deficiency and ionizing radiation cause DNA breaks in primary human lymphocytes: a comparison. *The FASEB journal*, **18**, 209-211.

134. Fenech, M.F. (2010) Dietary reference values of individual micronutrients and nutriomes for genome damage prevention: current status and a road map to the future. *American Journal of Clinical Nutrition*, **91**, 1438S-1454S.
135. MacGregor, J.T., Wehr, C.M., Hiatt, R.A., Peters, B., Tucker, J.D., Langlois, R.G., Jacob, R.A., Jensen, R.H., Yager, J.W., Shigenaga, M.K., Frei, B., Eynon, B.P., and Ames, B.N. (1997) 'Spontaneous' genetic damage in man: evaluation of interindividual variability, relationship among markers of damage, and influence of nutritional status. *Mutation Research*, **377**, 125-135.
136. Beetstra, S., Thomas, P., Salisbury, C., Turner, J., and Fenech, M. (2005) Folic acid deficiency increases chromosomal instability, chromosome 21 aneuploidy and sensitivity to radiation-induced micronuclei. *Mutation Research*, **578**, 317-326.
137. Kim, Y.I., Pogribny, I.P., Basnakian, A.G., Miller, J.W., Selhub, J., James, S.J., and Mason, J.B. (1997) Folate deficiency in rats induces DNA strand breaks and hypomethylation within the p53 tumor suppressor gene. *American Journal of Clinical Nutrition*, **65**, 46-52.
138. Blount, B.C., Mack, M.M., Wehr, C.M., MacGregor, J.T., Hiatt, R.A., Wang, G., Wickramasinghe, S.N., Everson, R.B., and Ames, B.N. (1997) Folate deficiency causes uracil misincorporation into human DNA and chromosome breakage: implications for cancer and neuronal damage. *Proceedings of the National Academy of Sciences*, **94**, 3290-3295.
139. Guo, X., Ni, J., Zhu, Y., Zhou, T., Ma, X., Xue, J., and Wang, X. (2017) Folate deficiency induces mitotic aberrations and chromosomal instability by compromising the spindle assembly checkpoint in cultured human colon cells. *Mutagenesis*, **32**, 547-560.
140. Bull, C.F., Mayrhofer, G., Zeegers, D., Mun, G.L., Hande, M.P., and Fenech, M.F. (2012) Folate deficiency is associated with the formation of complex nuclear anomalies in the cytokinesis-block micronucleus cytome assay. *Environmental and Molecular Mutagenisis*, **53**, 311-323.
141. Bull, C.F., Mayrhofer, G., O'Callaghan, N.J., Au, A.Y., Pickett, H.A., Low, G.K., Zeegers, D., Hande, M.P., and Fenech, M.F. (2014) Folate deficiency induces dysfunctional long and short telomeres; both states are associated with hypomethylation and DNA damage in human WIL2-NS cells. *Cancer Prevention Research* **7**, 128-138.
142. Guo, X., Dai, X., Ni, J., Cao, N., Yang, G., Xue, J., and Wang, X. (2019) High concentration of sugars is genotoxic to folate-deficient cells. *Mutation Research*, **814**, 15-22.
143. Marzio, A., Merigliano, C., Gatti, M., and Verni, F. (2014) Sugar and chromosome stability: clastogenic effects of sugars in vitamin B6-deficient cells. *PLoS Genetics*, **10**, e1004199.

2 Chapter 2. Methylglyoxal induces chromosomal instability and mitotic dysfunction in lymphocytes

The information presented in this Chapter is reproduced from an article published in Mutagenesis:

Donnellan, L., Simpson, B., Dhillon, V.S., Costabile, M., Fenech, M. and Deo, P., 2021. Methylglyoxal induces chromosomal instability and mitotic dysfunction in lymphocytes. *Mutagenesis*, *36*(5), pp.339-348. 10.1093/mutage/geab028

For continuity and ease of reading the following article is presented here in chapter format. See Appendix A for authorship statement. All **Tables** and **Figures** that correspond to the supplementary documentation within this chapter can be accessed via the appropriate Digital Object Identifier (DOI) listed above.

Preamble

It is well known that MGO can modify both proteins and DNA, and several studies have shown it contains genotoxic activity. The following study aims to expand on these results by measuring the genotoxicity of MGO, using the gold standard CBMNcyt assay which assesses various types of DNA damage. Furthermore, using LC-MS/MS techniques we explore whether the observed DNA damage is associated with protein or DNA glycation. Lastly, we utilise fluorescent *in situ* techniques to determine the type of DNA damage that is occurring in the CBMNcyt assay.

2.1 Abstract

Type 2 diabetes is associated with elevated levels of DNA damage, in particular micronuclei (MNi) which are formed by acentric chromosome fragments caused by double-stranded DNA breaks (DSBs), or whole chromosomes which fail to segregate during mitosis. We investigated if methylglyoxal (MGO), a reactive dicarbonyl known to be elevated in type 2 diabetes is capable of increasing chromosomal instability and DNA damage as measured by the cytokinesis block micronucleus cytome (CBMNcyt) assay in B-lymphoblastoid WIL2-NS cells and primary peripheral blood lymphocytes (PBL). We also investigated the level of various dicarbonyl stress biomarkers, including extracellular and intracellular MGO, protein and MGO modifications of DNA. WIL2-NS cells exposed to either MGO or a glyoxalase 1 inhibitor showed increases in MNi and nuclear buds, which were associated with an increase in intracellular MGO. DNA damage in the form of MNi and nucleoplasmic bridges were observed in primary PBL exposed to 10 μM MGO, suggesting low concentrations of MGO may be genotoxic. Furthermore, we showed, using fluorescent *in situ* hybridization, that the majority of MNi caused by MGO in WIL2-NS cells were caused by whole chromosome loss events, rather than DSBs. Our data suggest that MGO, a reactive metabolite elevated in type 2 diabetes and other pathologies, can affect genomic integrity by impairing chromosome segregation during mitosis.

2.2 Introduction

Micronuclei (MNi) are an important marker of genomic pathology and are associated with various metabolic, developmental and degenerative diseases such as aging and inflammation (1). Recently, two meta-analyses have been published showing that individuals with type 2 diabetes have an increased frequency of lymphocyte and exfoliated buccal cell MNi, and that MNi from both cell types are elevated in individuals with higher levels of advanced glycation endproducts (AGEs) and glycated haemoglobin (HbA1c) (2,3). Various mechanisms have been described to explain the elevated levels of DNA damage in these individuals, such as oxidative stress, inflammation and reduced DNA damage repair capacity, however, few mechanistic studies have been performed (4).

Metabolic processes produce various highly reactive intermediates that have been implicated in genomic damage. Methylglyoxal (MGO) is a by-product of glycolysis, formed by spontaneous degradation of intermediate triosephosphates (dihydroxyacetone phosphate and glyceraldehyde 3-phosphate) and shown to be elevated ~2-10 fold in type 2 diabetes (5,6). MGO non enzymatically generates stable protein post translational modifications (PTMs) with the amine side groups of arginine forming N^{δ}-(5-hydro-5-methyl-4-imidazolon2-yl)ornithine (MG-H1), and to a lesser extent the lysine adduct N^{ε}-(carboxyethyl)lysine (CEL), respectively (7). Deoxyguanosine residues are also vulnerable to MGO modification, producing 3-(2'eoxyribosyl)-6,7-dihydro-6,7-dihydroxy-6/7-methylimidazo-[2, deoxyguanosine] (MGdG) and N^2-(1,R/S-carboxyethyl)-deoxyguanosine (CEdG) (8). Under normal conditions, the majority of MGO is metabolised by the glyoxalase system which consists of glyoxalase (GLO) 1 and 2 and a catalytic amount of glutathione (9). Various proteins have been identified as targets of MGO including histones which play a crucial role in maintaining genomic integrity (1,10,11). Furthermore, histones are tightly regulated by PTMs which compete with MGO for lysine and arginine residues (10,11). Modification of DNA by MGO has also been implicated in DNA damage, by formation of double strand breaks (DSBs), depurination and increased mutation frequency, particularly in nucleotide excision repair deficient cells (8,12).

To assess the genotoxicity of MGO, we utilized the WIL2-NS B-lymphoblastoid cell line as an *in vitro* model to reflect the *ex vivo* lymphocyte CBMNcyt assay which has been used to measure DNA damage in type 2 diabetes (3). The p53 deficient status of WIL2-NS cells allows them to express DNA damage as MNi, nuclear buds (NBUDs) or nucleoplasmic bridges (NPBs) without undergoing

apoptosis, making them a useful tool for studying DNA damage mechanisms. We also investigated the genotoxicity of MGO in primary peripheral blood lymphocytes (PBL) to ensure that any effects observed were not unique to the WIL2-NS cell line. Herein, we reveal that MGO and inhibition of GLO1 increases MNi and other biomarkers of chromosomal instability in WIL2-NS cells and PBL. Furthermore, we provide evidence that the majority of MGO induced MNi were caused by whole chromosome malsegregation events.

2.3 Methods

2.3.1 Materials

All reagents, chemicals and enzymes were purchased from Sigma unless indicated otherwise. Isotopically labelled and unlabelled MG-H1, CEL and Lys were purchased from Iris biotech (Marktredwitz, Germany).

2.3.2 WIL2-NS cell culture

The WIL2-NS (ATCC CRL-8155) cell line was kindly gifted by Commonwealth Scientific Research Organisation (Adelaide, Australia). WIL2-NS cells were cultured in complete RPMI-1640 medium supplemented with 5% (v/v) Fetal Calf Serum (FCS), L-glutamine (1% v/v) and penicillin/ streptomycin (1% v/v) at 37°C in a humidified atmosphere with 5% CO_2. Cells were seeded at 3 x 10^5 cells/mL and incubated for 24 hours before being treated with MGO or S-p-Bromobenzylglutathione cyclopentyl diester (BBGC) for 48 hours. Cell proliferation and viability was measured using the trypan blue and MTT assays as per manufacturer's instructions (Promega, G4000). GLO1 activity was measured spectrophotometrically as previously described (13) and normalized to cell number.

2.3.3 Volunteers, sample collection and primary lymphocyte culture

Venous blood was collected from 4 healthy male volunteers and lymphocytes were isolated and cultured as previously described in complete RPMI with slight modifications (14). Briefly, mononuclear

lymphocytes were isolated by density gradient centrifugation (Ficoll Paque), washed 2x with HBSS and 1x with complete RPMI. Cells were seeded to 3 x 10^5 cells/mL in a T25 flask and stimulated with 2 µg/mL phytohemagglutinin (PHA). After 24 hours MGO was added and cells were grown for a further 96 hours and assessed for DNA damage by the CBMNcyt assay. The study was approved by the Human Research Ethics Committee of University of South Australia (Application ID: 203348) and written informed consent was obtained from all participants.

2.3.4 CBMNcyt assay/ multipolar assay with MGO/ Glo1 inhibitor

The CBMNcyt assay is a comprehensive system for measuring DNA damage, cytostasis and cytotoxicity. DNA damage events are scored specifically in once-divided binucleated (BN) cells and include (a) micronuclei (MNi), a biomarker of chromosome breakage and/or whole chromosome loss, (b) nucleoplasmic bridges (NPBs), a biomarker of DNA misrepair and/or telomere end-fusions, and (c) nuclear buds (NBUDs), a biomarker of elimination of amplified DNA and/or unresolved DNA repair complexes. Cytostatic effects are measured via the proportion of mono-, bi- and multinucleated cells to calculate the nuclear division index (NDI) and cytotoxicity is determined via necrotic and/or apoptotic cell ratios. These biomarkers are identified microscopically using well-established and validated criteria as previously described (14). Following treatment with MGO or BBGC, cells (WIL2-NS and primary PBL) were washed 1x with HBSS and 1x with complete RPMI and then cultured in the presence of 4.5 µg/mL cytochalasin-B (cyt-B) for 24 hours before being harvested onto slides by cytocentrifugation (14). Slide preparation and scoring of the CBMNcyt assay was performed as described previously (14,15) using a NanoZoomer S60 (Hammatsu Photonics). For determination of multipolar mitosis, cells were treated as for the CBMNcyt assay, with the exception that cyt-B was omitted. Cells in anaphase, telophase or cytokinesis were scored for the presence of two or more mitotic poles or nuclei (16).

2.3.5 Fluorescent *in situ* hybridization (FISH)

Origin of MNi was determined using FITC-conjugated peptide nucleic acid probes specific for pancentromeric regions of DNA to determine centromeric positive (+ve) or centromeric negative (-ve)

state. Cells were treated as for the CBMNcyt assay and transferred onto slides after fixation in suspension as described previously in (15). For FISH, slides were prepared as previously described (17). Slide images were acquired with the Zeiss CellDiscoverer 7 (Carl Zeiss AG, Jena, Germany) using a combination of two LED modules: 385 and 495 nm wavelengths in combination with a quad-band bandpass filter. A Plan-Apochromat 20x/0.8NA objective with a 1x tube lens and an Axiocam 506 monochrome-camera were used for image acquisition. Acquired images were processed using ZEN Blue software (Carl Zeiss AG, Jena, Germany).

2.3.6 Synthesis of CEdG and 13C$_3$-CEdG

Synthesis of CEdG and $^{13}C_3$-CEdG were achieved by reactions of 2-deoxyguanosine (2-dG) with DL-glyceraldehyde and $^{13}C_3$-DL-glyceraldehyde (Omicron biochemicals, GLE-007), respectively (18). Isotopically labelled $^{13}C_3$-DL-glyceraldehyde was supplied as a 0.1M solution and was therefore lyophilized prior to the reaction, all subsequent steps were the same as unlabeled CEdG. Briefly, DL-glyceraldehyde and 2-dG were reacted in a 3:1 mole ratio under buffered conditions at 37°C, for 17 days. Products were purified by reverse-phase (RP) high performance liquid chromatography (HPLC) on a Luna C_{18} column, 250 × 10 mm i.d., 5 µm particle size, 100 Å pore size (Phenomenex, Torrance, CA, USA) on a Shimadzu LC-6A system. Injection volume was 100-300 µL and mobile phase were 0.1% (v/v) formic acid and 95% (v/v) acetonitrile / 0.1% (v/v) formic acid at a flow rate of 4 mL/min (chromatographic conditions and representative chromatogram in supplementary table 1 and supplementary figure 1, respectively). Collected fractions were pooled and dried under nitrogen to remove residual acetonitrile and then lyophilized. Mass analyses of the unlabelled and labelled diastereomers was conducted using a Sciex 6500+ QTRAP mass spectrometer in positive ion mode. The most intense ions observed were for the *m/z* 340.3 and 343.3 for CEdG and $^{13}C_3$-CEdG, respectively. Collision induced dissociation gave rise to ion with *m/z* 224 and 227 for CEdG and $^{13}C_3$-CEdG, respectively. ^{1}H NMR of the two epimers corresponded with previous studies. ^{1}H NMR assignments for CEdG$_a$: ^{1}H NMR (400 MHz, DMSO-d6,18 °C): δ 10.68 (s, 1H, N1-H), δ 7.96 (s, 1H, C8-H), δ 6.84 (d, 1H, C2-NH), δ 6.15 (dd, 1H, C1′-H), δ 5.32 (d, 1H, C3′-OH), δ 4.91 (vbr, 1H, C5′-OH), δ 4.39 (m, 1H, C2-NH-CH), δ 4.36 (m, 1H, C4′-H), δ 3.84 (m, 1H, C3′-H), δ 3.56 (ddd, 2H, C5′-H$_2$), δ 2.69 (ddd, 1H,

C2'-H), δ 2.21 (m, 1H, C2'-H), δ 1.43 (d, 3H, C2-NH-CH-CH_3). ^{1}H NMR assignments for $CEdG_b$ are almost identical.

2.3.7 Quantification of dicarbonyl stress biomarkers by LC-MS/MS

MGO content of cells and culture medium was quantified as previously described (6,19) by derivatization with o-phenylenediamine. MG-H1 and CEL were quantified from intracellular protein extracts which underwent exhaustive enzymatic hydrolysis with pepsin, pronase E, prolidase and aminopeptidase as previously described (20). MG-H1 and CEL are reported as mmol/ mol unmodified Lysine. Due to the low abundance of MG-H1 and CEL in culture medium, quantification of these adducts in this matrix was performed following derivatization with 1-butanol under acidic conditions as previously described (21). The DNA adduct 8-Oxo-2'-deoxyguanosine (8-oxodG) was quantified in extracellular media as a surrogate measure of oxidative stress. Media was passed through a micro spin ultrafiltration (Amicon-Ultra; 10 kDa cut-off) column. Isotopically labelled 2-dG was spiked into sample to ensure both analytes were resolved to prevent over estimation of 8-oxodG by in source formation by oxidation of 2-dG. For quantification of CEdG from WIL2-NS cells, DNA was isolated as previously described (20), hydrolyzed by the addition of 10 µL of DNase II (2 U/ mg DNA) and 2 µL of phosphodiesterase II (1.5 U/ mg DNA) and incubated for 4 hours. Following this, 10 µL of acid phosphatase (35 U/ mg DNA) was added and the reaction incubated for 16 hours. Protein was removed by precipitation with acetonitrile: methanol (3:1) and centrifugation (17,000 *g*). The supernatant was dried under argon and resuspended in 5% (v/v) methanol. All analyses were performed using multiple reaction monitoring (MRM) in positive ion mode with an AB Sciex 6500+ QTRAP mass spectrometer. Analyte parameters and LOD/LOQ values are reported in supplementary table 2.

2.3.8 Statistical analysis

Data analysis was performed using Graph Pad Prism (San Diego, CA, USA, Version 8.0.0). One-way analysis of variance (ANOVA) followed by Dunnett post-hoc test was conducted when comparing more than two groups of data. Unpaired t-test was conducted when comparing two groups of data. A $p<0.05$

was considered significant and the results were expressed as mean ± standard deviation (SD) of 3-4 independent replicates.

2.4 Results

2.4.1 Dicarbonyl stress parameters are increased upon exposure to exogenous MGO

Cells are extremely efficient at detoxifying MGO, therefore we first sought to examine the level of various dicarbonyl stress parameters upon exposure to exogenous MGO to determine doses appropriate for further analysis. Viability studies were not conducted to determine doses as elevation of dicarbonyl stress biomarkers may occur at concentrations that do not cause a cytotoxic response but may result in chromosomal instability. Following exposure to 100, 500 and 1000 µM MGO for 48 hours, the level in the media had decreased to 1.67, 0.67 and 0.4% of the original level, respectively (Table 2.1). The majority of this decrease in media MGO is resultant of the efficient metabolism by WIL2-NS, however low concentrations of MG-H1 were observed in the media suggesting reactions of media MGO with free arginine (data not shown). The intracellular level of MGO in WIL2-NS increased in a dose-dependent manner, with a significant increase of 8.5 and 10.7-fold observed in cells exposed to 500 and 1000 µM MGO, respectively (Table 2.1). We also investigated the level of MGO derived protein and nucleotide modifications MG-H1, CEL and CEdG. Addition of 500 µM MGO led to significant increases in MG-H1 levels relative to control (Table 2.1). At 1000 µM MGO, MG-H1, CEL and CEdG were significantly increased, however, at this concentration the level of MG-H1 was increased >30-fold which is far beyond the upper limit of clinical dicarbonyl stress (≤ 10-fold) (Table 2.1) (5). We also investigated the medium concentration of 8-oxodG as a measure of oxidative stress, however, no significant difference was observed following treatment with MGO (supplementary table 3).

Table 2.1. Dicarbonyl stress biomarkers measured in WIL2-NS cells treated with MGO

	MGO (μM)			
Biomarker	0	100	500	1000
Media MGO (nM)	35.87 ± 4.60	1670.63 ± 410.28** (1.67%)	3333.11 ± 647.53**** (0.67%)	5036.27 ± 198.02**** (0.40%)
Cellular MGO (Relative level)	1.00 ± 0.30	2.63 ± 0.28	8.50 ± 3.12**	10.72 ± 2.35**
MG-H1 (mmol/mol lysine)	0.19 ± 0.03	0.15 ± 0.03	1.35 ± 0.66*	5.46 ± 0.46****
CEL (mmol/mol lysine)	0.20 ± 0.03	0.18 ± 0.04	0.45 ± 0.03	1.62 ± 0.51***
CEdG (adducts/ 10^6 dG)	2.66 ± 1.22	2.61 ± 1.00	6.43 ± 3.84	12.23 ± 5.88*

Data are mean ± SD, n=3. Significance: *p<0.05, **p<0.01, ***p<0.001, ****p<0.0001 when compared to 0 μM. Values in parentheses represent to the average percent of MGO remaining in the media after 48 hours exposure.

2.4.2 MGO increases DNA damage biomarkers measured by the CBMNcyt assay.

The cytostatic (NDI), cytotoxic (necrosis) and genotoxic (Figure 2.1a undamaged cell, 2.1b MNi, 2.1c NPB and 2.1d NBUDs) activity of MGO was determined using the CBMNcyt assay. Cells were treated with MGO for 48 hours as some types of DNA damage, such as DNA adducts and single strand DNA breaks may require more than one round of DNA replication for them to be converted to other lesions such as double strand DNA breaks that lead to acentric chromosome fragments from which MNi and NPBs originate (1). The frequency of necrotic cells was not significantly increased up to 500 μM MGO, however at 1000 μM the frequency of necrotic cells was 85.08 ± 10.96% (Figure 2.1e). No other biomarkers of the CBMNcyt assay were scored for 1000 μM MGO, due to low cell viability and inadequate numbers of binucleated cells required for MNi, NPB and NBUDs scoring. There was no significant difference in the NDI at 100 μM compared to the control, however, contrary to expectations, it was significantly increased at 500 μM compared to the control (Figure 2.1f).

The frequency of MNi was significantly increased at both 100 and 500 μM MGO when compared to the control (Figure 2.1g) with NBUDs significantly increased at 500 but not 100 μM MGO (Figure 2.1h). No significant increase was observed for NPBs using ANOVA, however they did show a significant trend to increase at higher concentrations of MGO (r=0.9337; *p*=0.0328). Total DNA damage (The sum of all MNi, NBUDs and NPBs) was also investigated. This was significantly increased at both

100 and 500 µM MGO (Figure 2.1j). To gain further insight into the potential relationship of MNi, NPBs and NBUDs under MGO stress conditions, correlation analysis was performed between the three, however no significant correlation was observed (data not shown).

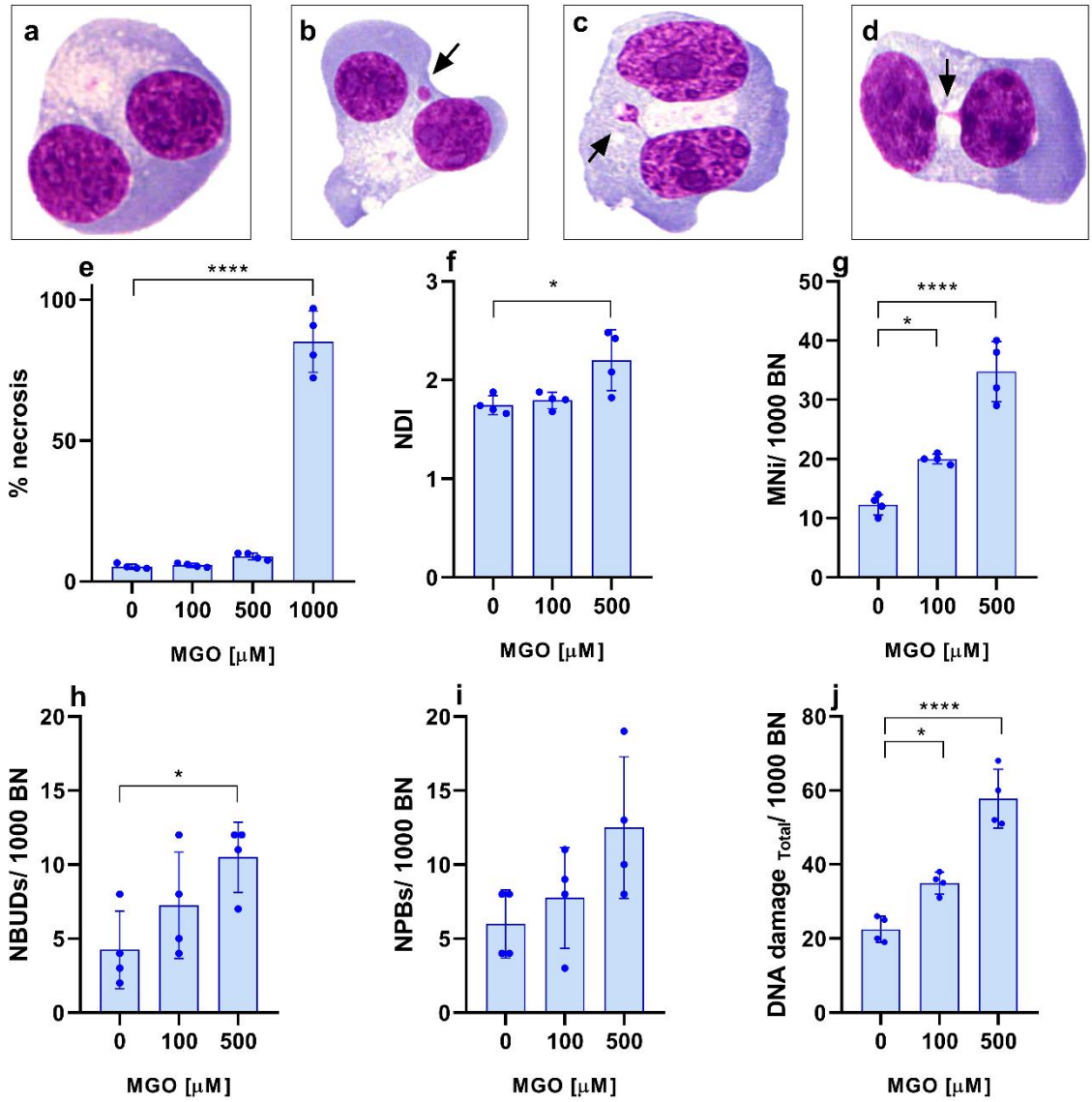

Figure 2.1. Methylglyoxal increases DNA damage biomarkers in WIL2-NS. (**a-d**) Representative photomicrographs of DNA damage biomarkers from CBMNcyt assay in binucleated (BN) cells (biomarkers indicated by small black arrows); (**a**) binucleated cell without damage, (**b**) micronuclei (MNi), **c** nuclear bud (NBUD) and (**d**) nucleoplasmic bridge (NPB), respectively. (**e**) Frequency of necrotic cells expressed as a percentage. (**f**) Nuclear division index (NDI). (**g**) Frequency of MNi per 1000 Binucleated (BN) cells. (**h**) Frequency of NBUDs per 1000 BN cells. (**i**) Frequency of NPBs per 1000 BN cells. (**j**) Frequency of total DNA damage per 1000 BN cells Data are mean ± SD, n=4. Significance: *p<0.05, ****p<0.0001 when compared to 0 µM.

2.4.3 MGO causes cells to undergo multipolar mitosis.

As revealed above, cells treated with 500 µM MGO had a higher NDI than control cells, suggesting an increase in proliferation. This result was unexpected as MGO is known to decrease cellular proliferation (22). Therefore, we first investigated the frequency of mono, bi and multinucleated cells to determine if this influenced the NDI. Cells treated with 500 µM MGO had a significantly higher frequency of multinucleated cells, a result consistent with an increased NDI (Figure 2.2a). We then sought to determine the proliferation of cells treated with MGO. Both the MTT and trypan blue exclusion assays showed no significant change at 100 µM MGO, but a ~20% decrease at 500 µM, contradicting the increase NDI and multinucleated cell frequency observation (Supplementary figure 2a,b). We hypothesized that these conflicting results may be due to centrosome replication defects or cytokinesis failure, which could explain the increased NDI and multinucleated cell frequency, despite a decrease in viable cell count. To confirm this, the CBMN assay was performed in the absence of cyt-B. To investigate this we measured the frequency of binucleated (BN) and multinucleated (>2 nuclei) cells which could indicate cytokinesis failure and centrosome replication defects, respectively. Indeed, we found a significant increase in both when cells were treated in 500 µM MGO, however, the relative increase in multinucleated cells was more pronounced than for BN cells. To further explore this, we measured the frequency of cells undergoing multipolar mitosis (Figure 2.2e-g), another indicator of centrosome replication defects. Mitotic cells were scored based on the criteria of possessing two or more poles (Figure 2.2c,d,e). Cells treated with 500 µM MGO had a 3.36-fold increase in the frequency of cells undergoing multipolar mitosis (Figure 2.2b). These results suggest that MGO may induce mitotic dysfunction by cytokinesis failure and defects in centrosome replication.

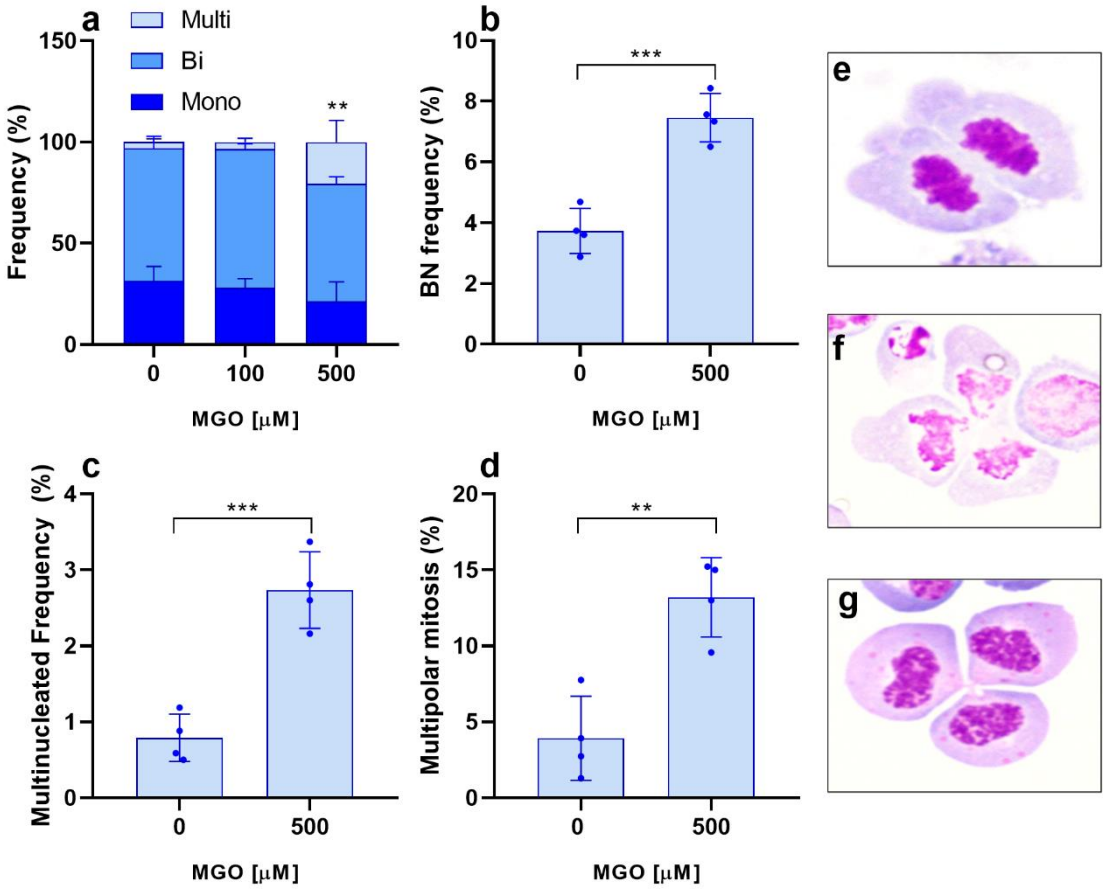

Figure 2.2. Methylglyoxal induces mitotic dysfunction. (**a**) Frequency of mono, bi and multinucleated cells following treatment with cyt-b. (**b**) Frequency of binucleated (BN) cells in non cyt-b treated experiments. (**c**) Frequency of multinucleated (>2 nuclei) cells in non cyt-b treated experiments. (**d**) Frequency of cells undergoing multipolar mitosis in non cyt-b treated cells expressed as a percentage of all mitotic cells. (**e-g**) Representative photomicrographs of cells undergoing normal (bipolar) mitosis and multipolar mitosis; normal (bipolar) mitosis (**e**), cells undergoing multipolar mitosis in telophase (**f**), cells undergoing multipolar mitosis in cytokinesis with formation of the cleavage furrow (**g**). Data are mean ± SD, n=4. Significance: **p<0.01, ***p<0.001 when compared to 0 μM.

2.4.4 Inhibition of GLO1 in WIL2-NS with BBGC increases MGO and DNA damage.

After establishing that exposure to exogenous MGO causes genomic instability, we next sought to confirm this by treating cells with the GLO1 inhibitor, BBGC. Since GLO1 is required to detoxify MGO, inhibition of this enzyme may result in increased concentrations of MGO and related modifications. To determine the appropriate concentration of BBGC to use, cells were exposed in a dose-dependent manner for 48 hours, at which point viability was measured colorimetrically by MTT

assay, which showed an EC_{50} of 21.9 ± 5.5 µM. Because 21.9 µM resulted in a 50% decrease in cell viability which may affect overall efficiency of scoring of the CBMNcyt assay, we chose 10 µM as the maximum concentration. We first evaluated the level of GLO1 activity in WIL2-NS cells exposed to BBGC. A trend of decreasing GLO1 activity with increasing concentrations of BBGC was observed, however a significant reduction (21.9%) was only observed at 10 µM (Table 2.2). This decrease in GLO1 activity at 10 µM BBGC was associated with a significant increase of MGO in the media (Table 2.2). However, no significant increase in intracellular MGO, MG-H1, CEL or CEdG was observed (Table 2.2). It has previously been shown that although an increase in adduct formation occurs, it may not be evident as the cell may remove damaged proteins and release free MG-H1, CEL or CEdG into the media (23). The level of free MG-H1 in the media was increased, although not significantly ($p=0.0755$) when treated with 10 µM BBGC (Table 2.2). There was no change in media concentrations of CEL, and CEdG was below the LOQ and thus could not be quantified (Table 2.2).

The NDI and frequency of necrotic cells was unchanged following exposure to BBGC (Figure 2.3a,b). Moreover, there was no change in the frequency of NBUDs and NPBs (Figure 2.3d,e). However, cells exposed to 10 µM BBGC had a significantly higher frequency of MNi and total DNA damage when compared to untreated cells (Figure 2.3c,f).

Table 2.2. Dicarbonyl stress biomarkers measured in WIL2-NS cells treated with the GLO1 inhibitor

	BBGC (µM)		
Biomarker	0	1	10
Glo1 activity (mU/ 10^6 cells)	1165.50 ± 112.79	990.68 ± 106.82	909.09 ± 121.12*
Media MGO (nM)	51.40 ± 6.75	57.32 ± 4.73	72.38 ± 6.54**
Cellular MGO (Relative level)	1.00 ± 0.27	0.95 ± 0.05	0.92 ± 0.08
MG-H1 (mmol/mol lysine)	0.19 ± 0.09	0.14 ± 0.06	0.16 ± 0.03
CEL (mmol/mol lysine)	0.21 ± 0.05	0.13 ± 0.04	0.17 ± 0.01
CEdG (adducts/ 10^6 dG)	1.19 ± 0.29	1.71 ± 0.46	1.57 ± 0.88
Media MG-H1 (nM)	43.55 ± 5.49	44.32 ± 7.18	53.04 ± 3.91
Media CEL (nM)	3.74 ± 0.14	2.97 ± 0.52	4.12 ± 0.31

Data are mean ± SD, n=3. Significance: *$p<0.05$, **$p<0.01$, when compared to 0 µM.

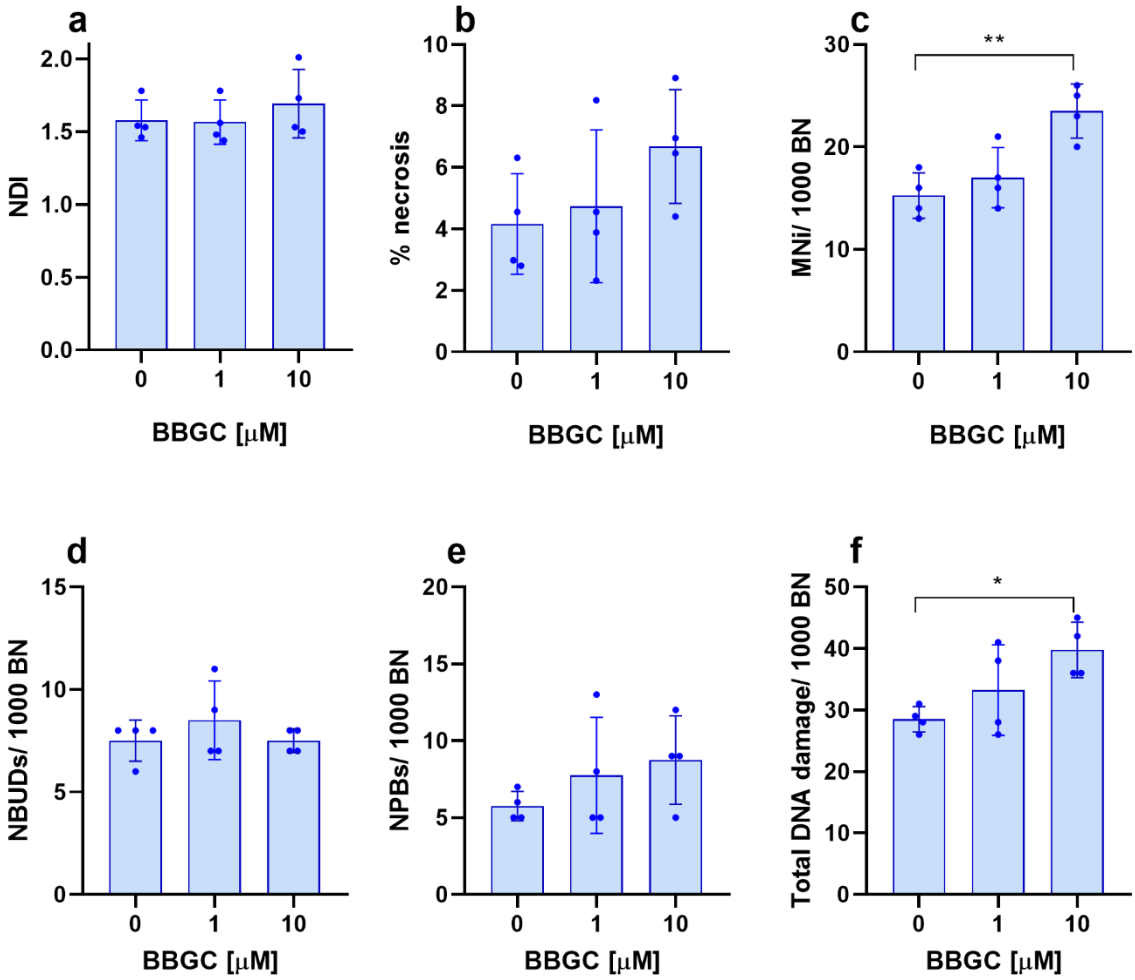

Figure 2.3. Inhibition of Glyoxalase 1 by BBGC increases DNA damage in WIL2-NS cells. (**a)** Nuclear division index (NDI). (**b**) Frequency of necrotic cells expressed as a percentage of all cells. (**c**) Frequency of MNi per 1000 BN cells. (**d**) Frequency of NBUDs per 1000 BN cells. (**e**) Frequency of NPBs per 1000 BN cells. (**f**) Frequency of total DNA damage per 1000 BN. Data are mean ± SD, n=4. Significance: *p<0.05, **p<0.01 when compared to 0 μM.

2.4.5 MGO induces DNA damage in peripheral blood lymphocytes (PBL)

After confirming that exposure to MGO and inhibition of GLO1 can induce DNA damage *in vitro*, we sought to confirm these results using primary PBL. Two rounds of mitotic division may be necessary for MGO-induced DNA damage to be expressed as MNi (1), and the growth of primary PBL is slower than that of WIL2-NS, therefore PBL cells were cultured for 96 hours following one dose of MGO. Preliminary studies showed primary PBL were much more sensitive to MGO than WIL2-NS and following exposure to 100 and 500 μM viable cell number was ~70 and 30% of the control, respectively (Supplementary figure 3). For this reason, primary PBL were exposed to MGO concentrations of 10 and 50 μM which caused only a small (~15%), but significant reduction in viable cell number.

MGO had no impact on the NDI, frequency of necrotic cells or NBUDs at either concentration tested (Figure 2.4a,c,f). However, apoptosis was significantly increased at both 10 and 50 µM (Figure 2.4b). The frequency of MNi and NPBs in primary PBL significantly increased at both 10 and 50 µM MGO (Figure 2.4d,e), however, total DNA damage was only significantly increased with 10 µM MGO (Figure 2.4g).

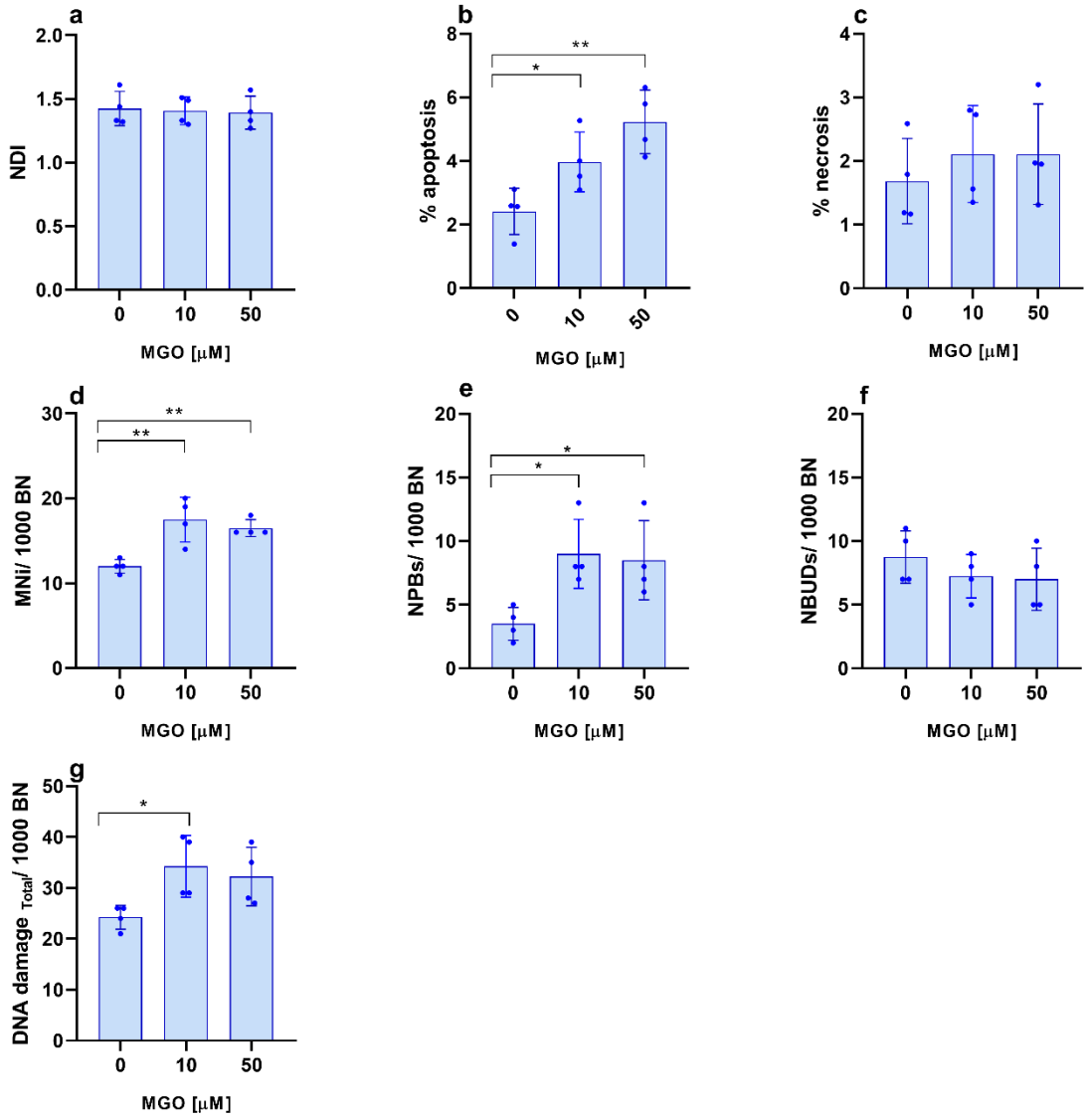

Figure 2.4. Methylglyoxal induces DNA damage in peripheral blood lymphocytes. (**a**) Nuclear division index (NDI). (**b**) Frequency of apoptotic cells expressed as a percentage. (**c**) Frequency of necrotic cells expressed as a percentage. (**d**) Frequency of MNi per 1000 BN cells. (**e**) Frequency of NBUDs per 1000 BN cells. (**f**) Frequency of NPBs per 1000 BN cells. (**g**) Frequency of total DNA damage per 1000 BN. Data are mean ± SD, n=4. Significance: *p<0.05, **p<0.01, ***p<0.001 when compared to 0 µM.

.

2.4.6 MGO causes whole chromosome loss in WIL2-NS

Given MNi can be caused by both acentric fragments as a result of DSBs and whole chromosomes which fail to segregate during mitosis, we sought to determine their origin using FISH. Peptide nucleic acid

probes, specific for pancentromeric DNA sequences were used to determine if MNi were centromere -ve (Figure 2.5a), indicating an acentric fragment or centromere +ve (Figure 2.5b), indicating a whole chromosome encased within the MNi. MNi from untreated cells were shown to contain 58% centromere -ve and 42% centromere +ve signals suggesting majority of spontaneous MNi occur from DSBs (Figure 2.5c). However, when treated with 500 µM MGO, frequency of centromere +ve MNi increased to 68% (Figure 2.5c). Based on the relative increase in MNi following exposure to 500 µM MGO (2.8-fold) from Figure 2.1g, the results suggest 88% of the MNi formed above background levels are centromere +ve and only 12% are centromere -ve. This data strongly suggests that MGO causes whole chromosome loss in dividing cells and as a consequence increases the rate of aneuploidy in their progeny (24).

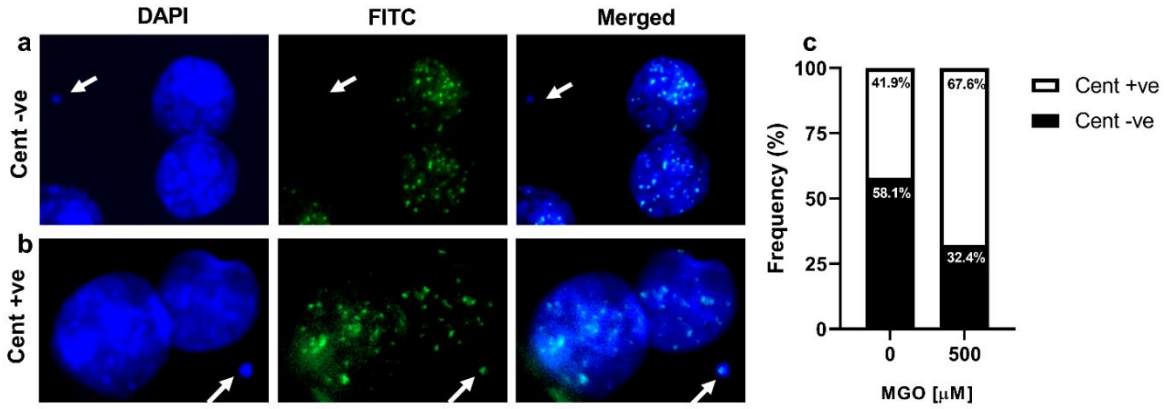

Figure 2.5. MGO induces whole chromosome loss in WIL2-NS cells. (**a**) Image of centromere -ve MNi. (**b**) Image of centromere +ve MNi. (**c**) Frequency of centromere -ve and centromere +ve MNi in control and MGO treated (500 µM). cent = centromere, -ve = negative, +ve = positive.

2.5 Discussion

In this study we revealed that dicarbonyl stress, induced with both exogenous MGO and inhibition of GLO1 can induce DNA damage in WIL2-NS, a B-lymphocyte cell line, and in primary PBL. Furthermore, we showed for the first time that MGO induces multiple mitotic aberrations, particularly multipolar mitosis and whole chromosome loss in WIL2-NS cells. To explore the genotoxicity of MGO, we employed the CBMNcyt assay, as it can measure simultaneously multiple forms of DNA damage that are evident at the cytological level as MNi, NPBs and NBUDs which are indicative of chromosomal instability. WIL2-NS cells exposed to either MGO or BBGC showed increased frequencies of these

DNA damage biomarkers, the most abundant being MNi. Interestingly, although increased MNi frequency was observed in cells exposed to BBGC, no increase in intracellular MGO or protein and DNA modifications was observed. A small increase in media MGO and MG-H1 was observed which may suggest mild increases in dicarbonyl stress, however, further studies using siRNA or CRISPR mediated knockdown of GLO1 would provide further evidence on the role this enzyme and MGO have on DNA damage. Low concentrations of MGO (10 μM) were shown to increase MNi and NPB frequency in primary PBL. Contrastingly, although WIL2-NS and primary PBL both showed elevated MNi, the former also showed elevated NBUDs, whereas the latter showed increased NPBs. This may suggest altered response to elevated MGO between WIL2-NS and primary PBL, which may result from differences in DNA repair profile or efficiency of the nuclear budding process to remove amplified DNA and unresolved DNA repair complexes.

A positive trend was observed between increasing intracellular MGO and MNi frequency, however no obvious association was seen between DNA damage biomarkers and MGO induced protein or DNA modifications. Methods used in this study to quantify these modifications only measured the whole intracellular level and not those on individual proteins or regions of DNA. It has been shown that low concentrations of MGO can increase the degree of modifications on specific proteins (e.g. histones), despite no observed increase in whole cell levels (11). Furthermore, MG-H1 modifications have been shown to localize to the nucleus following exposure to MGO (25). It may be that specific proteins, subcellular compartments or regions of chromosomes do experience an increase in MGO modifications, but the increase was insufficient to manifest their impact as MNi, NPB or NBUDs. Therefore, additional experiments that probe specific cellular compartments (e.g. nucleus) or proteins involved in DNA replication and chromosomal segregation (e.g. proteins involved in the mitotic process such as microtubules, kinetochores and centrosomes) may offer further insights. For example, it was recently shown that diabetics have increased centrosome amplification in peripheral blood mononuclear cells correlated with the levels of fasting blood glucose and HbA1c (26). Our results showing that MGO induces multi-polar mitoses suggest that increased MGO may also be one of the likely causes of centrosome amplification in diabetics.

Interestingly, we showed using FISH that the majority of MNi in WIL2-NS cells exposed to MGO were centromere +ve, suggesting that MGO-induced MNi were primarily caused by whole

chromosome loss events and not acentric chromosome fragments originating from DSBs, which has previously been shown to be induced by MGO (8,27,28). However, these studies employed techniques such as γH2AX or Terminal deoxynucleotidyl transferase dUTP nick end labeling (TUNEL) assay which are not capable of measuring whole chromosome loss events (8,27). Furthermore, DSBs in the study of Thornalley et al (8) was measured following 2 hours exposure to MGO, which suggest that DSBs are induced as a direct effect of MGO on DNA resulting in an acute response. In contrast, whole chromosome loss events may be a result of delayed response due to damage to mitotic proteins that requires prolonged chronic exposure to become evident; however, this remains to be determined. Nevertheless, a small number of the MNi caused by MGO were shown to be centromere -ve, suggesting a small percentage were probably caused by DSBs. Due to the non-specific nature of MGO modifications, there are numerous plausible mechanisms whereby it could cause chromosome malsegregation events. A previous study has shown MF-1 mouse oocytes exposed to MGO induced various mitotic aberrations, including tripolar spindle formation and failed congression which was associated with disturbances in spindle organization (29). Spindle or centrosome defects that impair correct segregation of chromosomes could account for multipolar cells and/ or whole chromosome loss events observed in this study. Moreover, modification and subsequent loss of activity of various proteins involved in mitotic processes such as kinetochores, microtubules and centrosomes could also result in whole chromosome loss events (1). Furthermore, several recent studies have shown core histone proteins (H2A, H2B, H3 and H4), are primary targets for MGO modification in mammalian cells (10,11). HEK293T cells treated with MGO and xenografted breast cancer tissue all showed higher histone modification relative to their control, while showing similar levels of glycation in the soluble fractions (non-histone protein fraction) (11). The abundance of lysine and arginine residues on the histones N-terminal tail which extends from the nucleosome increases its susceptibly to MGO modifications. Modification of these tail residues was shown to interfere with other histone PTMs such as methylation, acetylation and ubiquitination of lysine residues, suggesting MGO disrupts global histone enzymatic PTMs (10,11). Histone modifications are essential for kinetochore assembly (30). Thus, modification of histone residues by MGO that interfere with modifications required for binding of kinetochore proteins could result in compromised kinetochore assembly and kinetochore-microtubule

attachment. This could potentially result in chromosomes not being correctly segregated to the appropriate pole during mitosis, resulting in the formation of MNi.

MNi were the only form of DNA damage observed to be associated with MGO in all CBMNcyt experiments conducted as part of this study. We were able to show that the majority of MGO induced MNi in WIL2-NS were centromere +ve, suggesting MGO has aneugenic properties and impairs correct segregation of chromosomes during mitosis. Whether this is a result of direct MGO modifications, or a downstream effect remains to be determined. Proteomic studies and MG-H1 localization by immunofluorescence may be useful in determining underlying mechanisms by identifying protein modifications that could result in the DNA damage observed in this study

2.6 Conclusion

Together, the results obtained in this study indicate that MNi formation, caused by whole chromosome loss events are a pathophysiological outcome of dicarbonyl stress. Various diseases such as type 2 diabetes and cancer are associated with perturbed metabolic state, which results in elevated concentrations of MGO and related protein and DNA adducts (31,32). Furthermore, centrosome abnormalities/ amplification leading to multipolar mitoses are common in cancer and type 2 diabetes (26,33,34). Therefore, results from this study may provide mechanistic insight into the elevated frequency of MNi and multipolar mitosis seen in these diseases.

References

1. Fenech, M., Knasmueller, S., Bolognesi, C., Bonassi, S., Holland, N., Migliore, L., Palitti, F., Natarajan, A.T., and Kirsch-Volders, M. (2016) Molecular mechanisms by which in vivo exposure to exogenous chemical genotoxic agents can lead to micronucleus formation in lymphocytes in vivo and ex vivo in humans. *Mutation Research*, **770**, 12-25.
2. Kirsch-Volders, M., Bolognesi, C., Ceppi, M., Bruzzone, M., and Fenech, M. (2020) Micronuclei, inflammation and auto-immune disease. *Mutation Research*, **786**, 108335.
3. Deo, P., Fenech, M., and Dhillon, V.S. (2021) Association between glycation biomarkers, hyperglycemia, and micronucleus frequency: A meta -analysis. *Mutation Research/Reviews in Mutation Research*, **787**.
4. Kumar, V., Agrawal, R., Pandey, A., Kopf, S., Hoeffgen, M., Kaymak, S., Bandapalli, O.R., Gorbunova, V., Seluanov, A., Mall, M.A., Herzig, S., and Nawroth, P.P. (2020) Compromised DNA repair is responsible for diabetes-associated fibrosis. *The EMBO Journal*, **39**, e103477.
5. McLellan, A.C., Thornalley, P.J., Benn, J., and Sonksen, P.H. (1994) Glyoxalase system in clinical diabetes mellitus and correlation with diabetic complications. *Journal of Clinical Science*, **87**, 21-29.
6. Scheijen, J.L., and Schalkwijk, C.G. (2014) Quantification of glyoxal, methylglyoxal and 3-deoxyglucosone in blood and plasma by ultra performance liquid chromatography tandem mass spectrometry: evaluation of blood specimen. *Clinical Chemistry and Laboratory Medicine*, **52**, 85-91.
7. Thornalley, P.J., Battah, S., Ahmed, N., Karachalias, N., Agalou, S., Babaei-Jadidi, R., and Dawnay, A. (2003) Quantitative screening of advanced glycation endproducts in cellular and extracellular proteins by tandem mass spectrometry. *Biochemical Journal*, **375**, 581-592.
8. Thornalley, P.J., Waris, S., Fleming, T., Santarius, T., Larkin, S.J., Winklhofer-Roob, B.M., Stratton, M.R., and Rabbani, N. (2010) Imidazopurinones are markers of physiological genomic damage linked to DNA instability and glyoxalase 1-associated tumour multidrug resistance. *Nucleic Acids Research*, **38**, 5432-5442.
9. Rabbani, N., and Thornalley, P.J. (2015) Dicarbonyl stress in cell and tissue dysfunction contributing to ageing and disease. *Biochemical and Biophysical Research Communications*, **458**, 221-226.
10. Galligan, J.J., Wepy, J.A., Streeter, M.D., Kingsley, P.J., Mitchener, M.M., Wauchope, O.R., Beavers, W.N., Rose, K.L., Wang, T., Spiegel, D.A., and Marnett, L.J. (2018) Methylglyoxal-derived posttranslational arginine modifications are abundant histone marks. *Proceedings of the National Academy of Sciences of the United States of America*, **115**, 9228-9233.
11. Zheng, Q., Omans, N.D., Leicher, R., Osunsade, A., Agustinus, A.S., Finkin-Groner, E., D'Ambrosio, H., Liu, B., Chandarlapaty, S., Liu, S., and David, Y. (2019) Reversible histone glycation is associated with disease-related changes in chromatin architecture. *Nature Communications*, **10**, 1289.
12. Tamae, D., Lim, P., Wuenschell, G.E., and Termini, J. (2011) Mutagenesis and repair induced by the DNA advanced glycation end product N2-1-(carboxyethyl)-2'-deoxyguanosine in human cells. *Biochemistry*, **50**, 2321-2329.
13. Arai, M., Nihonmatsu-Kikuchi, N., Itokawa, M., Rabbani, N., and Thornalley, P.J. (2014) Measurement of glyoxalase activities. *Biochemical Society Transactions*, **42**, 491-494.
14. Fenech, M. (2007) Cytokinesis-block micronucleus cytome assay. *Nature Protocols*, **2**, 1084-1104.
15. Jaunay, E.L., Dhillon, V.S., Semple, S.J., Simpson, B.S., Deo, P., and Fenech, M. (2020) Can a digital slide scanner and viewing technique assist the visual scoring for the cytokinesis-block micronucleus cytome assay? *Mutagenesis*, **35**, 311-318.
16. Guo, X., Ni, J., Zhu, Y., Zhou, T., Ma, X., Xue, J., and Wang, X. (2017) Folate deficiency induces mitotic aberrations and chromosomal instability by compromising the spindle assembly checkpoint in cultured human colon cells. *Mutagenesis*, **32**, 547-560.
17. Lindberg, H.K., Wang, X., Jarventaus, H., Falck, G.C., Norppa, H., and Fenech, M. (2007) Origin of nuclear buds and micronuclei in normal and folate-deprived human lymphocytes. *Mutation Research*, **617**, 33-45.
18. Synold, T., Xi, B., Wuenschell, G.E., Tamae, D., Figarola, J.L., Rahbar, S., and Termini, J. (2008) Advanced glycation end products of DNA: quantification of N 2-(1-carboxyethyl)-2′-

deoxyguanosine in biological samples by liquid chromatography electrospray ionization tandem mass spectrometry. *Chemical Research in Toxicology*, **21**, 2148-2155.
19. Rabbani, N., and Thornalley, P.J. (2014) Measurement of methylglyoxal by stable isotopic dilution analysis LC-MS/MS with corroborative prediction in physiological samples. *Nature Protocols*, **9**, 1969-1979.
20. Rabbani, N., Shaheen, F., Anwar, A., Masania, J., and Thornalley, P.J. (2014) Assay of methylglyoxal-derived protein and nucleotide AGEs. *Biochemical Society Transactions*, **42**, 511-517.
21. Martens, R.J.H., Broers, N.J.H., Canaud, B., Christiaans, M.H.L., Cornelis, T., Gauly, A., Hermans, M.M.H., Konings, C., van der Sande, F.M., Scheijen, J., Stifft, F., Wirtz, J., Kooman, J.P., and Schalkwijk, C.G. (2019) Relations of advanced glycation endproducts and dicarbonyls with endothelial dysfunction and low-grade inflammation in individuals with end-stage renal disease in the transition to renal replacement therapy: A cross-sectional observational study. *PLoS One*, **14**, e0221058.
22. Wang, Y., Hall, L.M., Kujawa, M., Li, H., Zhang, X., O'Meara, M., Ichinose, T., and Wang, J.M. (2019) Methylglyoxal triggers human aortic endothelial cell dysfunction via modulation of the KATP/MAPK pathway. *American Journal of Physiology-Cell Physiology*, **317**, C68-C81.
23. Stratmann, B., Engelbrecht, B., Espelage, B.C., Klusmeier, N., Tiemann, J., Gawlowski, T., Mattern, Y., Eisenacher, M., Meyer, H.E., Rabbani, N., Thornalley, P.J., Tschoepe, D., Poschmann, G., and Stuhler, K. (2016) Glyoxalase 1-knockdown in human aortic endothelial cells - effect on the proteome and endothelial function estimates. *Scientific Reports*, **6**, 37737.
24. Fenech, M., Knasmueller, S., Bolognesi, C., Holland, N., Bonassi, S., and Kirsch-Volders, M. (2020) Micronuclei as biomarkers of DNA damage, aneuploidy, inducers of chromosomal hypermutation and as sources of pro-inflammatory DNA in humans. *Mutation Research/Reviews in Mutation Research*, **786**.
25. Wang, T., Streeter, M.D., and Spiegel, D.A. (2015) Generation and characterization of antibodies against arginine-derived advanced glycation endproducts. *Bioorganic & Medicinal Chemistry Letters*, **25**, 4881-4886.
26. Wang, P., Lu, Y.C., Wang, J., Wang, L., Yu, H., Li, Y.F., Kong, A., Chan, J., and Lee, S. (2018) Type 2 Diabetes Promotes Cell Centrosome Amplification via AKT-ROS-Dependent Signalling of ROCK1 and 14-3-3sigma. *Cellular Physiology and Biochemistry*, **47**, 356-367.
27. Morgenstern, J., Katz, S., Krebs-Haupenthal, J., Chen, J., Saadatmand, A., Cortizo, F.G., Moraru, A., Zemva, J., Campos, M.C., Teleman, A., Backs, J., Nawroth, P., and Fleming, T. (2020) Phosphorylation of T107 by CamKIIδ Regulates the Detoxification Efficiency and Proteomic Integrity of Glyoxalase 1. *Cell Reports*, **32**.
28. Richarme, G., Liu, C., Mihoub, M., Abdallah, J., Leger, T., Joly, N., Liebart, J.-C., Jurkunas, U.V., Nadal, M., and Bouloc, P. (2017) Guanine glycation repair by DJ-1/Park7 and its bacterial homologs. *Science*, **357**, 208-211.
29. Tatone, C., Heizenrieder, T., Di Emidio, G., Treffon, P., Amicarelli, F., Seidel, T., and Eichenlaub-Ritter, U. (2011) Evidence that carbonyl stress by methylglyoxal exposure induces DNA damage and spindle aberrations, affects mitochondrial integrity in mammalian oocytes and contributes to oocyte ageing. *Human Reproduction*, **26**, 1843-1859.
30. Wang, F., and Higgins, J.M. (2013) Histone modifications and mitosis: countermarks, landmarks, and bookmarks. *Trends in Cell Biology*, **23**, 175-184.
31. Luengo, A., Abbott, K.L., Davidson, S.M., Hosios, A.M., Faubert, B., Chan, S.H., Freinkman, E., Zacharias, L.G., Mathews, T.P., Clish, C.B., DeBerardinis, R.J., Lewis, C.A., and Vander Heiden, M.G. (2019) Reactive metabolite production is a targetable liability of glycolytic metabolism in lung cancer. *Nature Communications*, **10**, 5604.
32. Bellier, J., Nokin, M.J., Caprasse, M., Tiamiou, A., Blomme, A., Scheijen, J.L., Koopmansch, B., MacKay, G.M., Chiavarina, B., Costanza, B., Rademaker, G., Durieux, F., Agirman, F., Maloujahmoum, N., Cusumano, P.G., Lovinfosse, P., Leung, H.Y., Lambert, F., Bours, V., Schalkwijk, C.G., Hustinx, R., Peulen, O., Castronovo, V., and Bellahcene, A. (2020) Methylglyoxal Scavengers Resensitize KRAS-Mutated Colorectal Tumors to Cetuximab. *Cell Reports*, **30**, 1400-1416 e1406.
33. Levine, M.S., Bakker, B., Boeckx, B., Moyett, J., Lu, J., Vitre, B., Spierings, D.C., Lansdorp, P.M., Cleveland, D.W., Lambrechts, D., Foijer, F., and Holland, A.J. (2017) Centrosome Amplification Is Sufficient to Promote Spontaneous Tumorigenesis in Mammals. *Developmental Cell*, **40**, 313-322 e315.

34. Carroll, P.E., Okuda, M., Horn, H.F., Biddinger, P., Stambrook, P.J., Gleich, L.L., Li, Y.-Q., Tarapore, P., and Fukasawa, K. (1999) Centrosome hyperamplification in human cancer: chromosome instability induced by p53 mutation and/or Mdm2 overexpression. *Oncogene*, **18**, 1935-1944.

3 Chapter 3. Folic acid deficiency increases sensitivity to DNA damage by glucose and methylglyoxal

The information presented in this Chapter is reproduced from an article published in Mutagenesis.

Donnellan, L., Simpson, B.S., Dhillon, V.S., Costabile, M., Fenech, M., and Deo, P. (2022) Folic acid deficiency increases sensitivity to DNA damage by glucose and methylglyoxal. *Mutagenesis*, **37**, 24-33. 10.1093/mutage/geac003

The above manuscript was selected as Editor's Choice for Volume 37, Issue 1.

For continuity and ease of reading the following article is presented here in chapter format. See Appendix B for authorship statement. All **Table**s and **Figures** that correspond to the supplementary documentation within this chapter can be accessed via the appropriate Digital Object Identifier (DOI) listed above.

Preamble

In the previous chapter, we found that MGO can induce DNA damage, as measured by the CBMNcyt assay in WIL2-NS and PBL. It has recently been shown that high concentrations of various sugars, including glucose can induce DNA damage under folic acid deficient conditions. As MGO is formed as a by-product of glycolysis, we explored whether this increased susceptibility to glucose under folic acid deficient conditions was the result of increased MGO. We also explore the relationship between folic acid deficiency and the concentration of MGO and MGO glycation adducts.

3.1 Abstract

Type 2 diabetes (T2D) is associated with elevated frequencies of micronuclei (MNi) and other DNA damage biomarkers. Interestingly, individuals with T2D are more likely to be deficient in micronutrients (folic acid, pyridoxal-phosphate, cobalamin) that play key roles in one-carbon metabolism and maintaining genomic integrity. Furthermore, it has recently been shown that deficiencies in these nutrients, in particular folic acid leaves cells susceptible to glucose induced DNA damage. Therefore, we sought to investigate if the B lymphoblastoid WIL2-NS cell line cultured under folic acid deficient conditions was more sensitive to DNA damage induced by glucose, or the reactive glycolytic byproduct methylglyoxal and subsequent advanced glycation endproduct formation. Here, we show that only WIL2-NS cultured under folic acid deficient conditions (23 nmol/L) experience an increase in MNi frequency when exposed to high concentrations of glucose (45 mmol/L) or methylglyoxal (100 µmol/L). Furthermore, we showed aminoguanidine, a well validated methylglyoxal and free radical scavenger was able to prevent further MNi formation in folic acid deficient cells exposed to high glucose, which may be due to a reduction in methylglyoxal induced oxidative stress. Interestingly, we also observed an increase in methylglyoxal and other dicarbonyl stress biomarkers in folic acid deficient cells, irrespective of glucose concentrations. Overall, our evidence shows that folic acid deficient WIL2-NS cells are more susceptible to glucose and/or methylglyoxal induced MNi formation. These results suggest that individuals with T2D experiencing hyperglycemia and folic acid deficiency may be at higher risk of chromosomal instability.

3.2 Introduction

Micronutrients play a key role in maintaining genomic integrity because of their function as substrates or cofactors for enzymes involved in DNA synthesis and repair and DNA methylation (1). The B group vitamins folate (B9), pyridoxine (B6) and cobalamin (B12), in their various bioactive forms such as methyl-tetrahydrofolate, pyridoxal-phosphate and methyl-cobalamin, respectively, are critical for one-carbon metabolism. This process is required for the synthesis of deoxythymidine monophosphate (dTTP) from deoxyuridine monophosphate (dUMP) and remethylation of homocysteine to methionine and ultimately S-adenosyl methionine required for maintenance of DNA methylation patterns (2). Deficiency in these vitamins is associated with genomic instability, caused primarily by uracil misincorporation into DNA and induction of micronuclei (MNi), which can be measured by the cytokinesis block micronucleus cytome (CBMNcyt) assay (3,4). Moreover, deficiencies in pyridoxine and folic acid are associated with whole chromosome loss events, chromosomal rearrangement and telomere attrition (4,5). Interestingly, deficiencies in these vitamins are associated with increased cellular susceptibility to DNA damage by other genotoxins. For example, B lymphoblastoid WIL2-NS cells grown in folic acid deficient RPMI are more sensitive to radiation induced DNA damage (1.5 Gy), experiencing a ~two-fold increase in MNi and nucleoplasmic bridges (NPBs) compared to controls grown in standard RPMI (6). Therefore, it is important to consider how vitamin deficiencies may alter cellular responses to other genotoxic stresses, as various pathological conditions are associated with altered metabolic states.

Chromosomal instability (CIN) has been observed in individuals with Type 2 Diabetes (T2D). The CBMNcyt assay has been used to demonstrate that peripheral blood lymphocytes (PBL) and buccal cells from T2D patients contain elevated levels of MNi and other DNA damage biomarkers (7-11). Two recent meta-analyses have shown the meta-MR (mean ratio) for micronucleus frequency in lymphocytes in those with diabetes mellitus is 1.99 ($P<0.01$; T2D) and 1.74 ($P<0.001$; T2D and T1D) when compared to control groups (11,12). Despite this association, very few studies have investigated the potential underlying mechanisms. Interestingly, several studies have shown that individuals with T2D are more likely to be folate deficient than healthy controls, which may contribute to this observed CIN (13,14). We have recently shown that the reactive dicarbonyl compound methylglyoxal (MGO), which is

elevated in T2D, increases MNi frequency in WIL2-NS and cultured primary PBL by inducing chromosome malsegregation during mitosis (15). MGO is formed as a by-product of glycolysis, which may suggest elevated glycolytic flux, as seen in hyperglycemic states, may impact CIN in T2D (16). High concentrations of glucose have also been shown to induce MNi and other chromosomal aberrations in folic acid deficient, normal human colon mucosal cell lines (NCM460, CCD841) and human liver (L02) cells (17). Moreover, pyridoxal-phosphate deficient HeLa cells and brain cells isolated from *Drosophila melanogaster* have also been shown to be sensitive to glucose-induced DNA damage (18,19). The cause for the interaction between glucose and folic acid was not investigated. However, the glucose-induced DNA damage in pyridoxal-phosphate deficient HeLa cells was shown to be associated with the formation of advanced glycation endproducts (AGEs), a class of post-translational modifications, several of which are formed by MGO. Moreover, pyridoxal phosphate acts a cofactor for the enzyme serine hydroxymethyltransferase, which is directly involved in folate mediated one-carbon metabolism (specifically the synthesis of 5,10 methylene tetrahydrofolate required for the synthesis of dTTP from dUMP). Therefore, alterations in this pathway may leave cells susceptible to DNA damage caused by elevated glucose and/or glycolytic by-products which may adduct onto DNA or proteins involved in DNA synthesis/ repair processes or mitosis (20-22).

The aim of this study was to determine if folic acid deficiency alters cellular sensitivity of WIL2-NS to glucose-induced DNA damage. Furthermore, we investigated the role dicarbonyl stress may have on this increased susceptibility to DNA damage under folic acid deficient conditions. Herein we reveal a significant interaction between folic acid and glucose or MGO with respect to MNi frequency. Furthermore, we show that aminoguanidine, which can scavenge both MGO and free radicals, was able to prevent glucose-induced DNA damage in folic acid deficient cells. Our results suggest that glucose-induced dicarbonyl and oxidative stress exacerbates DNA damage under folic acid deficient conditions.

3.3 Methods

3.3.1 Materials

All reagents, chemicals and enzymes were purchased from Sigma unless indicated otherwise. All reagents for cell culture were of cell culture grade. Isotopically labelled and unlabelled MG-H1, CEL and Lysine were purchased from Iris biotech (Marktredwitz, Germany).

3.3.2 Media preparation

High glucose RPMI (45 mmol/L) was prepared by dissolving 6.1 g of glucose (G7021, Sigma) in 1 L of standard RPMI (R0883, Sigma; LG,11.1 mmol/L glucose). Media was then passed through a 0.2 µm filter under vacuum directly into a sterile container and stored at 4°C.

For the preparation of media with different concentrations of folic acid, RPMI-1640, 10x without folic acid (R1145, Sigma), was diluted 1:10 with 900 mL of pre autoclaved Milli-Q. Sodium bicarbonate (2.0 g) was added, and the solution passed through a 0.2 µm filter under vacuum directly into a sterile container. This was repeated with the inclusion of 6.1 g of glucose for high glucose folic acid-free RPMI. For the preparation of 23 (deficient) and 226 (medium) nmol/L folic acid RPMI, standard RPMI (Replete; 2264 nmol/L) was diluted 1:100 and 1:10, respectively, with either low or high glucose folic acid-free RPMI to achieve the required final concentration of each ingredient.

3.3.3 WIL2-NS cell culture

The WIL2-NS (ATCC CRL-8155) cell line was kindly gifted by the Commonwealth Scientific Research Organization (Adelaide, Australia). Cells were grown in RPMI supplemented with 5% (v/v) Fetal Calf Serum (FCS), L-glutamine (1% v/v) and penicillin/streptomycin (1% v/v) at 37°C in a humidified atmosphere with 5% CO_2. This study involved three experiments, which differed based on the medium composition of folic acid, glucose or MGO as well as culturing duration and are described in figure 3.1. Briefly, in experiment #1, cells were seeded at 3 x 10^5 cells/mL and subcultured back to the original

seeding density every 3.5 days. On day 7 and 14, an aliquot of cells (1.5 x 10^5 cells) was used for the CBMNcyt assay in which cytochalasin-B (cyt-B; 4.5 µg/mL) was added and cells harvested 24 hours later and prepared as described below. For experiment #2, cells were seeded at 3 x 10^5 cells/mL and subcultured back to original seeding density on day 3.5 and treated with vehicle (HBSS) or MGO (100 µmol/L) on day 5. The CBMNcyt assay was set up on day 7 by the addition of cyt-B (4.5 µg/mL) and harvested 24 hours later. For experiment #3, the folic acid concentration was kept constant at 23 nmol/L across all samples, and glucose concentrations were either 11.1 (low) or 45 mmol/L (high). Cells were either cultured in the presence of aminoguanidine (MGO scavenger; 100 µmol/L) or vehicle (HBSS). Cells were seeded at 3 x 10^5 and subcultured back to original seeding density every 3.5 days. On day 7, an aliquot of cells (1.5 x 10^5 cells) was removed for the CBMNcyt assay (as described for experiment #1 and #2) and remainder were harvested for quantification of dicarbonyl stress biomarkers.

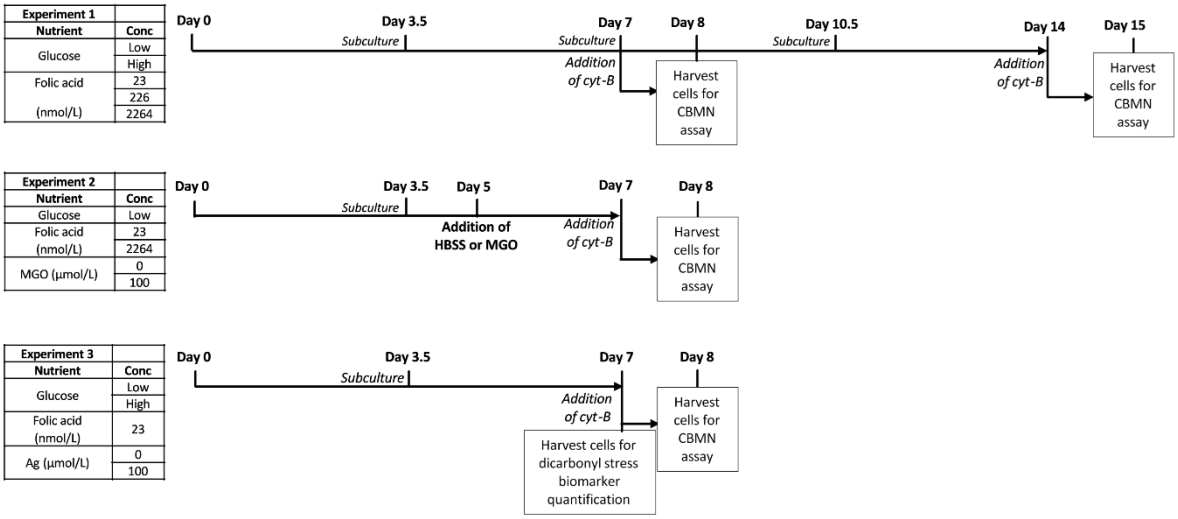

Figure 3.1. Culturing procedure for experiments 1-3. Experiment 1; WIL2-NS were cultured in LG or HG with varying concentrations of folic acid for 14 days. Cells were subcultured every 3.5 days and CBMNcyt assay performed on day 7 and 14. Experiment 2; WIL2-NS were cultured under folic acid deficient or replete conditions for 7 days and subcultured after 3.5 days MGO or vehicle (HBSS; Hanks balanced salt solution) was added to the media on day 5 for a further 48 hours and CBMNcyt assay was performed on day 7. Experiment 3; Cells were cultured under folic acid conditions in either LG or HG media for 7 days. Cells were also cultured in the presence or absence of aminoguanidine (100 µmol/L). Cells were subcultured on day 3.5 and CBMNcyt assay was performed on day 7. LG; low glucose (11.1 mmol/L glucose). HG; high glucose (45 mmol/L glucose). MGO; methylglyoxal. Ag; aminoguanidine. Cyt-b; cytochalasin-b.

3.3.4 CBMNcyt assay

The CBMNcyt assay is a comprehensive system for measuring DNA damage, cytostasis and cytotoxicity. DNA damage events are scored specifically in once-divided binucleated (BN) cells and include (a) micronuclei (MNi), a biomarker of chromosome breakage and/or whole chromosome loss, (b) nucleoplasmic bridges (NPBs), a biomarker of DNA misrepair and/or telomere end-fusions, and (c) nuclear buds (NBUDs), a biomarker of elimination of amplified DNA and/or unresolved DNA repair complexes. Cytostatic effects are measured via the proportion of mono-, bi- and multinucleated cells to calculate the nuclear division index (NDI), and cytotoxicity is determined via necrotic and/or apoptotic cell ratios. These biomarkers are identified microscopically using well-established and validated criteria as previously described (23). At day 7 and/ or 14, an aliquot of cells were removed and subcultured to 3 x 10^5 cells/mL (in 0.5 mL of media) and treated with cytochalasin-B (cyt-B; 4.5 µg/mL) (23). Cells were harvested 24 hours later, and slide preparation and scoring of the CBMNcyt assay was performed as described previously (23,24) using a NanoZoomer S60 (Hammatsu Photonics).

3.3.5 Quantification of MGO in cells and media

MGO was quantified by derivatization with o-phenylenediamine (O-PD) to 2-methylquinoxaline (2-MQ) as previously described with some modification (25,26). Briefly, 20 µL of 20% TCA (w/v)/ 0.9 % saline (w/v) was added to 40 µL of media or cell pellet (~$2x10^6$ cells resuspended in 40 µL of ddH_2O). Samples were briefly vortexed, and 40 µL of ddH_2O was added to the sample. Cell samples were sonicated for 30 seconds at 35% intensity (Misonix, NY, USA). Samples were then placed on a rotating incubator (150 rpm) for 10 min before being centrifuged at 14,000 g for 10 min. An aliquot (70 µL) was removed and mixed with 10 µL of 3% (w/v) sodium azide and 20 µL of 500 µM O-PD (in 200 mM HCl/ 500 µM diethylenetriaminepentaacetic acid). Samples were derivatized for 4 hours in the dark. Following derivatization, 5 µL of pre-synthesized d_4-2-MQ was added (prepared as above by reacting MGO with d_4-O-PD (Toronto Research Chemicals, P319842)). Ten microliters of the derivatized solution were chromatographed with a 100 x 3 mm, 3 µm Gemini C18 (Phenomenex, Torrance, CA, USA) column with a linear gradient of 0.1 % formic in water (Buffer A) and 0.1% formic acid in acetonitrile (Buffer B) over 9 min at a flow rate of 0.5 mL/ min. Multiple reaction monitoring (MRM) was conducted in positive mode using an AB Sciex 6500+ QTRAP mass spectrometer with the following transitions: *m/z* 145.1 > 77.1 (2-MQ); *m/z* 149.1 > 77.1 (d_4 2-MQ).

3.3.6 Quantification of protein-bound MG-H1, CEL and Lysine

Measurement of AGEs from total cellular protein was performed as previously described with some modifications (27). Briefly, cells (~5 x 10^6) were collected and washed twice with PBS. Cells were lysed by sonication at 35% for 90 seconds and the supernatant collected following centrifugation (17,000 *g* for 10 min). A total of 100 ug of protein was precipitated with ice-cold acetonitrile: methanol (3:1) and stored for 20 min at -20°C and then collected by centrifugation (17,000 *g* for 10 min). Supernatant was discarded and residual acetonitrile was removed under a stream of nitrogen. Samples were reconstituted in 20 µL of water. Following this, 10 µL of 100 mM HCl, 5 µL of pepsin (2 mg/mL in 20 mM HCl) and 5 µL of thymol solution (1 mg/mL in 20 mM HCl) were added. Samples were incubated at 37°C for 24

hours on a shaking incubator (150 rpm). Following incubation, 12.5 µL of 100 mM potassium phosphate buffer, pH 7.4, was added to the sample. After this, 5 µL of 260 mM KOH, 5 µL of Pronase E (2 mg/mL in 10 mM potassium phosphate buffer pH 7.4) and 5 µL of Pen-Strep (1000 units/ mL and 1 mg/mL, respectively) were added to the mixture and samples were further incubated at 37°C for 24 hours in a rotating incubator (150 rpm). Following this, 5 µL of aminopeptidase (2 mg/mL in 10 mM potassium phosphate buffer pH 7.4) and 5 µL of prolidase (2 mg/mL in 10 mM potassium phosphate buffer pH 7.4) was added, and samples were further incubated at 37°C for 48 hours in a rotating incubator. Sample (1 µL) was injected and analytes were separated using a 150 × 4.6 mm, 4 µm Phenomenex C18 column (Phenomenex, Torrance, CA, USA) with a linear gradient of 0.1 % formic in water (Buffer A) and 0.1% formic acid in acetonitrile (Buffer B) over 5 min at a flow rate of 0.6 mL/ min. Multiple reaction monitoring (MRM) was conducted in positive mode using an AB Sciex 6500+ QTRAP mass spectrometer with the following transitions *m/z* 147.4 > 83.9 (lysine), 151.2 > 87.9 (d_4 lysine), 219.2 > 130.2 (CEL), 222.2 > 134.2 (d_4 CEL), 229.2 > 116.1 (MG-H1) 232.2 > 116.1 (d_3 MG-H1).

3.3.7 Quantification of free MG-H1 and CEL

Due to the low concentration of MG-H1 and CEL in cell culture media, a derivatization step was used to increase the sensitivity of their detection as previously described (28). An aliquot of internal standard (100 nmol/L) was added to cell culture media (100 µL), which was deproteinized with acetonitrile: methanol (3:1). The supernatant was collected following centrifugation (17, 000 *g*, 10 min) and dried under a stream of nitrogen. The sample was reconstituted in 1-butanol:HCl (3:1) and heated at 70°C for 90 min. The samples were then dried under nitrogen and reconstituted in 5% (v/v) MeOH. Standards were prepared identically to samples. Sample (5 µL) was injected and analytes were separated using a 150 × 4.6 mm, 4 µm Phenomenex C18 column (Phenomenex, Torrance, CA, USA) with 0.1 % (v/v) formic in water (Buffer A) and 0.1% (v/v) formic acid in acetonitrile (Buffer B) over 10 min at a flow rate of 0.7 mL/ min. Multiple reaction monitoring (MRM) was conducted in positive mode using an AB Sciex 6500+ QTRAP mass spectrometer with the following transitions *m/z* 331.1 > 186.1 (CEL), 335.2 > 190.1 (d_4 CEL), 285.1 > 172.1 (MG-H1), 288.0 > 172.1 (d_3 MG-H1).

3.3.8 Quantification of media 8-Oxo-2'-deoxyguanosine (8-oxodG)

An aliquot of media was passed through a micro spin ultrafiltration (Amicon-Ultra; 10 kDa cut-off) column. Internal standard ([15N, $13C_2$] 8-oxodG) was added to a final concentration of 10 nmol/L. Sample (10 µL) was injected and the analyte was separated using a 100 x 3 mm, 3 µm Gemini C18 (Phenomenex, Torrance, CA, USA) column with 0.1 % (v/v) formic in water (Buffer A) and 0.1% (v/v) formic acid in acetonitrile (Buffer B) over 10 min at a flow rate of 0.5 mL/ min. An aliquot of [$15N_5$, $13C_{10}$] 2-deoxyguanosine (2-dG) was also added (10 nmol/L) to ensure both analytes were resolved to prevent overestimation of 8-oxodG by in source formation from oxidation of 2-dG. Multiple reaction monitoring (MRM) was conducted in positive mode using an AB SCIEX 6500+ QTRAP with the following transitions: *m/z* 284.2 > 168.0 (8-oxodG), 287.2 > 171.0 ([15N, $13C_2$] 8-oxodG).

3.3.9 Statistical Analysis

Data analysis was performed using GraphPad Prism (San Diego, CA, USA, Version 8.0.0). For experiments 1 and 2, a two-way analysis of variance (ANOVA) followed by Bonferroni post-hoc test was conducted to compare the statistical significance of differences in the effect of glucose or MGO at each concentration of folic acid and to determine the percentage of variance explained by each variable and their interaction. One-way analysis of variance (ANOVA) followed by Dunnett post-hoc test was conducted when comparing between groups of experiment 3. A $p<0.05$ was considered significant, and the results were expressed as mean ± standard deviation (SD) from 3-4 independent experiments.

3.4 Results

3.4.1 Folic acid deficient cells are sensitive to glucose-induced DNA damage.

We hypothesized that the interaction between folic acid and glucose was a result of elevated dicarbonyl stress. To address this, we first evaluated the intracellular MGO concentrations of WIL2-NS cells cultured under high glucose (45 mmol/L) versus low glucose (11.1 mmol/L) conditions. Cells cultured in high glucose for 7-days showed a 6-fold increase in the concentration of intracellular MGO compared

to those cultured under low glucose, thus confirming it as an appropriate model of dicarbonyl stress (Supplementary Figure 1). We next evaluated the interaction between folic acid and glucose with respect to cell viability, proliferation and DNA damage biomarkers as measured by the CBMNcyt assay (NDI, necrosis, MNI, NPB, NBUD). Folic acid deficiency caused a dose-dependent reduction in proliferation and viability over a 14-day period, though, at 2264 and 226 nmol/L, the addition of high glucose had no impact (Supplementary Figure 2A, B). However, at 23 nmol/L folic acid, high glucose resulted in a further significant reduction in proliferation and viability on day 14 (Supplementary Figure 2A, B). To confirm this effect of high glucose in a folic acid deficient environment was not caused by osmotic stress, the additional glucose in these cultures was replaced with non-metabolizable mannitol. No significant difference was observed between high mannitol and low glucose at any concentration of folic acid for proliferation and viability (Supplementary Figure 2C, D).

We next measured cytogenetic and DNA damage biomarkers on day 7 and 14. No significant difference was observed between low and high glucose cultures at any concentration of folic acid for NDI, frequency of necrotic cells, NBUDs or NPBs at day 7 or day 14 (Supplementary Figure 3A-D, Figure 3.2B-D, F, G). However, at days 7 and 14, high glucose increased the frequency of MNi in cells cultured in 23 nmol/L folic acid, but not in 226 or 2264 nmol/L (Figure 3.2A, E). Furthermore, high glucose increased total DNA damage in folic acid deficient cells on day 14 (Figure 3.2H). To confirm the observed increase in MNi frequency and total DNA damage was not a result of osmotic stress, high mannitol cultures were used. No significant difference was observed for MNi frequency or total DNA damage between low glucose and high mannitol under folic acid deficient conditions at day 7 or day 14 (Supplementary Figure 4A-C). This supports our hypothesis that the effect of glucose in folic acid deficient cells is a downstream effect of glucose metabolism. A two-way ANOVA was conducted to determine if there was a significant interaction between folic acid and glucose concentration on cytogenetic and DNA damage biomarkers. No significant interaction was observed at day 7 for any biomarker. However, on day 14, a significant interaction was observed for MNi frequency and total DNA damage (Table 3.1). These results corroborate previous findings demonstrating folic acid deficient cells are more sensitive to glucose-induced DNA damage than those under replete conditions (17).

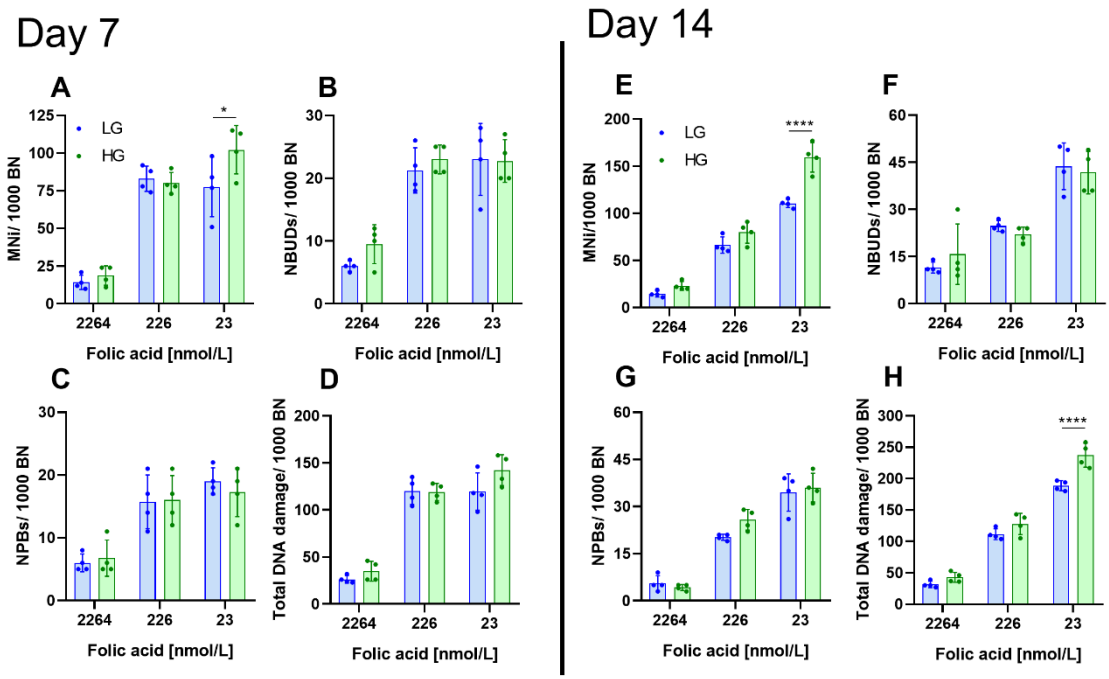

Figure 3.2. Folic acid deficient WIL2-NS cells are sensitive to glucose induced DNA damage. **A-D)** are DNA damage biomarkers measured at day 7, **E-F)** are DNA damage biomarkers measured at day 14. **A,E)** MNi/ 1000 BN. **B,F)** NBUDs/ 1000 BN. **C,G)** NPBs/ 1000 BN and **D,H)** Total DNA damage/ 1000 BN. LG; low glucose. HG; High glucose. Values represent mean ± SD of n=4. *p<0.05,****p<0.0001

Table 3.1. Two-way ANOVA of CBMNcyt assay biomarkers to determine effect of folic acid, glucose and their interaction.

		Source of Variation					
		Day 7			Day 14		
		Folic acid	**Glucose**	**Interaction**	**Folic acid**	**Glucose**	**Interaction**
NDI	Percentage (%)	5.46	0.19	9.53	15.09	2.95	5.35
	P value	0.19	0.84	0.38	0.1983	0.4159	0.5450
Necrosis (%)	Percentage (%)	**79.63**	0.059	0.65	**46.49**	**10.83**	5.69
	P value	**<0.0001**	0.82	0.74	**0.0007**	**0.0339**	0.2761
MNi	Percentage (%)	**87.22**	1.55	2.79	**88.79**	**5.51**	**3.20**
	P value	**<0.0001**	0.0855	0.0768	**<0.0001**	**<0.0001**	**0.0006**
NBUDs	Percentage (%)	**82.35**	1.180	01.00	**83.89**	0.00	1.409
	P value	**<0.0001**	0.2566	0.5700	**<0.0001**	0.9541	0.4385
NPBs	Percentage (%)	**75.90**	0.046	0.8537	**92.74**	0.55	1.14
	P value	**<0.0001**	0.8527	0.7224	**<0.0001**	0.2001	0.1860
Total DNA	Percentage (%)	**91.63**	1.179	1.084	**93.83**	**2.94**	**1.23**
	P value	**<0.0001**	0.0787	0.2299	**<0.0001**	**<0.0001**	**0.0135**

Source of variation was measured by two-way ANOVA and expressed as percentage with corresponding p-value. Values in **bold** are considered a significant source of variation to that biomarker.

3.4.2 Folic acid deficient cells are sensitive to MGO

Elevated concentrations of glucose can increase intracellular levels of MGO (21,29). Therefore, we sought to determine if folic acid deficient cells (23 nmol/L) are more sensitive to MGO than those under replete conditions (2264 nmol/L). To test this, cells were cultured for 7 days in either folic acid replete or deficient media and treated either with HBSS (vehicle) or MGO (100 µmol/L) on day 5 for 48 hours. Under folic acid replete conditions, MGO had no effect on any of the DNA damage biomarkers measured (Figure 3.3A-D). However, under folic acid deficient conditions, the frequency of MNi and total DNA damage was significantly increased compared to untreated cells (Figure 3.3A-D). Furthermore, two-way ANOVA analysis showed the interaction between folic acid and MGO was a significant source of variation for MNi and total DNA damage (Table 3.2).

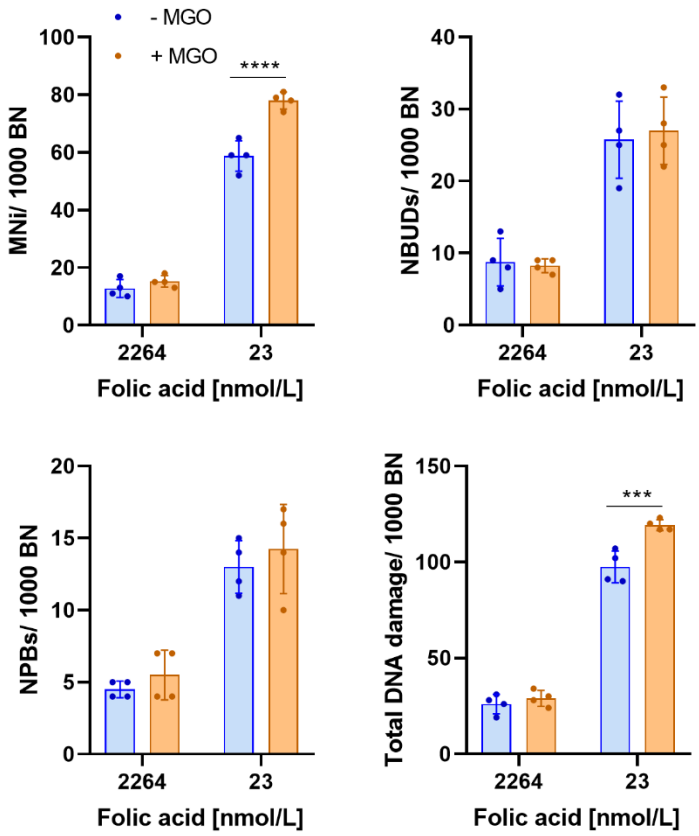

Figure 3.3. Folic acid deficient WIL2-NS cells are sensitive to MGO induced DNA damage. WIL2-NS cells were cultured under low (22.64 nmol/L) or high folic acid (2264 nmol/L) and treated with either HBSS (vehicle) or MGO (100 µmol/L) on day 5. **A)** MNi/ 1000 BN. **B)** NBUDs/ 1000 BN. **C)** NPBs/ 1000 BN and **D)** Total DNA damage/ 1000 BN. Values represent mean ± SD of n=4. ***p<0.001,****p<0.0001

Table 3.2. Two-way ANOVA of CBMNcyt assay biomarkers to determine effect of folic acid, MGO and their interaction.

		Source of Variation		
		Folic acid	**MGO**	**Interaction**
MNi	Percentage (%)	**92.89**	**3.72**	**2.20**
	P value	**p<0.0001**	**p<0.0001**	**p=0.0005**
NBUDs	Percentage (%)	**86.95**	0.04	0.21
	P value	**p<0.0001**	p=0.8530	p=0.6665
NPBs	Percentage (%)	**84.67**	1.44	0.18
	P value	**p<0.0001**	p<0.2861	p=0.9033
Total DNA	Percentage (%)	**95.17**	**2.23**	**1.28**
	P value	**p<0.0001**	**p<0.0007**	**p=0.0052**

Source of variation was measured by two-way ANOVA and expressed as percentage with corresponding p-value. Values in **bold** are considered a significant source of variation to that biomarker.

3.4.3 Aminoguanidine rescues high glucose-induced DNA damage in folic acid deficient cells

We next investigated if the sensitivity of folic acid deficient cells to glucose-induced DNA damage was a result of elevated MGO. To test this, cells were cultured in low or high glucose under folic acid deficient conditions (23 nmol/L) and exposed to either vehicle (HBSS) or aminoguanidine (100 µmol/L), a well-validated MGO scavenger (30). Consistent with our previous results, high glucose increased the frequency of MNi in folic acid deficient conditions (Figure 3.4A). Interestingly, when exposed to aminoguanidine, high glucose no longer increased MNi frequency under folic acid deficient conditions (Figure 3.4A). To ensure the protective effect of aminoguanidine was specific to high glucose cultures, cells under low glucose and folic acid deficient conditions were also exposed to 100 µmol/L aminoguanidine. Aminoguanidine did not reduce the frequency of MNi in cells cultured under folic acid deficient and low glucose conditions. This supports our hypothesis that the interaction between glucose and folic acid was at least in part due to glucose-induced dicarbonyl stress.

To further explore the interaction between glucose induced MNi under folic acid deficient conditions and what role dicarbonyl stress may have had, we investigated various dicarbonyl stress biomarkers.

High glucose significantly increased the concentration of cellular MGO by ~4-fold when compared to low glucose under folic acid deficient conditions; however, this was not impacted by the presence of aminoguanidine (Table 3.3). Furthermore, no differences were observed for the media concentration of MGO, protein-bound and free concentrations of MG-H1 and CEL when high glucose cells were exposed to aminoguanidine (Table 3.3). Since glucose has previously been shown to induce oxidative DNA damage, we quantified the media concentration of 8-Oxo-2'-deoxyguanosine (8oxodG) as a surrogate measure of oxidative stress. No significant difference was observed between low and high glucose cultures regardless of treatment with aminoguanidine (Figure 3.4B); however, 8-oxodG was significantly correlated with the frequency of MNi (R^2=0.9301; *p*=0.0356).

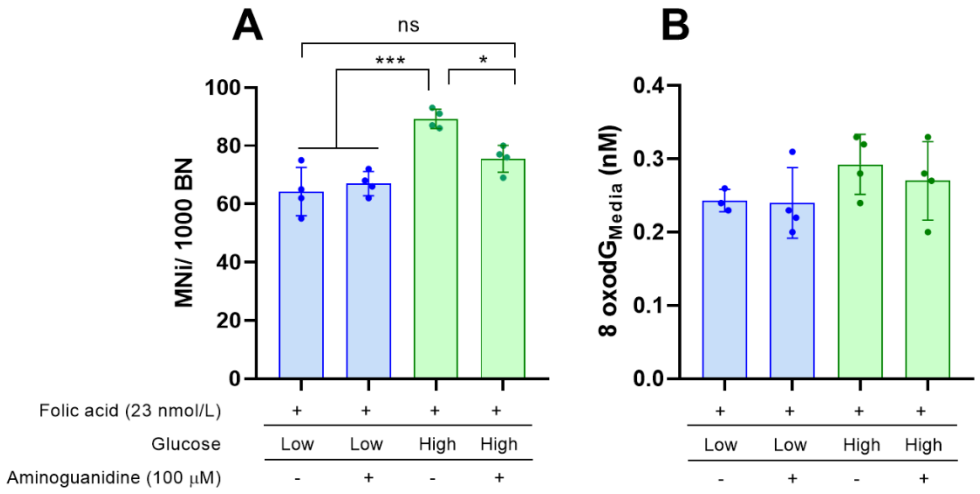

Figure 3.4. Aminoguanidine prevents glucose-induced DNA damage in folic acid-deficient cells. WIL2-NS cells were cultured in folic acid-deficient (23 nmol/l) RPMI under low or high glucose with or without aminoguanidine (100 µmol/l. (A) MNi/1000 BN. (B) Medium 8-oxodG (nM). Values represent mean ± SD of n = 4. ∗P < .05, ∗∗∗P < .001.

Table 3.3. Dicarbonyl stress biomarkers measured in WIL2-NS cells cultured under folic acid deficient conditions (23 nmol/L) in LG or HG, with or without aminoguanidine.

	Sample			
Biomarker	LG	LG +	HG	HG +
Media MGO (pmol/ 10^6 cells)	39.70 ± 11.74	43.88 ± 5.67	46.04 ± 4.49	39.23 ± 11.27
Cellular MGO (Relative abundance)	1.00 ± 0.26	1.22 ± 0.41	3.43 ± 1.15**	3.95 ± 1.33**
MG-H1 (mmol/mol lysine)	0.15 ± 0.05	0.13 ± 0.04	0.18 ± 0.04	0.12 ± 0.04
CEL (mmol/mol lysine)	0.06 ± 0.02	0.04 ± 0.02	0.05 ± 0.01	0.04 ± 0.01
$MG\text{-}H1_{media}$ (pmol/10^6 cells)	79.14 ± 8.11	65.02 ± 15.56	76.57 ± 23.51	61.27 ± 21.41
CEL_{media} (pmol/10^6 cells)	1.60 ± 0.38	0.91 ± 0.33	1.08 ± 0.18	1.43 ± 0.60

Data are mean ± SD, n=4. Significance: **p<0.01 when compared to LG. LG; low glucose. HG; high glucose.

3.4.4 Folic acid deficiency increases dicarbonyl stress biomarkers

Interestingly, we observed from the previous section that under folic acid deficient conditions, cells cultured under high glucose experience a smaller increase (3.4-fold; Table 3.3) in intracellular MGO than those cultured under folic acid replete conditions (6-fold; Supplementary Figure 1). We hypothesized that this may be due to folic acid deficient cells already having higher levels of intracellular MGO than those under replete conditions, which would account for the smaller increase in MGO following addition of high glucose. Therefore, we compared the concentration of various dicarbonyl stress biomarkers between WIL2-NS in folic acid replete and deficient media. We found a significant increase in both cellular (2.14-fold) and media (2.36-fold) concentrations of MGO in folic acid deficient cells when compared to replete controls (Figure 3.5A,B). We next investigated the concentration of protein bound MG-H1 and CEL, however no difference was observed between folic acid replete and deficient controls (Figure 3.5C, D). Lastly, we measured the media concentration of MG-H1 and CEL. From this, we found no significant difference in media CEL, however, media concentrations of MG-H1 significantly increased from 26.21 ± 3.40 pmol/10^6 cells in folic acid replete controls to 79.14 ± 8.11 pmol/ 10^6 cells in deficient cells (Figure 3.5E, F). This suggests that folic acid

deficient cells may experience higher levels of dicarbonyl stress, irrespective of glucose concentration.

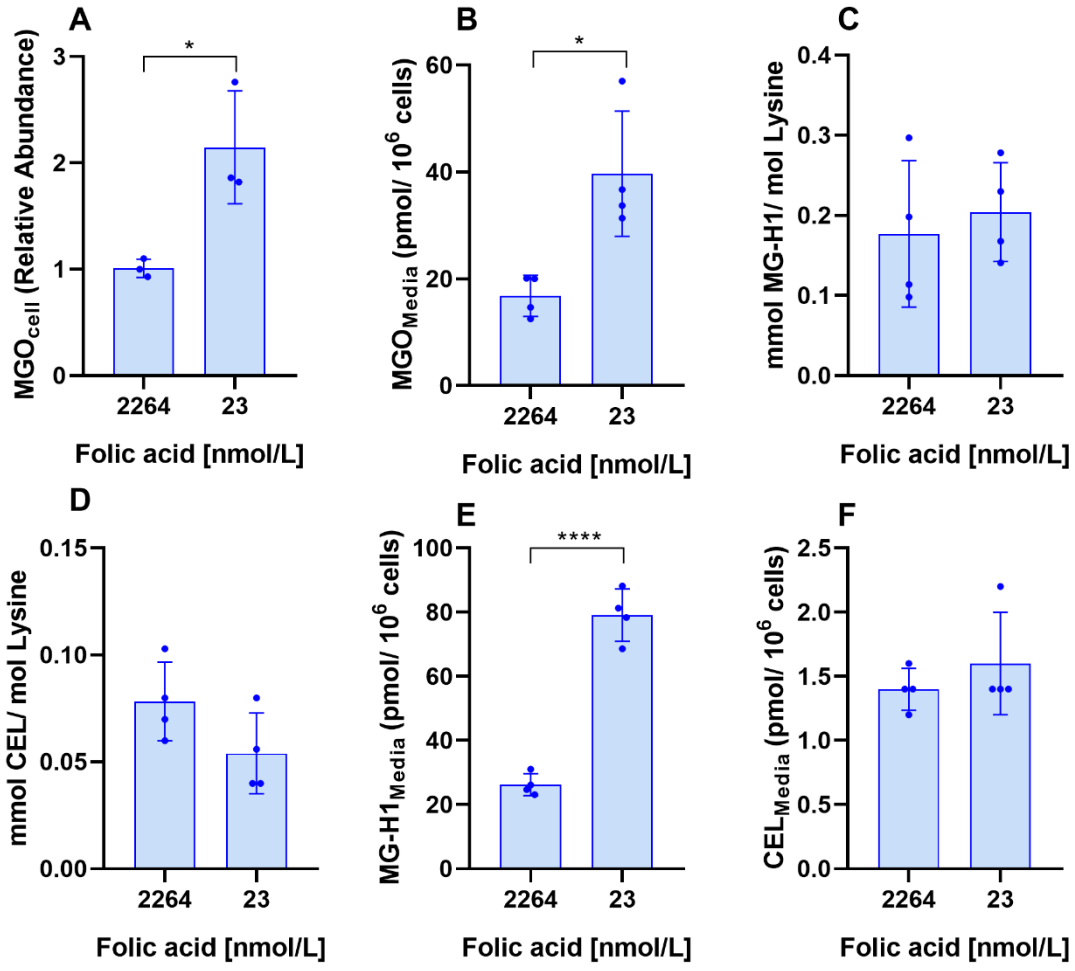

Figure 3.5. Folic acid deficiency increases concentration of dicarbonyl stress biomarkers. WIL2-NS cells were cultured in folic acid replete (2264 nmol/L) or deficient (23 nmol/L) RPMI under LG for 7-days. **A)** Intracellular MGO expressed as relative abundance to control. **B)** Medium MGO normalized to cell number (pmol/ 10^6 cells). **C)** Protein bound concentration of MG-H1 normalized to lysine content (mmol/ mol lysine). **D)** Protein bound concentration of CEL normalized to lysine content (mmol/ mol lysine). **E)** Medium concentration of MG-H1 normalized to cell number (pmol/ 10^6 cells). **E)** Medium concentration of CEL normalized to cell number (pmol/ 10^6 cells). Values represent mean ± SD of n=3-4. *p<0.05, ****p<0.0001.

3.5 Discussion

Accumulation of intracellular MGO and the formation of AGEs have been implicated in the pathogenesis of various diabetic complications. However, little is known about their role in chromosomal instability (CIN). We recently reported that MGO induces CIN and mitotic dysfunction in WIL2-NS and peripheral blood lymphocytes (15). In this current study, we show that cells deficient in folic acid are more sensitive to glucose or MGO-induced DNA damage. We also provide evidence that the increased sensitivity to glucose under folic acid deficient conditions may be in part be due to elevated concentrations of cellular MGO. Furthermore, we reveal that deficiency in folic acid leads to elevated MGO and other dicarbonyl stress biomarkers. Understanding these interactions is important as various pathological states, such as T2D, are associated with altered metabolism and/or deficiencies in various micronutrients.

Data herein supports previous findings that folic acid deficient cells are more sensitive to glucose-induced DNA damage than those under replete conditions (17).

Under folic acid deficient conditions, WIL2-NS cells showed an elevated propensity for MNi induction when exposed to glucose or MGO. The reactive glycolytic by-product MGO, is a major metabolite produced under hyperglycemic conditions and can be elevated up to 8-fold in T2D (31). Under *in vitro* conditions, high concentrations of glucose can increase intracellular MGO concentrations by up to 6-fold, which is consistent with the increase observed in this study (21,32). To determine if elevated MGO influenced the interaction between folic acid and glucose with respect to MNi frequency, the dicarbonyl scavenger aminoguanidine was used. Under folic acid conditions, the addition of aminoguanidine to high glucose cultures reduced the MNi frequency back to similar levels seen in the low glucose cultures. Furthermore, we showed that this protective effect of aminoguanidine was specific to high glucose cultures and showed no benefit under folic acid deficient conditions when glucose levels were low. However, although aminoguanidine did reduce the frequency of MNi, it had no effect on intracellular MGO or other dicarbonyl stress biomarkers. Therefore, this suggests the protective effect of aminoguanidine is independent of its MGO scavenging activity. Aminoguanidine has previously been shown to inhibit inducible nitric oxide synthase (iNOS) and contain radical scavenging activity (33,34). High concentrations of glucose in cell culture model systems has been shown to increase the production of reactive oxygen species (ROS), which can cause oxidative DNA damage and subsequently MNi

formation (35,36). In this study, we showed that MNi frequency was significantly correlated with the medium concentration of 8-oxodG. Therefore, high glucose may have stimulated ROS production, further increasing DNA damage and MNi formation, which was then rescued by radical scavenging activity of aminoguanidine. A significant interaction was also observed between folic acid and MGO. MGO has also been shown to stimulate production of ROS, which may have further influenced MNi formation (37). Furthermore, we have shown MGO induces whole chromosome loss events in WIL2-NS cells which may have been perpetuated under folic acid conditions, which has been shown to impair spindle assembly checkpoints (15,38).

Interestingly, in the previous study by Guo et.al (2019) the authors also observed an interaction between folic acid and other sugars, fructose, galactose and sucrose with respect to DNA damage biomarkers. (17). When studying glycation, glucose is usually the metabolite of interest due to its high intracellular concentrations, relative to other sugar. However, other reducing sugars, such as fructose and galactose can also react with lysine and arginine residues via the Maillard reaction forming AGEs (39,40). The concentration of these sugars in most tissues is significantly lower than glucose, however, in cells from kidney and lens, especially in diabetic patients where concentration of fructose can reach up to 15 mM, their effect may be more pronounced (41). Furthermore, fructose is metabolized by the liver, and enters the glycolytic pathway where it may contribute to MGO formation (42). Therefore, under folic acid conditions, other sugar metabolites may also be genotoxic due to their glycation potential which have contributed to the interaction with folic acid observed previously (17).

In this study, we found that cells deficient in folic acid had significantly higher levels of cellular MGO amongst other dicarbonyl stress biomarkers. Interestingly, it has previously been shown that pyridoxal-phosphate (active form of vitamin B6), which is also critical in one-carbon metabolism deficiency increases the concentration of AGEs in HeLa and *Drosophila melanogaster*, and this was associated with increased CIN (18). Furthermore, pyridoxal-phosphate deficiency was associated with elevated intracellular glucose concentrations, however, as this vitamin is a cofactor for many enzymes, it is unclear if its role in one-carbon metabolism was involved (18,19). Although MGO is primarily formed as a byproduct of glycolysis, other pathways such as threonine and glycine interconversion can also contribute under specific circumstances (43-45). Origin of MGO can be discerned by stable isotope experiments with [U-$^{13}C_6$] glucose and [U-$^{13}C_2$] glycine where the former produces fully labeled MGO

(mass + 3 Da) and the latter produces MGO with one labeled carbon (mass + 1 Da) (46). Nevertheless, it seems unlikely the elevated concentration of endogenous MGO significantly contributed to the observed DNA damage in folic acid deficient cells, as addition of aminoguanidine showed no protective benefit. However, the large increase in DNA damage (4.6-fold) induced by folic acid deficiency may also have overshadowed any impact by MGO. Nevertheless, persistent dicarbonyl stress, even at low levels may have significant pathophysiological impacts.

Numerous studies have observed elevated frequency of MNi in T2D (7-11). MNi frequency has been shown to be a prospective biomarker for cancer incidence with a 1.84 and 1.53-fold increase in relative risk for individuals with medium and high MNi frequency, respectively (47). This is important considering the observations that individuals with T2D have an increased cancer risk (48). Therefore, based on the results observed in this study, folic acid deficiency in T2D may potentiate the genotoxic effects of elevated glucose concentrations which may be associated with increased cancer risk observed in these individuals. In support of this, several studies have shown a decrease in MNi frequency of T2D following folic acid supplementation (49,50). However, whether this has any effect on cancer incidence has not been previously reported.

Overall, we found that folic acid deficient WIL2-NS cells are sensitive to high concentrations of glucose, or the glycolytic by-product MGO with respect to MNi formation. Furthermore, we showed that this interaction may be exacerbated by the production of ROS, which may be dependent on MGO formation. The present study provides further insight into the genotoxic interaction between folic acid and glucose, which is of significant importance due to the association between folate deficiency and T2D (13,14).

References

1. Fenech, M. (2012) Folate (vitamin B9) and vitamin B12 and their function in the maintenance of nuclear and mitochondrial genome integrity. *Mutation Research*, **733**, 21-33.
2. Clare, C.E., Brassington, A.H., Kwong, W.Y., and Sinclair, K.D. (2019) One-Carbon Metabolism: Linking Nutritional Biochemistry to Epigenetic Programming of Long-Term Development. *Annual Review of Animal Biosciences*, **7**, 263-287.
3. Crott, J.W., Mashiyama, S.T., Ames, B.N., and Fenech, M. (2001) The effect of folic acid deficiency and MTHFR C677T polymorphism on chromosome damage in human lymphocytes in vitro. *Cancer Epidemiology Prevention Biomarkers*, **10**, 1089-1096.
4. Wu, X., Xu, W., Zhou, T., Cao, N., Ni, J., Zou, T., Liang, Z., Wang, X., and Fenech, M. (2016) The Role of Genetic Polymorphisms as Related to One-Carbon Metabolism, Vitamin B6, and Gene-Nutrient Interactions in Maintaining Genomic Stability and Cell Viability in Chinese Breast Cancer Patients. *International Journal of Molecular Sciences*, **17**.
5. Bull, C.F., Mayrhofer, G., O'Callaghan, N.J., Au, A.Y., Pickett, H.A., Low, G.K., Zeegers, D., Hande, M.P., and Fenech, M.F. (2014) Folate deficiency induces dysfunctional long and short telomeres; both states are associated with hypomethylation and DNA damage in human WIL2-NS cells. *Cancer Prevention Research* **7**, 128-138.
6. Beetstra, S., Thomas, P., Salisbury, C., Turner, J., and Fenech, M. (2005) Folic acid deficiency increases chromosomal instability, chromosome 21 aneuploidy and sensitivity to radiation-induced micronuclei. *Mutation Research*, **578**, 317-326.
7. Shaik, N.A., Shaik, J.P., Ali, S., Imran, A., and Rao, D.K. (2010) Increased frequency of micronuclei in diabetes mellitus patients using pioglitazone and glimepiride in combination. *Food and Chemical Toxicology*, **48**, 3432-3435.
8. Shettigar, S.K., Shailaja, C., and Kulkarni, R.K. (2012) Elevated micronuclei frequency in type 2 diabetes with high glycosylated hemoglobin. *Diabetes Research and Clinical Practice*, **95**, 246-250.
9. Corbi, S.C., Bastos, A.S., Orrico, S.R., Secolin, R., Dos Santos, R.A., Takahashi, C.S., and Scarel-Caminaga, R.M. (2014) Elevated micronucleus frequency in patients with type 2 diabetes, dyslipidemia and periodontitis. *Mutagenesis*, **29**, 433-439.
10. Harishankar, M.K., Logeshwaran, S., Sujeevan, S., Aruljothi, K.N., Dannie, M.A., and Devi, A. (2015) Genotoxicity evaluation of metformin and glimepiride by micronucleus assay in exfoliated urothelial cells of type 2 diabetes mellitus patients. *Food and Chemical Toxicology*, **83**, 146-150.
11. Kirsch-Volders, M., Bolognesi, C., Ceppi, M., Bruzzone, M., and Fenech, M. (2020) Micronuclei, inflammation and auto-immune disease. *Mutation Research*, **786**, 108335.
12. Deo, P., Fenech, M., and Dhillon, V.S. (2021) Association between glycation biomarkers, hyperglycemia, and micronucleus frequency: A meta -analysis. *Mutation Research/Reviews in Mutation Research*, **787**.
13. Al-Maskari, M.Y., Waly, M.I., Ali, A., Al-Shuaibi, Y.S., and Ouhtit, A. (2012) Folate and vitamin B12 deficiency and hyperhomocysteinemia promote oxidative stress in adult type 2 diabetes. *Nutrition*, **28**, e23-26.
14. Nilsson, E., Matte, A., Perfilyev, A., de Mello, V.D., Kakela, P., Pihlajamaki, J., and Ling, C. (2015) Epigenetic Alterations in Human Liver From Subjects With Type 2 Diabetes in Parallel With Reduced Folate Levels. *The Journal of Clinical Endocrinology and Metabolism*, **100**, E1491-1501.
15. Donnellan, L., Simpson, B., Dhillon, V.S., Costabile, M., Fenech, M., and Deo, P. (2021) Methylglyoxal induces chromosomal instability and mitotic dysfunction in lymphocytes. *Mutagenesis*, **36**, 339-348.
16. Schalkwijk, C.G., and Stehouwer, C.D.A. (2020) Methylglyoxal, a Highly Reactive Dicarbonyl Compound, in Diabetes, Its Vascular Complications, and Other Age-Related Diseases. *Physiological Reviews*, **100**, 407-461.
17. Guo, X., Dai, X., Ni, J., Cao, N., Yang, G., Xue, J., and Wang, X. (2019) High concentration of sugars is genotoxic to folate-deficient cells. *Mutation Research*, **814**, 15-22.
18. Marzio, A., Merigliano, C., Gatti, M., and Verni, F. (2014) Sugar and chromosome stability: clastogenic effects of sugars in vitamin B6-deficient cells. *PLoS Genetics*, **10**, e1004199.

19. Merigliano, C., Mascolo, E., La Torre, M., Saggio, I., and Verni, F. (2018) Protective role of vitamin B6 (PLP) against DNA damage in Drosophila models of type 2 diabetes. *Scientific Reports*, **8**, 11432.
20. Thornalley, P.J., Waris, S., Fleming, T., Santarius, T., Larkin, S.J., Winklhofer-Roob, B.M., Stratton, M.R., and Rabbani, N. (2010) Imidazopurinones are markers of physiological genomic damage linked to DNA instability and glyoxalase 1-associated tumour multidrug resistance. *Nucleic Acids Research*, **38**, 5432-5442.
21. Galligan, J.J., Wepy, J.A., Streeter, M.D., Kingsley, P.J., Mitchener, M.M., Wauchope, O.R., Beavers, W.N., Rose, K.L., Wang, T., Spiegel, D.A., and Marnett, L.J. (2018) Methylglyoxal-derived posttranslational arginine modifications are abundant histone marks. *Proceedings of the National Academy of Sciences of the United States of America*, **115**, 9228-9233.
22. Blount, B.C., Mack, M.M., Wehr, C.M., MacGregor, J.T., Hiatt, R.A., Wang, G., Wickramasinghe, S.N., Everson, R.B., and Ames, B.N. (1997) Folate deficiency causes uracil misincorporation into human DNA and chromosome breakage: implications for cancer and neuronal damage. *Proceedings of the National Academy of Sciences*, **94**, 3290-3295.
23. Fenech, M. (2007) Cytokinesis-block micronucleus cytome assay. *Nature Protocols*, **2**, 1084-1104.
24. Jaunay, E.L., Dhillon, V.S., Semple, S.J., Simpson, B.S., Deo, P., and Fenech, M. (2020) Can a digital slide scanner and viewing technique assist the visual scoring for the cytokinesis-block micronucleus cytome assay? *Mutagenesis*, **35**, 311-318.
25. Rabbani, N., and Thornalley, P.J. (2014) Measurement of methylglyoxal by stable isotopic dilution analysis LC-MS/MS with corroborative prediction in physiological samples. *Nature Protocols*, **9**, 1969-1979.
26. Scheijen, J.L., and Schalkwijk, C.G. (2014) Quantification of glyoxal, methylglyoxal and 3-deoxyglucosone in blood and plasma by ultra performance liquid chromatography tandem mass spectrometry: evaluation of blood specimen. *Clinical Chemistry and Laboratory Medicine*, **52**, 85-91.
27. Rabbani, N., Shaheen, F., Anwar, A., Masania, J., and Thornalley, P.J. (2014) Assay of methylglyoxal-derived protein and nucleotide AGEs. *Biochemical Society Transactions*, **42**, 511-517.
28. Martens, R.J.H., Broers, N.J.H., Canaud, B., Christiaans, M.H.L., Cornelis, T., Gauly, A., Hermans, M.M.H., Konings, C., van der Sande, F.M., Scheijen, J., Stifft, F., Wirtz, J., Kooman, J.P., and Schalkwijk, C.G. (2019) Relations of advanced glycation endproducts and dicarbonyls with endothelial dysfunction and low-grade inflammation in individuals with end-stage renal disease in the transition to renal replacement therapy: A cross-sectional observational study. *PLoS One*, **14**, e0221058.
29. Irshad, Z., Xue, M., Ashour, A., Larkin, J.R., Thornalley, P.J., and Rabbani, N. (2019) Activation of the unfolded protein response in high glucose treated endothelial cells is mediated by methylglyoxal. *Scientific Reports*, **9**, 7889.
30. Thornalley, P.J., Yurek-George, A., and Argirov, O.K. (2000) Kinetics and mechanism of the reaction of aminoguanidine with the α-oxoaldehydes glyoxal, methylglyoxal, and 3-deoxyglucosone under physiological conditions. *Biochemical Pharmacology*, **60**, 55-65.
31. Fleming, T., Cuny, J., Nawroth, G., Djuric, Z., Humpert, P.M., Zeier, M., Bierhaus, A., and Nawroth, P.P. (2012) Is diabetes an acquired disorder of reactive glucose metabolites and their intermediates? *Diabetologia*, **55**, 1151-1155.
32. Dhar, A., Desai, K., Kazachmov, M., Yu, P., and Wu, L. (2008) Methylglyoxal production in vascular smooth muscle cells from different metabolic precursors. *Metabolism*, **57**, 1211-1220.
33. Griffiths, M., Messent, M., MacAllister, R., and Evans, T. (1993) Aminoguanidine selectively inhibits inducible nitric oxide synthase. *British journal of pharmacology*, **110**, 963-968.
34. Yildiz, G., Demiryürek, A.T., Sahin-Erdemli, I., and Kanzik, I. (1998) Comparison of antioxidant activities of aminoguanidine, methylguanidine and guanidine by luminol-enhanced chemiluminescence. *British journal of pharmacology*, **124**, 905-910.
35. Kumar, P., Natarajan, K., and Shanmugam, N. (2014) High glucose driven expression of pro-inflammatory cytokine and chemokine genes in lymphocytes: molecular mechanisms of IL-17 family gene expression. *Cell Signal*, **26**, 528-539.
36. Umegaki, K., and Fenech, M. (2000) Cytokinesis-block micronucleus assay in WIL2-NS cells: a sensitive system to detect chromosomal damage induced by reactive oxygen species and activated human neutrophils. *Mutagenesis*, **15**, 261-269.

37. Riboulet-Chavey, A., Pierron, A., Durand, I., Murdaca, J., Giudicelli, J., and Van Obberghen, E. (2006) Methylglyoxal impairs the insulin signaling pathways independently of the formation of intracellular reactive oxygen species. *Diabetes*, **55**, 1289-1299.
38. Guo, X., Ni, J., Zhu, Y., Zhou, T., Ma, X., Xue, J., and Wang, X. (2017) Folate deficiency induces mitotic aberrations and chromosomal instability by compromising the spindle assembly checkpoint in cultured human colon cells. *Mutagenesis*, **32**, 547-560.
39. Ledesma-Osuna, A.I., Ramos-Clamont, G., and Vázquez-Moreno, L. (2008) Characterization of bovine serum albumin glycated with glucose, galactose and lactose. *Acta Biochimica Polonica*, **55**, 491-497.
40. Gugliucci, A. (2017) Formation of Fructose-Mediated Advanced Glycation End Products and Their Roles in Metabolic and Inflammatory Diseases. *Advanced Nutrition*, **8**, 54-62.
41. Zhao, W., Devamanoharan, P.S., and Varma, S.D. (2000) Fructose-mediated damage to lens α-crystallin: prevention by pyruvate. *Biochimica et Biophysica Acta (BBA) - Molecular Basis of Disease*, **1500**, 161-168.
42. Hannou, S.A., Haslam, D.E., McKeown, N.M., and Herman, M.A. (2018) Fructose metabolism and metabolic disease. *Journal of Clinical Investigation*, **128**, 545-555.
43. Lyles, G.A., and Chalmers, J. (1992) The metabolism of aminoacetone to methylglyoxal by semicarbazide-sensitive amine oxidase in human umbilical artery. *Biochemical pharmacology*, **43**, 1409-1414.
44. Kazachkov, M., and Yu, P.H. (2005) A novel HPLC procedure for detection and quantification of aminoacetone, a precursor of methylglyoxal, in biological samples. *Journal of Chromatography B*, **824**, 116-122.
45. Phillips, S.A., and Thornalley, P.J. (1993) The formation of methylglyoxal from triose phosphates: investigation using a specific assay for methylglyoxal. *European Journal of Biochemistry*, **212**, 101-105.
46. Luengo, A., Abbott, K.L., Davidson, S.M., Hosios, A.M., Faubert, B., Chan, S.H., Freinkman, E., Zacharias, L.G., Mathews, T.P., Clish, C.B., DeBerardinis, R.J., Lewis, C.A., and Vander Heiden, M.G. (2019) Reactive metabolite production is a targetable liability of glycolytic metabolism in lung cancer. *Nature Communications*, **10**, 5604.
47. Bonassi, S., Znaor, A., Ceppi, M., Lando, C., Chang, W.P., Holland, N., Kirsch-Volders, M., Zeiger, E., Ban, S., Barale, R., Bigatti, M.P., Bolognesi, C., Cebulska-Wasilewska, A., Fabianova, E., Fucic, A., Hagmar, L., Joksic, G., Martelli, A., Migliore, L., Mirkova, E., Scarfi, M.R., Zijno, A., Norppa, H., and Fenech, M. (2007) An increased micronucleus frequency in peripheral blood lymphocytes predicts the risk of cancer in humans. *Carcinogenesis*, **28**, 625-631.
48. Ling, S., Brown, K., Miksza, J.K., Howells, L., Morrison, A., Issa, E., Yates, T., Khunti, K., Davies, M.J., and Zaccardi, F. (2020) Association of Type 2 Diabetes With Cancer: A Meta-analysis With Bias Analysis for Unmeasured Confounding in 151 Cohorts Comprising 32 Million People. *Diabetes Care*, **43**, 2313-2322.
49. Zuniga-Gonzalez, G.M., Batista-Gonzalez, C.M., Gomez-Meda, B.C., Ramos-Ibarra, M.L., Zamora-Perez, A.L., Munoz-Magallanes, T., Ramos-Valdes, C., and Gallegos-Arreola, M.P. (2007) Micronuclei in diabetes: folate supplementation diminishes micronuclei in diabetic patients but not in an animal model. *Mutation Research*, **634**, 126-134.
50. Gomez-Meda, B.C., Zamora-Perez, A.L., Munoz-Magallanes, T., Sanchez-Parada, M.G., Garcia Banuelos, J.J., Guerrero-Velazquez, C., Sanchez-Orozco, L.V., Vera-Cruz, J.M., Armendariz-Borunda, J., and Zuniga-Gonzalez, G.M. (2016) Nuclear abnormalities in buccal mucosa cells of patients with type I and II diabetes treated with folic acid. *Mutation Research/Genetic Toxicology and Environmental Mutagenesis*, **797**, 1-8.

4 Chapter 4. Methylglyoxal impairs sister chromatid separation in Lymphocytes

The information presented in this Chapter is reproduced from an article published in International Journal of Molecular Sciences:

Donnellan, L., Young, C., Simpson, B.S., Dhillon, V.S., Costabile, M., Hoffmann, P., Fenech, M., and Deo, P. (2022) Methylglyoxal Impairs Sister Chromatid Separation in Lymphocytes. *International Journal of Molecular Sciences*, **23.** 10.3390/ijms23084139.

For continuity and ease of reading the following article is presented here in chapter format. See Appendix C for authorship statement. All **Tables** and **Figures** that correspond to the supplementary documentation within this chapter can be accessed via the appropriate Digital Object Identifier (DOI) listed above.

Preamble

In chapter 2, we showed that MGO induces whole chromosome loss events in WIL2-NS. Furthermore, we found that MGO induced DNA damage was more closely associated with protein glycation, as opposed to DNA glycation. We explored this relationship between protein glycation and DNA damage by measuring the formation of CEL and MG-H1 over time. Furthermore, using shot-gun proteomics, we explored the presence of mitotic proteins harbouring MGO modifications. Lastly, using chromosome spread and other cytological analysis, we found that MGO induced DNA damage is consistent with impairment of sister chromatid separation.

4.1 Abstract

The accurate segregation of sister chromatids is complex, and errors that arise throughout this process can drive chromosomal instability and tumorigenesis. We recently showed that methylglyoxal (MGO), a glycolytic by-product, can cause chromosome missegregation events in lymphocytes. However, the underlying mechanisms of this were not explored. Therefore, in this study, we utilised shotgun proteomics to identify MGO-modified proteins, and label-free quantitation to measure changes in protein abundance following exposure to MGO. We identified numerous mitotic proteins that were modified by MGO, including those involved in the separation and cohesion of sister chromatids. Furthermore, the protein abundance of Securin, an inhibitor of sister chromatid separation, was increased following treatment with MGO. Cytological examination of chromosome spreads showed MGO prevented sister chromatid separation, which was associated with the formation of complex nuclear anomalies. Therefore, results from this study suggest MGO may drive chromosomal instability by preventing sister chromatid separation.

4.2 Introduction

The separation of sister chromatid into daughter cells is an incredibly complex process involving the coordinated efforts of hundreds of proteins (1). Unsurprisingly, the errors that arise in this process can cause missegregation of chromosomes resulting in the generation of aneuploidy in the offspring (1,2). Because most tumours harbour aneuploid cells, mechanisms that lead to this may be causally implicated in tumour development (3). Chromosome missegregation events can originate from a variety of factors including i) erroneous or failed attachment of kinetochores to spindle microtubules (4), ii) abnormal centrosome amplification and multipolar spindle formation (5) and iii) defects in sister chromatid cohesion causing premature chromatid separation or inability of sister chromatids to separate (6,7).

We recently showed that methylglyoxal (MGO), a glycolytic by-product is capable of inducing chromosome missegregation events in WIL2-NS B-lymphoblastoid cells and peripheral blood lymphocytes (8). MGO is a highly reactive electrophilic metabolite that can react with the nucleophilic side chains of arginine and lysine residues on proteins forming a variety of advanced glycation endproducts (AGEs) such as N^{ε}-(carboxyethyl)lysine (CEL) and N^{δ}-(5-hydro-5-methyl-4-imidazolon2-

yl)ornithine (MG-H1) (9). Although it is well known that MGO can modify proteins, only several proteins have been identified as specific targets of MGO in robust biological and chemical detail. These include hypoxia inducible factor-1α (HIF-1α), all canonical histone proteins, glyceraldehyde-phosphate dehydrogenase and Kelch-like ECH-associated protein 1 (10-13). Modification of proteins by MGO has previously been shown to alter protein function. For example, modification of histone proteins causes ablation of electrostatic interactions between histones and DNA due to the neutralization of arginine and lysine positive charges, altered surface topology and interference with other post-translational modifications (9,14,15). Therefore, we hypothesized that MGO modification of proteins involved in the accurate segregation of sister chromatids may cause chromosome missegregation events.

To investigate this, we utilized liquid chromatography-mass spectrometry (LC-MS) to identify mitotic proteins harbouring MGO modifications. Furthermore, we performed label-free quantitation (LFQ) to determine the change in abundance of proteins after MGO exposure. Overall, we found numerous mitotic proteins to be modified by MGO, particularly those involved in the separation and cohesion of sister chromatids. Moreover, we observed that MGO increased the protein abundance of several cell cycle proteins involved in the separation of sister chromatids. Cytological examination of metaphase spreads confirmed the impairment of sister chromatid separation, which resulted in various, complex nuclear anomalies.

4.3 Methods

4.3.1 Materials

All reagents, chemicals and enzymes were purchased from Sigma (*St. Louis, MO, USA*) unless indicated otherwise. Isotopically labelled and unlabelled MG-H1, CEL and Lysine were purchased from Iris Biotech (Marktredwitz, Germany). Trypsin Gold (Promega, V5280) and ProAlanase (Promega, VA2161) were purchased from Promega (Madison, WI, USA).

4.3.2 WIL2-NS cell culture

The WIL2-NS (ATCC CRL-8155) cell line was kindly gifted by Commonwealth Scientific Research Organisation (Adelaide, Australia). WIL2-NS cells were cultured in complete RPMI-1640 medium supplemented with 5% (v/v) fetal calf serum (FCS), L-glutamine (1% v/v) and penicillin/streptomycin (1% v/v) at 37°C in a humidified atmosphere with 5% CO_2. Cells were seeded at $5x10^5$ cells/mL and incubated for 24 h before being treated with 100 and 500 µmol/L of MGO for 24 or 48 h (as indicated) for each experiment.

4.3.3 Identification of DNA damage biomarkers

Micronuclei (MNi) multiple MNi (≥ 2), nucleoplasmic bridges (NPBs), nuclear buds (NBUDs) and fused nuclei (Fused) were scored in binucleated cells using the cytokinesis-block micronucleus cytome assay (CBMNcyt) (16). Briefly, following treatment with MGO for 24 or 48 h, cells were washed twice with Hanks balanced salt solution and resuspended in RPMI-1640 containing 4.5 µg/ mL cytochalasin-b (cyt-b) for 24 h. After cytokinesis block, cells were harvested onto slides by cytocentrifugation (16). Slide preparation and scoring of the CBMNcyt assay was performed as described previously using a NanoZoomer S60 (Hammatsu Photonics, Shizuoka, Japan) (16,17). Enlarged, misshapen and multinucleated cells were prepared the same as for the CBMNcyt assay, except cytochalasin-b was not added following treatment of MGO. Scoring criteria for the above biomarkers has previously been described (16,18). For mitotic index, cells which possessed condensed chromosomes were distinguished from interphase cells microscopically, as previously described (19).

4.3.4 Quantification of MG-H1 and CEL in whole cell extracts

WIL2-NS cells were lysed in ice-cold RIPA buffer with sonication over-ice for 2 x 10 s burst (Misonix, NY, USA). Cellular debris was removed by centrifugation (17,000 g for 10 min). Protein was precipitated by the addition of ice-cold acetone (4:1 ratio of acetone: sample). The sample was left overnight at -20°C before being centrifuged at 17,000 g for 10 min. Protein was washed twice with ice-

cold acetone before resuspension in 50 µL of 50 mM ammonium bicarbonate (pH 8). Samples were incubated at 37°C for 4 hours to aid protein solubilization. Undissolved protein was removed by centrifugation at 17,000 g for 10 min and protein concentration of the solution was measured by Bicinchoninic acid (BCA) assay following manufacturer's instructions. Trypsin (TPCK treated sequencing grade) was added at an enzyme to protein ratio (1:50) and sample was incubated at 37°C for 16 hours. Following incubation, the sample was heated to 95°C for 10 minutes to denature the trypsin. Following this, the sample was cooled to room temperature and Pronase E and Aminopeptidase were added at an enzyme to protein ratio (1:50) for a further 24 hours. Enzymes were removed by the addition of ice-cold acetone and the sample was centrifuged at 17,000 g for 10 min. The supernatant was collected, dried under vacuum centrifugation and resuspended in 0.1% (v/v) formic acid containing an internal standard. Sample (2 µL) was injected and analytes were separated using a 150 × 4.6 mm, 4 µm Phenomenex C18 column (Phenomenex, Torrance, CA, USA) with a linear gradient of 0.1 % formic acid in water (Buffer A) and 0.1% formic acid in acetonitrile (Buffer B) over 5 min at a flow rate of 0.6 mL/ min. Multiple reaction monitoring (MRM) was conducted in positive-ion mode using an AB Sciex 6500+ QqQ mass spectrometer with the following transitions m/z 147.4 > 83.9 (lysine), 151.2 > 87.9 (d4 lysine), 219.2 > 130.2 (CEL), 222.2 > 134.2 (d4 CEL), 229.2 > 116.1 (MG-H1) 232.2 > 116.1 (d3 MG-H1). The concentration of MG-H1 and CEL was normalized to lysine content and expressed relative to control.

4.3.5 Sister chromatid resolution assay

Resolution of sister chromatids was scored in metaphase spreads of cells arrested in metaphase using Colcemid. Briefly, cells were treated with MGO for 24 h. Following treatment, colcemid (KaryoMAX, Thermofisher Scientific) was added to a concentration of 0.5 µg/ mL for 2 h. After metaphase arrest, cells were gently centrifuged and the supernatant was removed. Cells were resuspended in hypotonic 0.075 M KCl solution and incubated at 37°C for 10 min. The supernatant was removed and ice-cold fixative (1:3 acetic acid: methanol) was added dropwise and cells incubated at 4°C for 10 min. After the fixative was removed, the cells were resuspended in approximately 100 µL of fresh fixative and dropped onto microscope slides. Slides were air-dried and stained as described previously (17). Metaphase

spreads were scored microscopically using an Olympus CX43 at 100 x objective lens. Mitotic cells in metaphase spread experiments were categorized into three groups according to their morphology as previously described (20,21): (1) Resolved, where the arms of each sister chromatid were separated (i.e. resolved) but remained connected at the centromere. (2) Partially resolved, where sister chromatid could be distinguished from one and other but were still connected along the length of the arms and centromere. (3) Unresolved; where sister chromatid could not be distinguished from one and other and had an arm closed morphology. Metaphase spreads consisting of multiple morphologies were scored as the morphology accounting for the largest percentage of chromosomes.

4.3.6 Proteomic analysis of WIL2-NS

Samples were prepared for LC-MS as described previously using trypsin and proalanase in separate digests (22). Raw MS files were analysed using Proteome Discoverer 2.4 (Thermo Scientific). Data were processed with the Sequest HT search engine against a concatenated database containing the 74811 forward entries from the UniProt human database (December 1, 2019) and their respective decoy counterparts. Trypsin or ProAlanase (cleaves C-terminal to proline and alanine residues) was specified as the enzyme and a maximum of five missed cleavages was allowed. Precursor and fragment mass tolerances were 10 ppm and 0.02 Da, respectively. Arginine and lysine carboxyethylation (+72.021129), arginine methylglyoxal-hydroimidazolone (+54.010565), methionine oxidation (+15.994915), N-terminal acetylation (+42.010565), N-terminal methionine loss (-131.040485), N-terminal methionine loss and acetylation (-89.02992) were set as dynamic modifications, with cysteine carbamidomethylation (+57.021464) designated a static modification. Protein and peptide false discovery rates were both set at 1%. LFQ was performed for Trypsin and ProAlanase digests separately and a Log2 cut-off of 0.5 was applied. Enrichment analysis was performed using the Database for Annotation, Visualization and Integrated Discovery (DAVID) v6.8 (https://david.ncifcrf.gov/) accessed 18/01/2022 (23). Raw MS files have been deposited to the ProteomeXchange Consortium via the PRIDE partner repository with the dataset identifier PXD032812 (24).

4.3.7 Data analysis

Data are expressed as mean ± SD of three independent experiments (*n*=3). A one-way or two-way analysis of variance (ANOVA) followed by a Dunnett *post hoc* test was conducted (depending on experimental design) to determine statistical significance using GraphPad prism (San Diego, CA, USA, Version 8.3.0). A $P<0.05$ was considered significant. Two-tailed Pearson correlations were used to analyze relationships between AGE biomarkers and MNi frequency.

4.4 Results

4.4.1 MGO induced micronuclei formation is associated with increased AGEs

In our previous study, we showed that MGO can induce the formation of micronuclei (MNi) and other DNA damage biomarkers (nuclear buds (Nbuds) and multipolar mitosis) in WIL2-NS cells after 48 h exposure [8]. As MGO can react rapidly with proteins, we investigated whether MNi formation was more pronounced at earlier time points and associated with the formation of MGO modifications. Therefore, WIL2-NS cells were exposed to 100 and 500 µmol/L MGO for 8, 24, and 48 h, followed by measurement of MGO modification levels (MG-H1 and CEL) and MNi. MG-H1 levels were significantly increased in cells exposed to 500 µmol/L MGO at all time points but not in cells exposed to 100 µmol/L (Figure 4.1A). CEL was significantly increased at both concentrations but only with 8 and 24 h treatments (Figure 4.1B). MNi were significantly increased at 8 and 24 h following exposure to both concentrations (Figure 4.1C). However, MNi were only elevated in cells exposed to 500 µmol/L at 48 h (Figure 4.1C). Correlation analysis was applied to explore the relationship between these MGO modifications and MNi formation. No significant correlation was observed for MG-H1; however, a significant correlation was observed for CEL ($r = 0.693$; $p = 0.038$) (Table 4.1). This suggests that CEL formation may be associated with the induction of MNi.

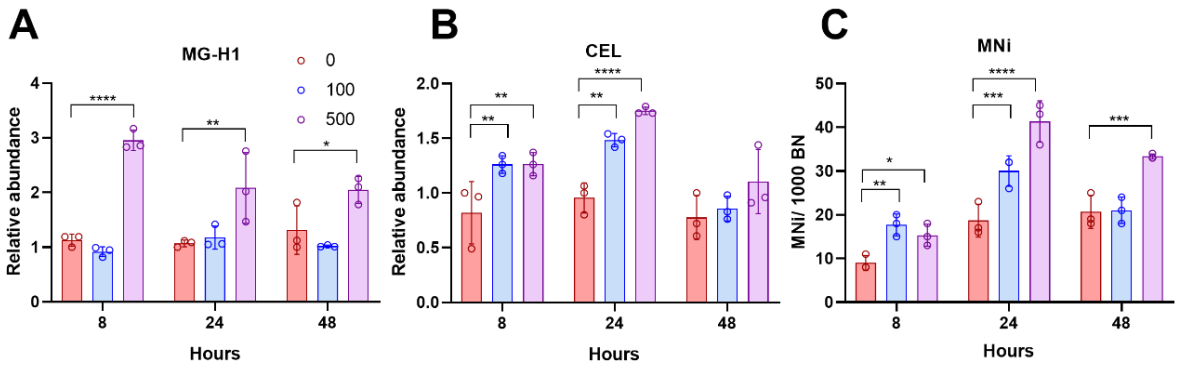

Figure 4.1. Time and dose dependent MG-H1, CEL and MNi formation. (A) MG-H1 concentration in whole-cell extracts at 8, 24, and 48 h normalised to control; (B) CEL concentration in whole-cell extracts at 8, 24, and 48 h normalised to control; (C) MNi formation, measured by CBMNcyt assay at 8, 24, and 48 h expr expressed as number of MNi/1000 Binucleated (BN) cells. Data are mean ± SD (n = 3). A two-way ANOVA followed by a Dunnett post hoc was conducted to determine statistical significance. * $p < 0.05$, ** $p < 0.01$, *** $p < 0.001$, **** $p < 0.0001$.

Table 4.1: Pearson correlation for relationship between AGE biomarkers and MNi

		MG-H1	**CEL**
MNi	r	0.26	0.693
	p	0.495	0.038

Two-tailed Pearson correlations were used to analyze relationships between AGE biomarkers and MNi frequency.

4.4.2 MGO modifies various components of the mitotic machinery

To better understand the role of MGO in MNi formation, which we previously observed were the result of missegregated chromosomes, a shot-gun proteomics experiment was conducted to investigate both changes in protein abundance and the modification of mitotic proteins by MGO (8). Based on time point studies, cells were treated with 500 µmol/L of MGO for 24 h for all proteomic experiments. Although correlation analysis suggested CEL modifications were more closely associated with MNi formation, we also searched for MG-H (isomers 1, 2 and 3) and carboxethylarginine (CEA) modifications. For a full list of proteins identified with MGO modifications, see previous study (22). Enrichment analysis using DAVID was performed on the proteins identified with MGO modifications, which showed several

overrepresented Reactome pathways, biological processes and cellular components associated with mitosis (Fig 2A). Specifically, more than 50 cell cycle associated proteins were revealed to contain MGO modifications, as well as the involvement of sister chromatid cohesion, where the cohesin complex is one of the most enriched processes/ pathways associated with these modifications.

We performed a LFQ study to ascertain changes in protein abundance resulting from MGO exposure, where 89 and 90 proteins exhibited a decrease or increase in abundance, respectively (Appendix A). Although enrichment analysis using DAVID on the down-regulated proteins showed no down regulation of pathways associated with mitosis, several pathways associated with various mitotic processes were upregulated (Fig 2B). Similar to the results obtained from the enrichment analysis of MGO modifications, pathways associated with the regulation of sister chromatid cohesin and separation were increased in cells treated with MGO. An example includes PTTG1 (securin), which is an inhibitor of ESPL1 (separase) and a cysteine protease that cleaves the cohesin complex that adheres sister chromatids to each other (Fig 2C/D). Securin remains bound to separase until the onset of anaphase where it is ubiquitinated by the anaphase promoting complex/ cyclosome (APC/C): CDC20 complex targeting it for ubiquitin mediated degradation, causing the release of separase and subsequent sister chromatid separation (25). Other proteins, including CDC20, UBE2C, UBE2S and BUB1, all of which are involved in the regulation of sister chromatid separation were also upregulated (Fig 2C/D). The mitotic index for MGO untreated and treated cells was 7.67 ± 3.06% and 7.33 ± 1.53%, respectively, confirming the altered abundance of mitotic proteins was not due to the increased level of mitotic cells (Appendix 2).

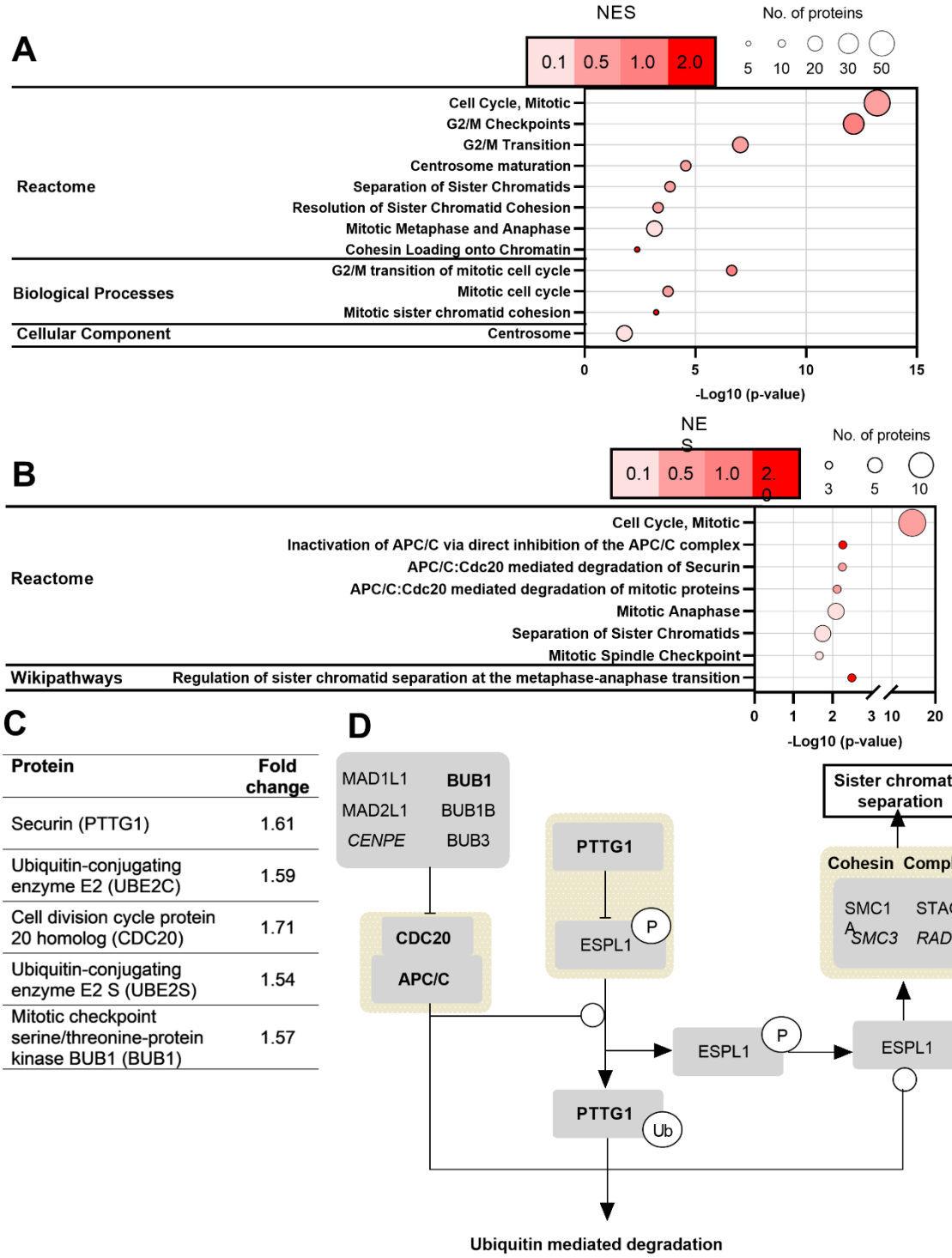

Figure 4.2: Enrichment analysis. **A**. Enrichment analysis of MGO modified proteins using DAVID. Due to the large number of enriched terms, only those associated with mitosis were included and redundant terms were excluded. NES; normalized enrichment score. NES was calculated by dividing the fold enrichment by average enrichment of all terms. **B.** Enrichment analysis of upregulated proteins following MGO treatment (500 µmol/L for 24 h). Due to the large number of enriched terms, only those associated with mitosis were included and redundant terms were excluded **C.** Fold change of proteins of interest following MGO treatment. **D.** Diagram showing the regulation of sister chromatid separation. Proteins in bold show increased abundance by MGO. Proteins in italics contain one or more MGO modifications.

4.4.3 Methylglyoxal impairs sister chromatid separation

Proteomic analysis revealed the possibility that proteins involved in the separation of sister chromatids were susceptible to both modification and increased protein abundance following MGO exposure and that this might cause disruption of the mitotic process. Therefore, using metaphase spreads, we investigated the resolution of sister chromatids, which is an indicator of their ability to dissociate from one another during the metaphase to anaphase transition. In control cells, we observed that the majority of metaphase spreads (51.1%) contained chromosomes in which sister chromatids were resolved from each other, whereas only 29.8% were 'partially resolved' and 19.1% were 'unresolved' (Figure 4.3A). In contrast, MGO exposure resulted in 61.1% of the metaphase spreads to contain 'unresolved' chromatids and only a small percentage (8.3%) were 'resolved'. To further explore the basis of this observation, we investigated various nuclear anomalies (Figure 4.3) which have been shown to occur due to impairment of sister chromatid separation (6,18). At 100 µmol/L, MGO increased the frequency of MNi, NPBs, Fused, Enlarged and Multinucleated cells after 24 hours (Figure 4.3B). These biomarkers, along with cells containing multiple (≥2) MNi and Nbuds were also increased at 500 µmol/L MGO (Figure 4.3B). Fused nuclei are a well described marker of failed sister chromatid separation and are thought to be caused by the presence of multiple ultrafine bridges which form when unseparated sister chromatid are pulled to opposite poles (26). In this situation, centromeric signals should be present in or very close to the fusion region. Indeed, the fusion regions contained numerous centromeric signals, determined using fluorescence *in situ* hybridization with pan centromeric probes (Figure 4.3C). This supports the hypothesis that fused nuclei are formed by the failed separation of sister chromatids and not by other mechanisms such as telomeric end fusion events which are less likely to contain centromeric signals.

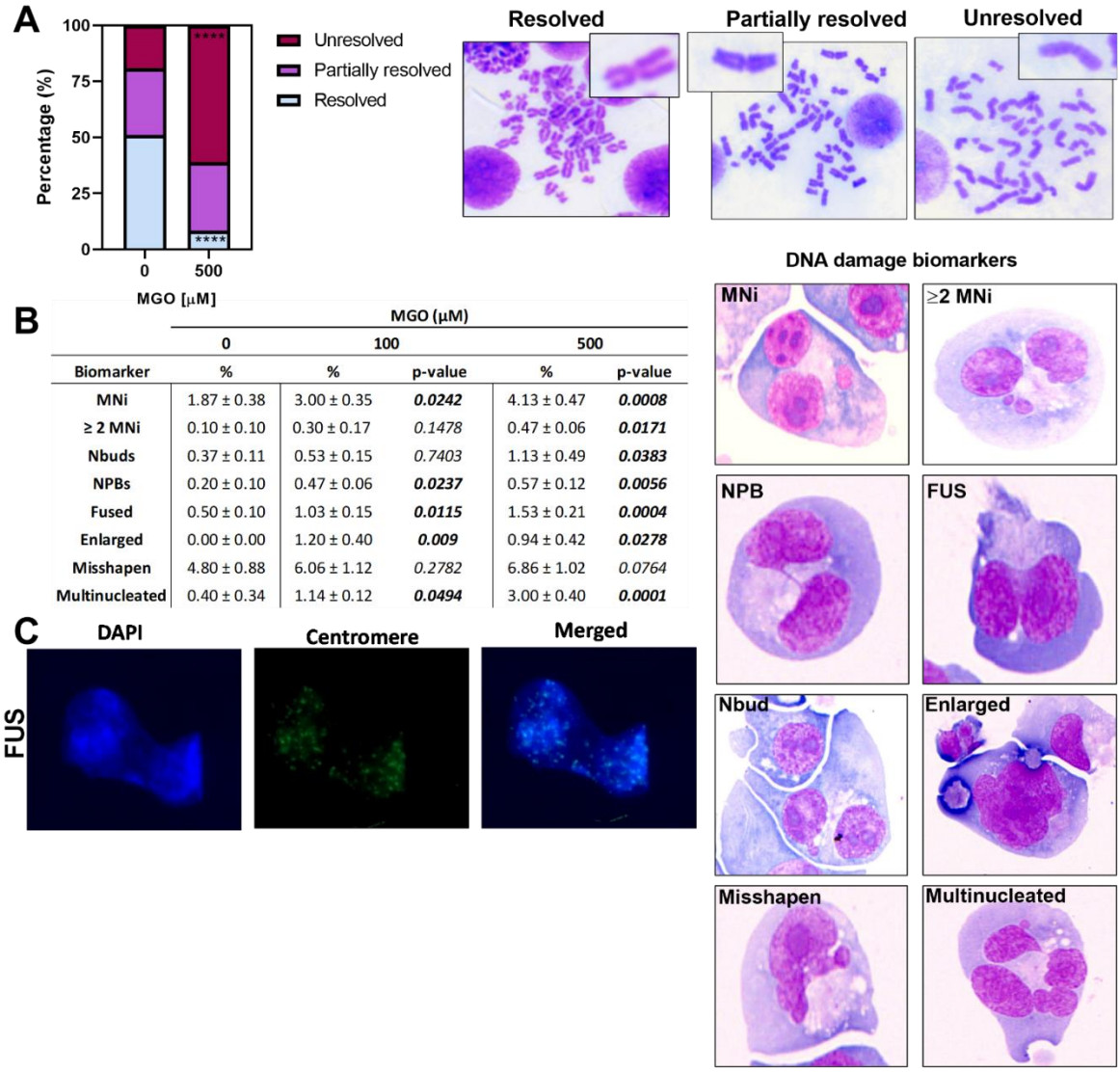

	MGO (µM)				
	0	100		500	
Biomarker	%	%	p-value	%	p-value
MNi	1.87 ± 0.38	3.00 ± 0.35	***0.0242***	4.13 ± 0.47	***0.0008***
≥ 2 MNi	0.10 ± 0.10	0.30 ± 0.17	*0.1478*	0.47 ± 0.06	***0.0171***
Nbuds	0.37 ± 0.11	0.53 ± 0.15	*0.7403*	1.13 ± 0.49	***0.0383***
NPBs	0.20 ± 0.10	0.47 ± 0.06	***0.0237***	0.57 ± 0.12	***0.0056***
Fused	0.50 ± 0.10	1.03 ± 0.15	***0.0115***	1.53 ± 0.21	***0.0004***
Enlarged	0.00 ± 0.00	1.20 ± 0.40	***0.009***	0.94 ± 0.42	***0.0278***
Misshapen	4.80 ± 0.88	6.06 ± 1.12	*0.2782*	6.86 ± 1.02	*0.0764*
Multinucleated	0.40 ± 0.34	1.14 ± 0.12	***0.0494***	3.00 ± 0.40	***0.0001***

Figure 4.3: MGO impairs sister chromatid separation. **A.** Analysis of sister chromatid resolution, scored as (i) resolved, (ii) partially resolved and (iii) unresolved. **B.** Analysis of DNA damage biomarkers. Columns show the percentage of cells displaying each biomarker and its significance determined by one-way ANOVA when compared to the control. Representative photomicrographs of each nuclear anomaly are displayed on the right. MNi, ≥2 MNi, NPB, FUS and Nbuds were scored in binucleated cells using the CBMNcyt assay. Enlarged, misshapen and multinucleated cells were scored in normally dividing cells. **C.** Fluorescence in situ hybridization analysis of fused nuclei. Data are mean ± SD (n=3). A one-way ANOVA followed by a Dunnett post hoc was conducted to determine statistical significance ****P<0.0001.

4.5 Discussion

In this study, we found that MGO impairs sister chromatid separation in WIL-2NS cells, causing various nuclear anomalies associated with chromosomal instability (CIN). LC/MS revealed the identification of numerous mitotic proteins containing various MGO modifications, most of which were CEL modifications. Furthermore, we observed an increased abundance in several proteins involved in the regulation of sister chromatid separation. Most notably, we found treatment with MGO increased the protein abundance of the separase inhibitor, securin. Securin inhibits the cysteine protease separase until the onset of anaphase, at which point it is ubiquitinated by the anaphase promoting complex/ cyclosome (APC/C) ubiquitin ligase (E3) and degraded by the 26S proteasome system (27). This process releases separase which cleaves the double-strand-break repair protein rad21 homolog (RAD21) of the cohesin complex which binds together sister chromatids, allowing them to separate. Overexpression or expression of non-degradable securin results in incomplete sister chromatid separation and gives rise to chromosomes (or sister chromatids) with an 'unresolved' phenotype (Fig 3A) (25,28). Furthermore, increased abundance of securin has been shown to causes various nuclear anomalies, most notably MNi, NPBs and multinucleated cells (25,28,29). This is consistent with studies showing that expression of non-cleavable RAD21 (target of separase) prevents sister chromatid separation and causes similar morphologies as observed in this study (6). Although prevention of sister chromatid separation by increased abundance of securin could account for the results observed in this study, other changes may also be contributing to the observed CIN. For example, cohesin can also be removed from chromosome arms by cleavage independent mechanisms (6). During DNA replication in S phase, soronin associates with chromatin, which is facilitated by acetylation of structural maintenance of chromosome 3 (Smc3) (30). Soronin binds to Pds5, which alters the topology of Pds5 and Wap1, producing a stable closed cohesin complex (30). Both sister chromatid cohesion protein PDS5 homolog B (Pds5B) and Smc3 contained MGO modifications in this study. While it is uncertain what impact this may have on cohesin function, altered topology due to MGO modification may cause structural changes in cohesin, resulting in an unresolved phenotype. Furthermore, over expression of either CDC20 or UBE2C can increase the frequency of missegregated chromosomes resulting in aneuploidy, polyploidy and various other markers of CIN (31-33). Over expression of CDC20 was shown to promote premature anaphase, which is known to result in various aberrant phenotypes, including aneuploidy (31). Moreover, increased abundance of

securin, CDC20 and UBE2C were shown to be predictors of poor survival in patients with various cancers, including breast, colorectal, and gastric cancers (34-38). We also identified numerous proteins with critical roles in mitosis to be modified by MGO. MGO has been shown to induce several changes in activity, modification of active/ binding sites and competition with other post-translational modifications (13,15). MGO modifications have also been shown to cause structural changes in protein topology, likely caused by neutralizing charged residues (arginine and lysine) which are involved in intramolecular interactions (15,39). Therefore, modification of RAD21, or other cohesin complex proteins may have impaired cleavage by separase, preventing sister chromatid separation. Moreover, modification of other mitotic proteins, such as those involved in centrosome organization or kinetochore-microtubule attachments, may have also contributed to the CIN observed in this study (4). For example, impairment of the centrosome cycle can result in centrosome amplification (more than two centrosomes per cell) which causes multipolar spindle formation and merotelic (uneven) kinetochore-microtubule attachments (40). Extra centrosomes can cluster together such that the cell undergoes bipolar mitosis, however those chromosomes with merotelic kinetochore-microtubule attachments are prone to lagging at the metaphase plate to form MNi (40).

The presence of MGO modification cannot alone infer loss of protein function and further studies are required to characterize which MGO-modifications in mitotic proteins are strongly correlated with mitotic dysfunction and specific CIN phenotypes. Nevertheless, we showed that several critical proteins involved in mitosis are targets for MGO modification, particularly those involved in sister chromatid separation. Moreover, we showed MGO increased the abundance of securin, a separase inhibitor in which its increased abundance has been shown to cause CIN (28). These results further unravel the MGO-induced proteomic changes that are likely to cause MNi and provide information on the underlying mechanisms on missegregated chromosome events observed after exposure to MGO. Many of the CIN events observed after exposure to MGO are the same as those associated with tumorigenesis (3,41). Therefore, it is possible that MGO promotes tumorigenesis by driving increased CIN by preventing sister chromatid separation during mitosis.

References

1. Guo, X., Ni, J., Liang, Z., Xue, J., Fenech, M.F., and Wang, X. (2019) The molecular origins and pathophysiological consequences of micronuclei: New insights into an age-old problem. *Mutation Research/Reviews in Mutation Research*, **779**, 1-35.
2. Krupina, K., Goginashvili, A., and Cleveland, D.W. (2021) Causes and consequences of micronuclei. *Current Opinions in Cell Biology*, **70**, 91-99.
3. Ben-David, U., and Amon, A. (2020) Context is everything: aneuploidy in cancer. *Nature Reviews Genetics*, **21**, 44-62.
4. Thompson, S.L., and Compton, D.A. (2011) Chromosome missegregation in human cells arises through specific types of kinetochore-microtubule attachment errors. *Proceedings of the National Academy of Sciences*, **108**, 17974-17978.
5. Quintyne, N.J., Reing, J.E., Hoffelder, D.R., Gollin, S.M., and Saunders, W.S. (2005) Spindle multipolarity is prevented by centrosomal clustering. *Science*, **307**, 127-129.
6. Hauf, S., Waizenegger, I.C., and Peters, J.M. (2001) Cohesin cleavage by separase required for anaphase and cytokinesis in human cells. *Science*, **293**, 1320-1323.
7. Watrin, E., Schleiffer, A., Tanaka, K., Eisenhaber, F., Nasmyth, K., and Peters, J.M. (2006) Human Scc4 is required for cohesin binding to chromatin, sister-chromatid cohesion, and mitotic progression. *Current Biology*, **16**, 863-874.
8. Donnellan, L., Simpson, B., Dhillon, V.S., Costabile, M., Fenech, M., and Deo, P. (2021) Methylglyoxal induces chromosomal instability and mitotic dysfunction in lymphocytes. *Mutagenesis*, **36**, 339-348.
9. Zheng, Q., Maksimovic, I., Upad, A., and David, Y. (2020) Non-enzymatic covalent modifications: a new link between metabolism and epigenetics. *Protein Cell*, **11**, 401-416.
10. Ceradini, D.J., Yao, D., Grogan, R.H., Callaghan, M.J., Edelstein, D., Brownlee, M., and Gurtner, G.C. (2008) Decreasing intracellular superoxide corrects defective ischemia-induced new vessel formation in diabetic mice. *Journal of Biololgical Chemistry*, **283**, 10930-10938.
11. Bento, C.F., Fernandes, R., Ramalho, J., Marques, C., Shang, F., Taylor, A., and Pereira, P. (2010) The chaperone-dependent ubiquitin ligase CHIP targets HIF-1alpha for degradation in the presence of methylglyoxal. *PLoS One*, **5**, e15062.
12. Bollong, M.J., Lee, G., Coukos, J.S., Yun, H., Zambaldo, C., Chang, J.W., Chin, E.N., Ahmad, I., Chatterjee, A.K., Lairson, L.L., Schultz, P.G., and Moellering, R.E. (2018) A metabolite-derived protein modification integrates glycolysis with KEAP1-NRF2 signalling. *Nature*, **562**, 600-604.
13. Galligan, J.J., Wepy, J.A., Streeter, M.D., Kingsley, P.J., Mitchener, M.M., Wauchope, O.R., Beavers, W.N., Rose, K.L., Wang, T., Spiegel, D.A., and Marnett, L.J. (2018) Methylglyoxal-derived posttranslational arginine modifications are abundant histone marks. *Proceedings of the National Academy of Sciences of the United States of America*, **115**, 9228-9233.
14. Maksimovic, I., and David, Y. (2021) Non-enzymatic Covalent Modifications as a New Chapter in the Histone Code. *Trends in Biochemical Sciences*, **46**, 718-730.
15. Zheng, Q., Omans, N.D., Leicher, R., Osunsade, A., Agustinus, A.S., Finkin-Groner, E., D'Ambrosio, H., Liu, B., Chandarlapaty, S., Liu, S., and David, Y. (2019) Reversible histone glycation is associated with disease-related changes in chromatin architecture. *Nature Communications*, **10**, 1289.
16. Fenech, M. (2007) Cytokinesis-block micronucleus cytome assay. *Nature Protocols*, **2**, 1084-1104.
17. Jaunay, E.L., Dhillon, V.S., Semple, S.J., Simpson, B.S., Deo, P., and Fenech, M. (2020) Can a digital slide scanner and viewing technique assist the visual scoring for the cytokinesis-block micronucleus cytome assay? *Mutagenesis*, **35**, 311-318.
18. Bull, C.F., Mayrhofer, G., Zeegers, D., Mun, G.L., Hande, M.P., and Fenech, M.F. (2012) Folate deficiency is associated with the formation of complex nuclear anomalies in the cytokinesis-block micronucleus cytome assay. *Environmental and Molecular Mutagenisis*, **53**, 311-323.
19. Guo, X., Ni, J., Zhu, Y., Zhou, T., Ma, X., Xue, J., and Wang, X. (2017) Folate deficiency induces mitotic aberrations and chromosomal instability by compromising the spindle assembly checkpoint in cultured human colon cells. *Mutagenesis*, **32**, 547-560.
20. Yang, Y., Wang, W., Li, M., Gao, Y., Zhang, W., Huang, Y., Zhuo, W., Yan, X., Liu, W., Wang, F., Chen, D., and Zhou, T. (2019) NudCL2 is an Hsp90 cochaperone to regulate sister chromatid cohesion by stabilizing cohesin subunits. *Cellular and Molecular Life Sciences*, **76**, 381-395.

21. Ouyang, Z., Zheng, G., Song, J., Borek, D.M., Otwinowski, Z., Brautigam, C.A., Tomchick, D.R., Rankin, S., and Yu, H. (2013) Structure of the human cohesin inhibitor Wapl. *Proceedings of the National Academy of Sciences of the United States of America*, **110**, 11355-11360.
22. Donnellan, L., Young, C., Simpson, B.S., Acland, M., Dhillon, V.S., Costabile, M., Fenech, M., Hoffmann, P., and Deo, P. (2022) Proteomic Analysis of Methylglyoxal Modifications Reveals Susceptibility of Glycolytic Enzymes to Dicarbonyl Stress. *International Journal of Molecular Sciences*, **23**, 3689.
23. Huang da, W., Sherman, B.T., and Lempicki, R.A. (2009) Systematic and integrative analysis of large gene lists using DAVID bioinformatics resources. *Nature Protocols*, **4**, 44-57.
24. Perez-Riverol, Y., Csordas, A., Bai, J., Bernal-Llinares, M., Hewapathirana, S., Kundu, D.J., Inuganti, A., Griss, J., Mayer, G., Eisenacher, M., Perez, E., Uszkoreit, J., Pfeuffer, J., Sachsenberg, T., Yilmaz, S., Tiwary, S., Cox, J., Audain, E., Walzer, M., Jarnuczak, A.F., Ternent, T., Brazma, A., and Vizcaino, J.A. (2019) The PRIDE database and related tools and resources in 2019: improving support for quantification data. *Nucleic Acids Research*, **47**, D442-D450.
25. Jallepalli, P.V., Waizenegger, I.C., Bunz, F., Langer, S., Speicher, M.R., Peters, J.-M., Kinzler, K.W., Vogelstein, B., and Lengauer, C. (2001) Securin Is Required for Chromosomal Stability in Human Cells. *Cell*, **105**, 445-457.
26. Broderick, R., and Niedzwiedz, W. (2015) Sister chromatid decatenation: bridging the gaps in our knowledge. *Cell Cycle*, **14**, 3040-3044.
27. Park, J.H., Cosgrove, M.S., Youngman, E., Wolberger, C., and Boeke, J.D. (2002) A core nucleosome surface crucial for transcriptional silencing. *Nature Genetics*, **32**, 273-279.
28. Zur, A., and Brandeis, M. (2001) Securin degradation is mediated by fzy and fzr, and is required for complete chromatid separation but not for cytokinesis. *The EMBO journal*, **20**, 792-801.
29. Mora-Santos, M., Castilla, C., Herrero-Ruiz, J., Giraldez, S., Limon-Mortes, M.C., Saez, C., Japon, M.A., Tortolero, M., and Romero, F. (2013) A single mutation in Securin induces chromosomal instability and enhances cell invasion. *European Journal of Cancer*, **49**, 500-510.
30. Nishiyama, T., Ladurner, R., Schmitz, J., Kreidl, E., Schleiffer, A., Bhaskara, V., Bando, M., Shirahige, K., Hyman, A.A., Mechtler, K., and Peters, J.M. (2010) Sororin mediates sister chromatid cohesion by antagonizing Wapl. *Cell*, **143**, 737-749.
31. Mondal, G., Sengupta, S., Panda, C.K., Gollin, S.M., Saunders, W.S., and Roychoudhury, S. (2007) Overexpression of Cdc20 leads to impairment of the spindle assembly checkpoint and aneuploidization in oral cancer. *Carcinogenesis*, **28**, 81-92.
32. Li, M., Fang, X., Wei, Z., York, J.P., and Zhang, P. (2009) Loss of spindle assembly checkpoint-mediated inhibition of Cdc20 promotes tumorigenesis in mice. *Journal of Cell Biology*, **185**, 983-994.
33. van Ree, J.H., Jeganathan, K.B., Malureanu, L., and van Deursen, J.M. (2010) Overexpression of the E2 ubiquitin-conjugating enzyme UbcH10 causes chromosome missegregation and tumor formation. *Journal of Cell Biology*, **188**, 83-100.
34. Karra, H., Pitkanen, R., Nykanen, M., Talvinen, K., Kuopio, T., Soderstrom, M., and Kronqvist, P. (2012) Securin predicts aneuploidy and survival in breast cancer. *Histopathology*, **60**, 586-596.
35. Wu, W.-j., Hu, K.-s., Wang, D.-s., Zeng, Z.-l., Zhang, D.-s., Chen, D.-l., Bai, L., and Xu, R.-h. (2013) CDC20 overexpression predicts a poor prognosis for patients with colorectal cancer. *Journal of translational medicine*, **11**, 1-8.
36. Karra, H., Repo, H., Ahonen, I., Loyttyniemi, E., Pitkanen, R., Lintunen, M., Kuopio, T., Soderstrom, M., and Kronqvist, P. (2014) Cdc20 and securin overexpression predict short-term breast cancer survival. *British Journal of Cancer*, **110**, 2905-2913.
37. Gayyed, M.F., El-Maqsoud, N.M., Tawfiek, E.R., El Gelany, S.A., and Rahman, M.F. (2016) A comprehensive analysis of CDC20 overexpression in common malignant tumors from multiple organs: its correlation with tumor grade and stage. *Tumour Biology*, **37**, 749-762.
38. Zhang, H., Zhao, G., Ke, B., Ma, G., Liu, G., Liang, H., Liu, L., and Hao, X. (2018) Overexpression of UBE2C correlates with poor prognosis in gastric cancer patients. *European Review for Medical and Pharmacological Sciences*, **22**, 1665-1671.
39. Rabbani, N., Xue, M., and Thornalley, P.J. (2021) Dicarbonyl stress, protein glycation and the unfolded protein response. *Glycoconjugate Journal*, **38**, 331-340.
40. Ganem, N.J., Godinho, S.A., and Pellman, D. (2009) A mechanism linking extra centrosomes to chromosomal instability. *Nature*, **460**, 278-282.

41. Holland, A.J., and Cleveland, D.W. (2009) Boveri revisited: chromosomal instability, aneuploidy and tumorigenesis. *Nature Reviews Molecular Cell Biology*, **10**, 478-487.

5 Chapter 5. Proteomic analysis of methylglyoxal modifications reveals susceptibility of glycolytic enzymes to dicarbonyl stress

The information presented in this Chapter is reproduced from an article published in International Journal of Molecular Sciences:

Donnellan, L., Young, C., Simpson, B.S., Acland, M., Dhillon, V.S., Costabile, M., Fenech, M., Hoffmann, P., and Deo, P. (2022) Proteomic Analysis of Methylglyoxal Modifications Reveals Susceptibility of Glycolytic Enzymes to Dicarbonyl Stress. *International Journal of Molecular Sciences*, **23**, 3689. 10.3390/ijms23073689

For continuity and ease of reading the following article is presented here in chapter format. See Appendix D for authorship statement. All **Tables** and **Figures** that correspond to the supplementary documentation within this chapter can be accessed via the appropriate Digital Object Identifier (DOI) listed above.

Preamble

Identification of proteins harbouring methylglyoxal modifications is critical for understanding underlying mechanisms associated with elevated concentrations of this metabolite. The following chapter, although not directly associated with the core theme of this thesis, that being DNA damage, was produced by analysing the proteomics data generated in Aim 3 for non-mitotic proteins with methylglyoxal modifications. To date, only a handful of studies have analysed methylglyoxal modifications using shot-gun proteomics approach, with varying levels of success. This chapter suggests particular proteins may be more susceptible to methylglyoxal modifications than others, particularly those associated with glycolysis. Therefore, modification of proteins by methylglyoxal may not be random, and these results may suggest it may contain functional activity.

5.1 Abstract

Methylglyoxal (MGO) is highly reactive cellular metabolite that glycates lysine and arginine residues to form post translational modifications known as advanced glycation end-products. Because of their low abundance and low stoichiometry, few studies have reported their occurrence and site-specific locations in proteins. A proteomic analysis of WIL2-NS B lymphoblastoid cells in the absence and presence of exogenous MGO was conducted to investigate the extent of MGO modifications. We found over 500 MGO modified proteins, revealing an over representation of these modifications on many glycolytic enzymes, as well as ribosomal and spliceosome proteins. Moreover, MGO modifications were observed on the active site residues of glycolytic enzymes that could alter their activity. We similarly observed modification of glycolytic enzymes across several epithelial cell lines and peripheral blood lymphocytes, with modification of fructose bisphosphate aldolase being observed in all samples. These results indicate that glycolytic proteins could be particularly prone to the formation of MGO adducts.

5.2 Introduction

Post-translational modifications (PTMs) of proteins play an important role in biological events by regulating protein activity, interactions, stability and degradation (1). PTMs can be derived through enzymatic processes via specific proteins responsible for the addition or removal of modifications including phosphorylation, methylation, acetylation and ubiquitination (1). Moreover, PTMs can also be derived from non-enzymatic covalent modifications caused by electrophilic metabolites which react with the nucleophilic groups of arginine and lysine residues (2). These electrophilic metabolites include acetyl-CoA, malonyl-CoA, 4-hydroxynonenal, glyoxal and methylglyoxal (MGO) (2,3). MGO is a highly reactive 1,2-dicarbonyl compound formed as a by-product of glycolysis, in which intermediate triosephosphates (dihydroxyacetone phosphate and glyceraldehyde-3 phosphate) spontaneously degrade to generate MGO (4). Because MGO is formed via glucose metabolism it has been implicated in the pathogenesis of diabetic complications (5). Moreover, MGO has been shown to be elevated in cancer cells following the metabolic rewiring from oxidative phosphorylation to glycolysis (Warburg effect) as their primary energy source (6). Cellular MGO concentrations are maintained by the glyoxalase

system. MGO spontaneously reacts with glutathione forming a hemithioacetal that is recognized by glyoxalase 1 (GLO1) and converted to S-D-lactoylglutathione. This is subsequently recognized by GLO2 and converted to the non-reactive D-lactate and glutathione (7). MGO that is not sequestered by the glyoxalase system is able to react non-enzymatically to form methylglyoxal-hydroimidazolone (MG-H) isomers (1, 2 and 3) on arginine residues and carboxyethyl modifications on both arginine (N^{ϵ}-carboxyethylarginine (CEA)) and lysine (N^{ϵ}-carboxyethyllysine *(*CEL)) residues, amongst other less abundant modifications (8). Collectively, these modifications, as well as those formed by other metabolites (glucose, glyoxal and 3-deoxyglucosone) are referred to as Advanced Glycation Endproducts (AGEs) (9).

Detection of MGO modifications has been largely achieved by measuring the total cellular contribution, rather than its presence on specific proteins (10). This has primarily been performed utilising spectroscopic, immunochemical, chromatographic and mass spectrometric methods (11). While these approaches are effective for detecting changes in the abundance of the modification which can be used to infer biological significance, it lacks the specificity to directly identify target proteins which is crucial for elucidating underlying mechanisms. Unfortunately, measuring these modifications on specific proteins has proved challenging, due to their low abundance, low stoichiometry and heterogeneity which makes their detection and characterisation difficult. Only a few studies have attempted to measure site specific MGO modifications in mammalian cells with varying degrees of success (12-16). Initial studies struggled to identify MGO modifications under control conditions, requiring the use of exogenous MGO to increase the concentration of these modifications (12-14,16). While this is an effective approach for increasing the concentration of these modifications, these conditions may promote non-specific MGO modification of proteins or residues that would otherwise be unmodified under physiological or pathological conditions. Only recently has a comprehensive assessment of MGO modifications in HEK293T cells been applied. In this study, subcellular fractionation was applied to decrease sample complexity allowing for the identification of more than 600 MG-H modified proteins (14).

We recently applied bottom-up proteomics of whole WIL2-NS cell lysates to identify MGO modifications on mitotic proteins to gain deeper understanding on the aneugenic activity of MGO (17). While we were able to identify several mitotic proteins harbouring MGO modifications, we also identified an abundance of non-mitotic modified proteins. Therefore, using the entire inventory of MGO

modified proteins identified from our previous study, we performed several types of enrichment analysis to identify proteins and/or pathways that are most susceptible to MGO. Samples were digested with ProAlanase or Trypsin and analysed by LC-MS. In WIL2-NS cells we identified over 500 proteins with MGO modifications. Enrichment analysis revealed glycolytic enzymes are targets for MGO modifications, several of which occur on residues involved in substrate interactions and are likely to affect their activity. Furthermore, we showed that modification of glycolytic enzymes was not unique to WIL2-NS but was also present in several epithelial cell lines and peripheral blood lymphocytes *in vivo*, with modification of fructose bisphosphate aldolase being the most prevalent.

5.3 Methods

5.3.1 Materials

All reagents, chemicals and enzymes were purchased from Sigma unless indicated otherwise. Isotopically labelled and unlabelled MG-H1, CEL and Lys were purchased from Iris biotech (Marktredwitz, Germany). Trypsin Gold (Promega, V5280) and ProAlanase (Promega, VA2161) were purchased from Promega (Wisconsin, USA). Methylglyoxal solution was purchase from Sigma (M0252; Batch number BCBL7249V).

5.3.2 WIL2-NS cell culture

WIL2-NS cells (ATCC CRL-8155) was kindly gifted by Commonwealth Scientific Research Organisation (Adelaide, Australia). WIL2-NS cells were cultured in complete RPMI-1640 medium supplemented with 5% (v/v) fetal calf serum (FCS), l-glutamine (1% v/v) and penicillin/streptomycin (1% v/v) at 37°C in a humidified atmosphere with 5% CO_2. Cells were seeded at $5x10^5$ cells/ mL and incubated for 24 hours before being treated with 500 µmol/ L MGO for a further 24 hours.

5.3.3 Whole cell quantification of MG-H1 and CEL

WIL2-NS cells were lysed in ice-cold RIPA buffer with sonication over-ice for 2 x 10 second burst (Misonix, NY, USA). Cellular debris was removed by centrifugation (17,000 g for 10 min at RT).

Protein was precipitated by the addition of ice-cold acetone (4:1 ratio of acetone: sample). Sample was left overnight at -20°C before being centrifuged at 17,000 g for 10 min at RT. Precipitated protein was washed 2 x with ice-cold acetone before being resuspended in 50 mM ammonium bicarbonate (pH 8.0). Samples were incubated at 37°C for 4 hours to aid in the solubilization of protein. Undissolved protein was removed by centrifugation at 17,000 g for 10 min (RT) and protein concentration was quantified using a Bicinchoninic acid (BCA; Sigma) assay following the manufacturer's instructions. Trypsin (TPCK treated, ≥ 10,000BAEE units/ mg protein) was added at a protein to enzyme ratio (1:50) and sample was incubated at 37°C for 16 hours. Following incubation, sample was heated to 95°C for 10 minutes to denature the trypsin. Following this, sample was cooled to room temperature and Pronase E (≥ 3.5 units/ mg protein) and Aminopeptidase (≥ 12 units/ mg protein) were added at protein to enzyme ratio (1:50) for a further 24 hours. Enzymes were removed by the addition of ice-cold acetone (4:1 ration of acetone: sample) and sample was centrifuged at 17,000 g for 10 min at RT. Supernatant was collected, dried under vacuum centrifugation and resuspended in 0.1% formic acid (v/v) containing internal standard (100 nmol/L). Sample (2 µL) was injected and analytes were separated using a 150 × 4.6 mm, 4 µm Phenomenex C18 column (Phenomenex, Torrance, CA, USA) with a linear gradient of 0.1 % formic acid in water (Buffer A) and 0.1% formic acid in acetonitrile (Buffer B) over 5 min at a flow rate of 0.6 mL/ min. Multiple reaction monitoring (MRM) was conducted in positive mode using an AB Sciex 6500+ QTRAP mass spectrometer with the following transitions: m/z 147.4 > 83.9 (lysine), 151.2 > 87.9 (d_4 lysine), 219.2 > 130.2 (CEL), 222.2 > 134.2 (d_4CEL), 229.2 > 116.1 (MG-H1) 232.2 > 116.1 (d_3 MG-H1). The ion source parameters were as follows; source temperature (450°C), curtain gas (20 psi), collision gas (medium), ion spray voltage (5500 V) and ion source gas 1 and 2 (40 psi). The concentration of MG-H1 and CEL was normalized to lysine content and expressed as mmol analyte/ mol lysine. Concentration of MG-H1 and CEL are expressed as mean ± SD n=3. Student t-test was conducted to determine any significant difference ($P < 0.05$) using GraphPad Prism (San Diego, CA, USA, Version 8.3.0).

5.3.4 Isolation and purification of peripheral blood lymphocytes

Venous blood was collected and lymphocytes isolated as previously described from three healthy male volunteers, aged 25-45 years by density gradient centrifugation (18). Following isolation, PBL were

stored in liquid nitrogen. The study was approved by the Human Research Ethics Committee of University of South Australia (Application ID: 203348) and written informed consent was obtained from all participants. For PBL, only cytoplasmic proteins were isolated by separation of cytoplasmic fraction from nuclear fraction by cell lysis with buffer containing (320 mM sucrose, 10 mM tris-HCl, 5 mM $MgCl_2$ and 1% triton-X100). Supernatant was collected and protein precipitated with 3 volumes of ice-cold acetone and washed 3 times. Protein was dissolved in 8 M urea/ 50 mM ammonium bicarbonate and protein concentration determined by BCA assay following manufacturer's instructions.

5.3.5 Proteomic analysis of WIL2-NS and PBL

Cell lysis for and protein isolation for WIL2-NS was identical to whole cell quantification of MG-H1 and CEL, however, following this, protein was resuspended in 50 mM ammonium bicarbonate/ 8 M urea. Protein concentration was measured by BCA assay. Preparation of WIL2-NS and PBL for proteomic analysis was identical, except that PBL were only digested with trypsin. Briefly, 100 µg of protein was reduced and alkylated with 10 mM dithiothreitol and 15 mM chloroacetamide, respectively. Sample was diluted with 50 mM ammonium bicarbonate to reduce urea concentration to 0.8 M. Trypsin (Trypsin Gold, Promega, V5280, 2 µg) was added and samples were incubated for 8 hours at 37°C at 500 rpm. Following incubation, 10.2 µL of 100% (v/v) formic acid was added to terminate the reaction and acidify the sample. For ProAla digestion, 20 µg of protein was reduced and alkylated with 10 mM dithiothreitol and 15 mM chloroacetamide, respectively. Sample was diluted with 33 mM HCl to reduce Urea conc to 0.3 M and reduce pH to ~1.5. ProAlanase enzyme (Promega, VA2161, 0.2 µg) was added, and samples were incubated for 4 hours at 37°C. All subsequent steps were the same for trypsin and ProAla digests. Peptides were purified using in-house packed C18 stage tips. Stage tips were conditioned with 40 µL of 100% acetonitrile and equilibrated with 80 µL of 0.1% (v/v) formic acid. Samples were loaded onto the stage tip and washed with 40 µL of 0.1% (v/v) formic acid. Samples were then eluted with 50% (v/v) acetonitrile in 0.1% (v/v) formic acid. Eluates were dried using a Speed-Vac and reconstituted in 20 µL of 0.1% (v/v) formic acid. Peptide concentration was determined by measuring tryptophan concentration of the peptides using an Agilent Cary Eclipse Fluorescence Spectrophotometer. Briefly, samples diluted 1:10 in 8M urea/ 50 mM ammonium bicarbonate were

loaded into a 50 µL Quartz cuvette and fluorescence was measured at excitation and emission of 295 and 350, respectively. Concentration was determined by comparing against a standard curve generated using tryptophan. Protein concentration was deduced from tryptophan concentration assuming a tryptophan content of 1.17% in mammalian protein (19).

OV90 and Caov3 cell lines were prepared as described above except that a mixture of Trypsin/ Lys-C was used for the digestion and samples incubated overnight. These samples were prepared for another study, but raw data files were processed as described below for analysis of MGO modifications.

5.3.6 High resolution orbitrap mass spectrometry

LC-MS analysis was conducted on an EASY-nLC 1200 system coupled to an Orbitrap Exploris 480 mass spectrometer (Thermo Scientific, Bremen, Germany). Peptides from trypsin (1 ug) or ProAlanase (0.5 ug) digests were reconstituted in 0.1% formic acid and loaded onto a 25 cm fused silica column (75 um inner diameter, 360 um outer diameter) heated to 50°C. The column was in-house packed with 1.9 um ReproSil-Pur 120 C18-AQ particles (Dr. Maisch, Ammerbuch, Germany). Peptides were separated over a 70-minute linear gradient (3 to 20% acetonitrile in 0.1% formic acid) at a flow rate of 300 nl/min. A FAIMS Pro interface (Thermo Scientific) generated compensation voltages at -50 and -70 V to regulate the entry of ionized peptides into the mass spectrometer. MS scans (m/z 300 to 1500) were acquired at resolution 60000 (m/z 200) in positive ion mode. Peptide fragmentation (minimum threshold of 1×10^4 precursor ions) was performed with 27.5% HCD collision energy, with the resulting MS/MS scans (starting m/z 85) measured at resolution 15000. Cycle time was limited to 1.5 seconds, while the dynamic exclusion period was specified at 40 seconds.

5.3.7 Data analysis

Raw MS files were analysed using Proteome Discoverer 2.4 (Thermo Scientific). Data were processed with the Sequest HT search engine against a concatenated database containing the 74811 forward entries from the UniProt human database (December 1, 2019) and their respective decoy counterparts. Trypsin or ProAlanase (cleaves C-terminal to proline and alanine residues) was specified as the enzyme and a maximum of five miscleavages was allowed. Precursor and fragment mass tolerances were 10 ppm and

0.02 Da, respectively. Arginine and lysine carboxyethylation (+72.021129), arginine methylglyoxal-hydroimidazolone (54.010565), methionine oxidation (+15.994915), N-terminal acetylation (+42.010565), N-terminal methionine loss (-131.040485), N-terminal methionine loss and acetylation (-89.02992) were set as dynamic modifications, with cysteine carbamidomethylation (+57.021464) designated a static modification. Protein and peptide false discovery rates were both set at 1%. Raw MS files have been deposited to the ProteomeXchange Consortium via the PRIDE partner repository with the dataset identifier PXD032812 (20).

Enrichment analysis was performed using the Database for Annotation, Visualization and Integrated Discovery (DAVID) v6.8 (https://david.ncifcrf.gov/) (21). We used STRING database v11.5 (Search Tool for the Retrieval of Interacting Genes, available at: http://string-db.org/ (22)) for construction of the protein-protein interaction (PPI) network. Only interactions with an interaction score >0.95 were included and any disconnected nodes were removed. Remaining STRING network was exported to Cytoscape (23). Cluster labels were assigned based on the KEGG analyses of pathways that were associated with the greatest number of proteins in that cluster. Venn diagrams were generated using https://bioinformatics.psb.ugent.be/webtools/Venn/.

5.4 Results

5.4.1 Characterization of MGO modified proteins

To explore the potential impact of dicarbonyl stress (elevated MGO) on cellular function, we used an untargeted proteomic approach on whole cell extracts (WCE) from WIL2-NS cells to investigate modification of intracellular proteins following treatment with MGO. Cells were treated with 500 µmol/L MGO for 24 hours which led to a 2.2 and 1.8-fold increase in MG-H1 and CEL, respectively shown by LC-MS/MS analysis (Appendix A Figure 1A, B). This relative increase is consistent with those observed in pathological conditions such as diabetes and thus less likely to cause non-specific modifications (8).

Preparation of WCE for proteomics was performed using trypsin and Proalanase (ProAla) in separate digests. Overall, we identified 519 modified proteins (Full list in Appendix B). Majority of modifications were identified in trypsin digests, however, incorporation of ProAla in this study

increased the number of identified MGO modification sites by approximately 25% (Appendix A Figure 1C). Surprisingly, only 3.8% of the modification sites were detected in both ProAla and trypsin digested samples (Appendix A Figure 1C). This was mostly due to ProAla modified peptides contributing to increased sequence coverage where the corresponding modification sites were undetected by trypsin. For example, as shown for CEL modification of K20 of Transgelin-2 and K496 of RNA-splicing ligase Rtcb homolog (Figure 5.1A). Trypsin is commonly the protease of choice for MS-based proteomics because among other reasons it cleaves at the carboxyterminal of lysine and arginine causing a positive charge at the C-terminus of the peptide. This is advantageous for MS analysis as it influences the intensity of b and y ion series, which is particularly useful for identifying site-specific PTM residues. Abundant y and b ions were observed for MGO modified peptides produced in trypsin digested samples (Figure 5.1B). However, despite a C-terminus alanine or proline, abundant b and y ions could also be observed in ProAla digested samples (Figure 5.1C). Therefore, ProAla can be used in conjunction with trypsin for identification of MGO modifications. To gain insight into what factors may influence identification of MGO modified proteins we ranked the proteins from each digest based on their Log2 abundance. In both digests, modification of proteins by MGO was more often observed in higher abundant proteins with 45.8% and 61.9% of identifications occurring in the top 20% most abundant proteins for trypsin and ProAla, respectively (Figure 5.1D and Appendix A1.D). In the trypsin digest, 13 of the 20 most abundant proteins contained MGO modifications, consisting of 32 modification sites. Number of modifications per protein ranged from 1-19 sites, with beta-actin (ACTB) containing the highest number of MGO modification sites (Appendix A table 1 and Appendix A Figure 1E).

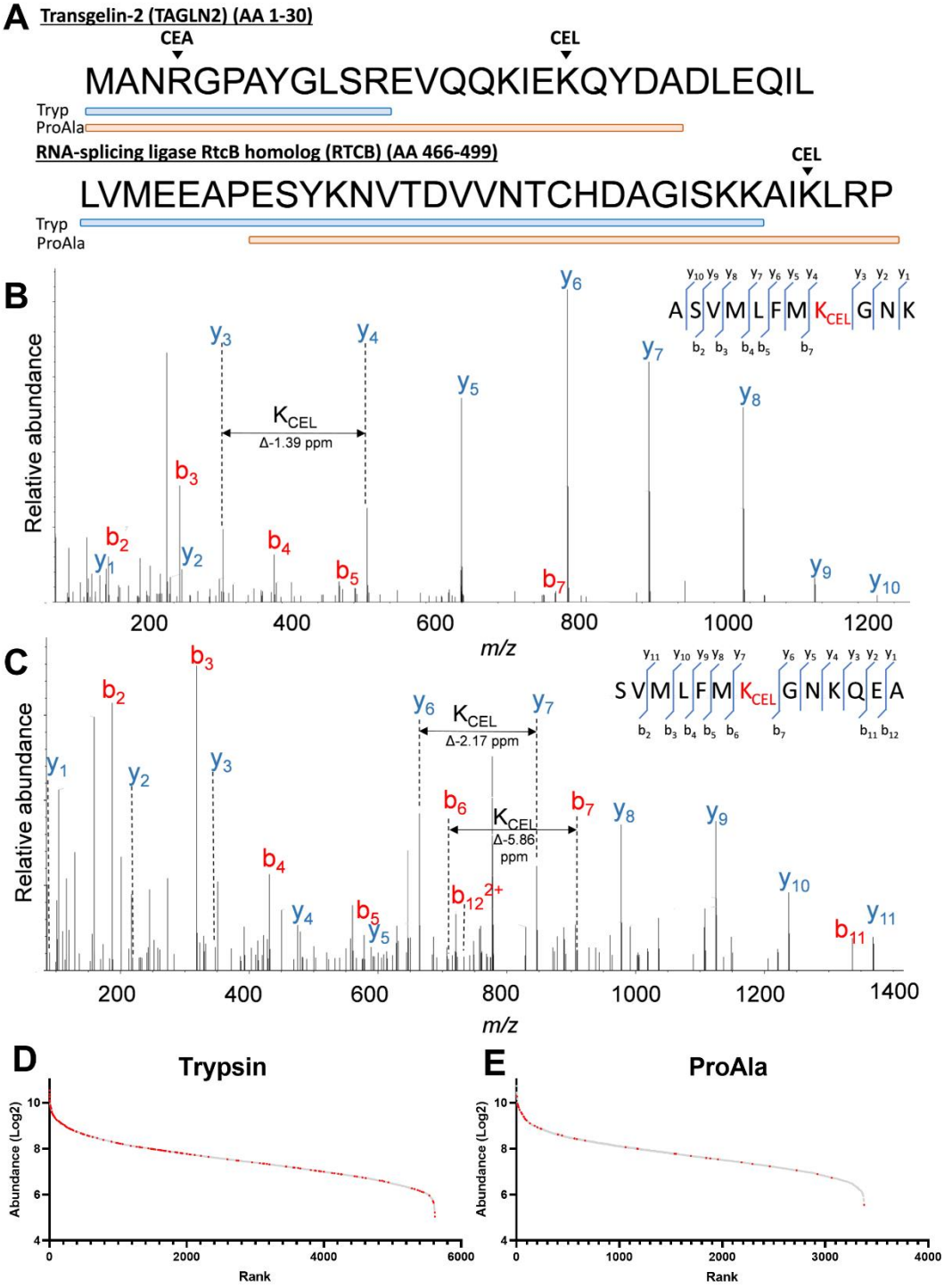

Figure 5.1. Proteomic analysis of MGO modifications. A. Sequence coverage plot of Transgelin-2 (top) and RNA-splicing ligase RtcB homolog (bottom) protein sequences obtained from Trypsin (blue) and ProAla (orange). B/C. MS/MS spectra of a CEL modification on Glutaredoxin at K253 generated by trypsin digestion (B) and ProAla digestion (C) (see also Appendix A Figure 2). **D/E**. Ranking plot of proteins in trypsin digestion (D) and ProAla digestion (E). Grey spots represent unmodified and red are those with MGO modifications.

5.4.2 Enrichment analysis of MGO modified proteins

To explore the functional impact of MGO modifications in WIL2-NS we performed enrichment analysis of biological processes with the DAVID gene ontology tool using all MGO-modified proteins generated in this study. MGO-modified proteins showed over representation in a diverse range of biological processes including canonical glycolysis, translation initiation, regulation of cellular response to heat, mRNA splicing via spliceosome, amongst others (Table 5.1). Canonical glycolysis was the most enriched biological process (13.4-fold enrichment). Pathways with the largest number of MGO-modified proteins included cell-cell adhesion, mRNA splicing via spliceosome, translation initiation and protein folding which all contained more than 20 modified proteins (Table 5.1). To further explore those pathways most impacted by MGO, we developed a protein-protein interaction (PPI) network with STRING. KEGG pathway enrichment analysis was performed to determine pathways associated with the remaining clusters which revealed glycolysis/ gluconeogenesis, spliceosome and ribosome as the pathways most affected by MGO modifications (Figure 5.2). Glycolysis involves the conversion of glucose to pyruvate in 10 enzyme mediated steps. Remarkably, 7 of the 10 steps contained MGO-modified proteins including glucose-6-phosphate isomerase (GPI), enolase 1/3 (ENO1/3), fructose bisphosphate aldolase A/C (ALDOA/C), triosephosphate isomerase (TPI), glyceraldehyde 3-phosphate dehydrogenase (GAPDH), phosphoglycerate kinase 1 (PGK1) and pyruvate kinase M (PKM) consisting of 20 modification sites in total (Figure 5.3A and Appendix C). The selective enrichment of glycolysis suggests MGO may modulate glucose metabolism by modification of enzymes involved in this pathway. To investigate potential impact of MGO modifications on these proteins we looked at the role of residues that were modified. ALDOA is a highly conserved glycolytic enzyme that catalyses the reaction that cleaves the aldol fructose 1,6-bisphosphate into triosephosphates dihydroxyacetone phosphate (DHAP) and glyceraldehyde 3-phosphate (G3P). Fructose 1,6-bisphosphate covalently binds to K229 followed by Schiff-base formation and carbon-carbon cleavage yielding triosephosphate formation. K229, as well as K146 and R42 which non-covalently interact with the substrate in the active site were modified by MGO suggesting modification of these sites is likely to interfere with its interaction with fructose 1,6-bisphosphate (Figure 5.3B). All 4 modification sites observed on ALDOA were observed within the active site, despite the presence of numerous other lysine and arginine resides on the protein, suggesting modification of these residues was not random (Figure 5.3B). Strikingly, ENO1, another glycolytic

enzyme that converts 2-phosphoglycerate to phosphoenolpyruvate was shown to contain 7 modification sites. Three of which were shown to occur on residues shown to contain other PTMs (Figure 5.3C). Several other MGO-modifications occurred on other glycolytic enzymes on residues of known PTMs, active sites or binding sites (Figure 5.3C).

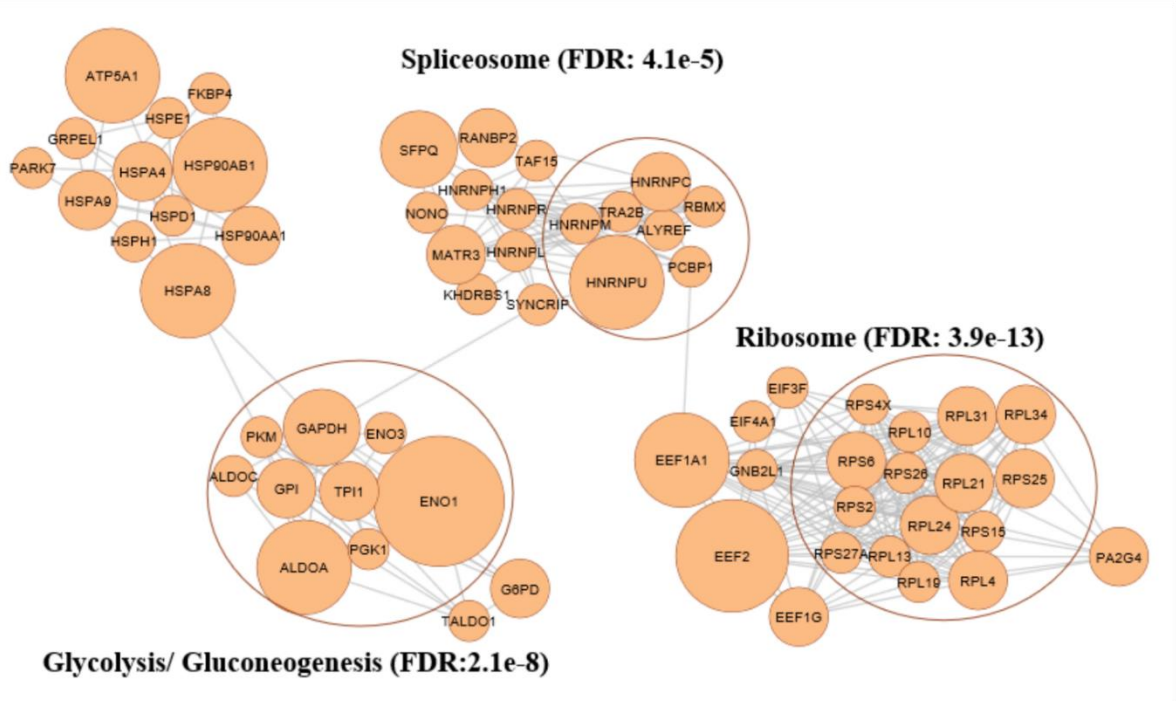

Figure 5.2. Protein-protein interaction network of MGO modified proteins generated using STRING database v11.5 and Cytoscape v3.9.0 [19]. Size of the node (protein) reflects the number of MGO modifications found on that protein (ranging from 1-7). FDR; false discovery rate.

Table 5.1 Enrichment analysis for biological processes enriched with MGO modifications.

Biological Process	**Count**	**Fold Enrichment**	**FDR**	**Genes**
Canonical Glycolysis	9	13.4	3.6E-5	**ALDOA**, **ALDOC**, **ENO1**, **ENO3**, GPI, GAPDH, **PGK1**, **PKM**, **TPI1**
Gluconeogenesis	9	7.9	1.6E-3	**ALDOA**, **ALDOC**, **ENO1**, **ENO3**, GPI, GOT2, GAPDH, **PGK1**, **TPI1**
Translation initiation	22	6.2	2.3E-8	**DDX3Y**, DHX29, EIF3F, EIF4A1, **PABPC1**, PAIP1, RPL10, **RPL13**, **RPL19**, **RPL21**, RPL24, **RPL31**, **RPL34**, **RPL4**, RPS15, RPS2, RPS25, RPS26, RPS27A, **RPS4X**, **RPS4Y1**, **RPS6**
Regulation of cellular response to heat	12	6.2	4.7E-4	FKBP4, **POM121C**, **POM121**, **RANBP2**, HSP90AA1, **HSP90AB1**, **HSPA8**, HSPH1, **NUP153**, NUPL2, **RPA3**, **YWHAE**
Nucleosome assembly	17	5.5	1.4E-5	ATRX, H2AFX, **H3F3A**, ANP32A, **ANP32B**, DAXX, **HMGB2**, **HIST1H1A**, HIST1H2BB, HIST1H2BD, **HIST1H2BK**, HIST1H2BM, HIST1H3A, **HIST1H4I**, HIST2H2BF, HIST2H3PS2, NPM1
Cell-cell adhesion	38	5.4	1.3E-13	**AHNAK**, DDX6, DHX29, **EHD4**, LASP1, **PARK7**, **RAB1A**, RANGAP1, **ALDOA**, CCT8, **CKAP5**, **ENO1**, EEF1G, EEF2, FASN, FLNB, **HSP90AB1**, **HSPA8**, HDLBP, HIST1H3A, HCFC1, LDHA, **PRDX1**, **PCBP1**, PSMB6, **PPME1**, **PKM**, RACK1, RPL24, **RPL34**, RPS2, RPS26, **SPTAN1**, SPTBN1, TAGLN2, **YWHAB**, **YWHAE**, **YWHAZ**
mRNA splicing, via spliceosome	26	4.5	2.4E-7	ALYREF, **DNAJC8**, **FUS**, **RBMX2**, **RBMX**, **POLR2B**, **CSTF2**, **HSPA8**, **HNRNPC**, **HNRNPH1**, **HNRNPH2**, **HNRNPL**, HNRNPM, HNRNPR, **HNRNPU**, NONO, **PPIE**, **PABPC1**,

				PCBP1, **SRSF2**, **SNRPB**, **SPEN**, **SF3B1**, **SF3B2**, SYNCRIP, TRA2B
Protein folding	21	4.5	9.9E-6	FKBP4, FKBP5, GRPEL1, HSPE1-MOB4, **RANBP2**, **CANX**, **CCT2**, CCT5, CCT8, HSP90AA1, **HSP90AA2P**, **HSP90AB1**, HSP90AB2P, **HSP90B1**, **HSPA8**, HSPA9, HSPE1, PPIA, **PPIE**, ST13, TXN
Protein sumoylation	13	4.3	5.2E-3	**POM121C**, **POM121**, **RAD21**, **RANBP2**, **BIRC5**, **HNRNPC**, IFIH1, **NUP153**, NUPL2, **RING1**, **SMC3**, **TRIM28**
G2/M transition of mitotic cell cycle	15	4.2	1.5E-3	ALMS1, **HAUS5**, **KHDRBS1**, **BIRC5**, CNTRL, **CEP250**, **CKAP5**, HSP90AA1, ODF2, PPP1CB, RPS27A, **TUBA4A**, TUBB4B, **YWHAE**

Pathway enrichment analysis was performed using Database for Annotation, Visualization and Integrated Discovery (DAVID) v6.8 (https://david.ncifcrf.gov/) (23). Biological Processes or proteins in **bold** were also observed in control (untreated) cells.

5.4.3 Modification of glycolytic enzymes

Following the identification of glycolytic enzymes as primary targets for MGO-modification in WIL2-NS we sought to determine if this was consistent across other cell types. Therefore, using previous data of epithelial cell lines; OV90 and Caov3 without (parental) and with chemoresistance to the chemotherapeutic drug carboplatin (CBPR) from our laboratory, raw data files were reprocessed for MGO modifications. As these cell lines were initially used for a different study, they were not treated with MGO and therefore modification sites represent those present under basal conditions. All cell lines, except for OV90 (parental) showed canonical glycolysis to be over-represented with MGO

modifications (Figure 5.4A). Next, using peripheral blood lymphocytes isolated from three separate healthy male donors, we investigated whether the same was true *in vivo*. As with epithelial cell lines, analysis of MGO modification sites was done without MGO treatment to determine modifications sites present under basal conditions only. Unfortunately, no significant enrichment was observed for MGO modifications on glycolytic enzymes in PBL, but modification of ALDOA was observed in PBL from all donors (Figure 5.4A, B). Furthermore, modification of ALDOA was observed in all epithelial cell lines (Figure 5.4B). We also investigated modification of other proteins that occurred across multiple cell types. Histone H1.1 R57 (CEA), AT-rich interactive domain-containing protein 2 (Fragment) R277 (CEA) and Neuroblast differentiation-associated protein AHNAK K1333 (CEL) being the most commonly identified modification sites (Appendix A Table 2).

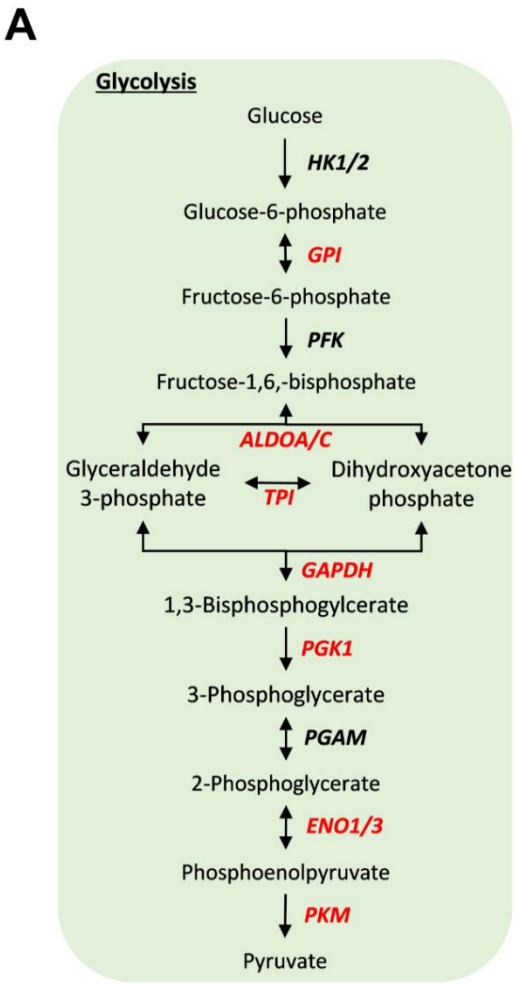

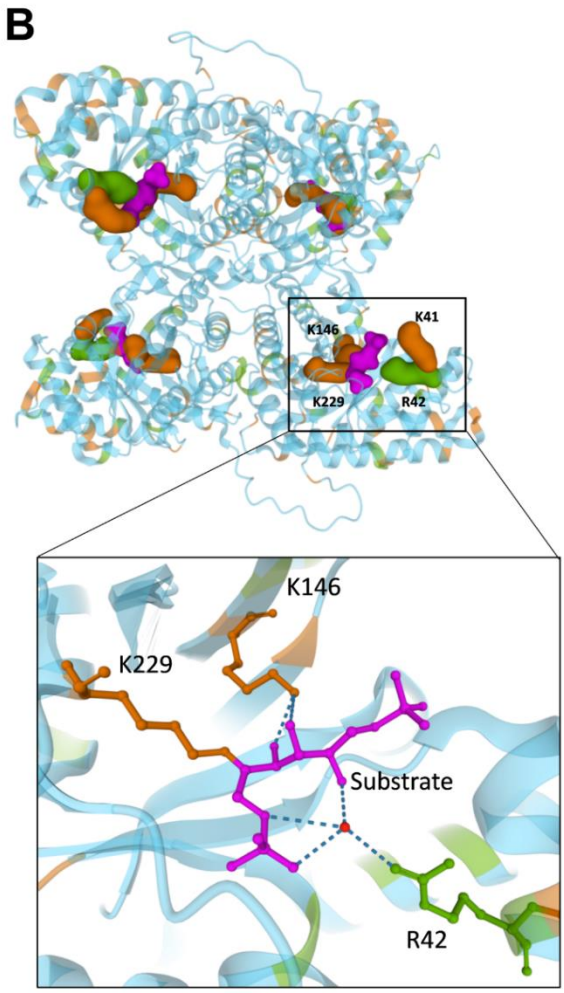

C

Protein	Residue	Description
ALDOA	K229	Active site
	K146, R42	Binding site: Substrate
	K41	PTM site: acetylation
ENO1	K228	PTM site: 2-hydroxyisobutyrylation
	K71, K193	PTM site: acetylation
GAPDH	K215, K263	PTM site: dimethylation
	R234	Binding site: Substrate
PKM	K305	PTM site: acetylation

Figure 5.3. MGO modifies critical residues of glycolytic enzymes. A. Flow diagram showing glycolysis. Enzymes highlighted in red contain MGO modifications detected by LC-MS/MS analysis. B. Three-dimensional structure of fructose bisphosphate aldolase A (ALDOA, PDB entry 1ZAI). MGO modified residues are labelled and all arginine (green) and lysine (orange) residues are shown. Active site bound to intermediate Schiff-base (substrate) is enlarged. **C.** Table of MGO modification sites that occur on residues involved in protein function. HK; hexokinase, GPI glucose-6-phosphate, PFK; phosphofructokinase, ALDO; fructose bisphosphate aldolase, TPI; triosephosphate isomerase, GAPDH; glyceraldehyde 3-phosphate dehydrogenase, PGK; phosphoglycerate kinase, PGM; phosphoglucomutase, ENO; enolase, PKM; pyruvate kinase M.

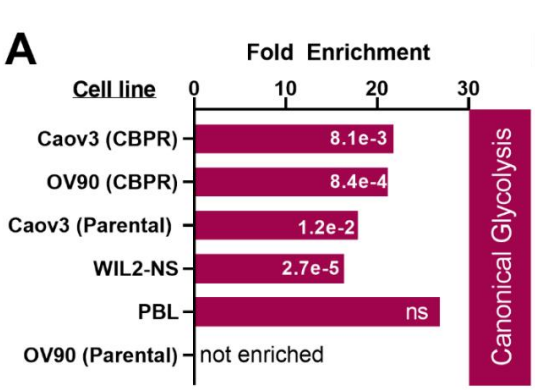

B

	ENO1/3	ALDOA/C	TPI	GAPDH	PGK1	PGM1	PKM
WIL2-NS	2	2	1	0	1	0	3
OV90 (P)	0	2	0	0	1	0	0
OV90 (CBPR)	0	3	0	0	2	1	0
Caov3 (P)	1	1	0	1	0	0	0
Caov3 (CBPR)	1	2	0	0	0	0	0
PBL 1	0	1	0	0	0	0	0
PBL 2	0	1	0	0	0	0	0
PBL 3	0	1	0	0	0	0	0

Figure 5.4. Modification of glycolytic enzymes by MGO is present across various cell lines. A. Enrichment of MGO modified glycolytic proteins in different cell types. For this analysis, all cells were untreated, including WIL2-NS. For PBL, modified proteins from all donors were collated into one list and enrichment analysis was performed. Values in white corresponds to the FDR. **B,** Occurrence of MGO modified glycolytic enzymes in different cell types. CBPR; chemoresistance to the chemotherapeutic drug carboplatin, PBL; peripheral blood lymphocytes, ENO; enolase, ALDO; fructose bisphosphate aldolase, TPI; triosephosphate isomerase, GAPDH; glyceraldehyde 3-phosphate dehydrogenase, PGK; phosphoglycerate kinase, PGM phosphoglucomutase, PKM; pyruvate kinase M, ns; not significant.

5.5 Discussion

Metabolite driven PTMs have a diverse role in regulating protein function, by altering enzyme activity, obstructing protein-protein interactions and by forming covalent crosslinks between proteins (1). To gain further insight into the role of PTMs, mapping of proteins and specific sites using proteomic techniques is an attractive approach. Therefore, we utilised LC-MS techniques to explore intracellular MGO modifications. Detection of MGO modifications, and other AGEs has remained difficult due to their low abundance, low stoichiometry and heterogeneity at modification sites and the lack of suitable enrichment techniques (24). An ideal approach would utilise pan-specific antibodies to enrich native modifications. Only one previous study has reported this approach for MGO modifications using antibodies specific to each MG-H isomer and CEA to enrich MGO modified histone peptides, however this yielded no enrichment (16). Interestingly, an antibody-based enrichment method was applied to N^{ε}-carboxymethyllysine (CML) modifications, another AGE using commercially available antibodies (25). This yielded a 10-fold increase in the identification of CML-modified peptides (25). Several commercially available antibodies exist for MGO modifications which may be more suitable for

antibody-based enrichment techniques then those previously used. An alternative enrichment technique was recently described using an alkyne-labelled MGO analogue (alkMGO) which can be enriched by click-chemistry based techniques (26). In this study, 71 MG-H, CEL and CEA modifications were identified in human serum incubated with 250 µmol/L of alkMGO and >300 in erythrocyte lysates treated with 500 µmol/L (26). Unfortunately, the alkMGO analogue is not commercially available which limits its use by other researchers. Similar to what we performed in this study the most common approach to increase identification of MGO modified proteins is to increase their concentration using exogenous MGO. This approach has been used to study MGO modification sites in Human microvascular endothelial cells (HMEC-1), periodontal ligament fibroblasts (PDLF) and HEK293T cells (12-14). In PDLF, only five proteins with MGO modifications were identified under control conditions (13). This increased to 172 proteins consisting of 353 sites following incubation of cell lysate with 500 µM MGO for 24 hours. Furthermore, the same authors recently provided a comprehensive assessment of the dicarbonyl proteome in HEK293T cells by incubation with 131 µmol/L of MGO followed by subcellular fractionation which resulted in the identification of more than 600 MG-H modified proteins (14). Similarly, Galligan et.al (2018) used exogenous MGO in GLO1 KO cells to study the site specific MGO modifications on histone proteins, from which they identified 21 sites across canonical histone proteins (16). While addition of exogenous MGO is useful for increasing the concentration of MGO modifications, several of the aforementioned studies have used concentrations which is likely to cause non-specific modification of proteins expected under physiological or pathological conditions. To prevent excessive modification of proteins, we ensured the concentration of MG-H1 and CEL following treatment were elevated to a level which reflects in vivo pathological conditions (i.e., less than 3-fold) to prevent non-specific modifications occurring (27). We also utilised a non-standard protease ProAla, in addition to trypsin to increase total sequence coverage. ProAla has recently been shown to be more effective than trypsin at peptide mapping and identifying PTMs on more basic proteins such as histones, which are known targets for MGO (16,28). Previous studies have also utilised other proteases such as Lys-C and Glu-C for the identification of various glycated proteins (12,29,30). For example, a study using Glu-C for digestion of diabetic serum was effective in the identification of glycated peptides (30). Therefore, use of other proteases such as Arg-C, Asp-N and Lys-N in conjunction with trypsin may be useful in identifying additional MGO modification sites (31).

Enrichment analysis of our inventory of MGO modified proteins using DAVID and STRING revealed distinct networks which were enriched with these modifications. Most enriched was canonical glycolysis, of which 7 steps of this 10-step process contained MGO modified proteins in WIL2-NS cells. Previous studies have shown various MGO modifications on arginine residues of glycolytic enzymes, however, in the current study, the majority of modified sites were on lysine residues (12,26). This may be due to treatment times as MG-H modifications occur more rapidly than carboxyethyl, but also have a shorter half-life. Interestingly, glycolysis is the major pathway responsible for the formation of MGO by spontaneous degradation of intermediate triosephosphates (4). Therefore, this may suggest a potential regulatory feedback mechanism whereby elevated MGO leads to modification of glycolytic proteins, decreasing their activity and reducing MGO back to a physiological concentration. Modification of fructose bisphosphate aldolase A at K229 or 146 was identified in all cell types analysed in this study, including PBL. Remarkably, all 4 modification sites of ALDOA are involved in its aldolase activity (32). K229 acts as a nucleophile in the formation of the Schiff-base with the C2-carbonyl group of the substrate fructose 1,6-bisphosphate, followed by cleavage of the C3-C4 bond releasing glycolytic intermediates G3P and DHAP (32). The charged from of K146 non-covalently interacts with the substrate and intermediates to stabilise negative charges and promotes the negative form of Y363 responsible for the reversible protonation of C3 of the substrate (32). K41 and R42 have also been shown to interact with the 6-phosphate of the substrate (33). All these interactions rely on the positively charged nucleophilic groups of the lysine or arginine residue which are lost following MGO modifications (34,35). Therefore, it is highly likely that MGO modification of ALDOA at these residues, in particular K229 will affect substrate binding and its catalytic activity, interfering with the progression of glycolysis. Moreover, modification of ENO1 was also shown to be a target of MGO containing 7 modifications sites following treatment with MGO. Regulation of ENO1 activity has recently been shown to occur, at least in part by p300 mediated 2-hydroxyisobutyrylation of K228, a site shown to be modified by MGO (36). Knockdown of p300, reducing the level of K228 2-hydroxyisobutyrylation, was shown to reduce enzyme activity and the concentration of glycolytic intermediates (36). Therefore, modification of K228 by MGO would prevent p300 mediated 2-hydroxyisobutyrylation which may cause a reduction in its activity. MGO has been shown to decrease the activity of glycolytic enzymes in vitro and alter the abundance of glycolytic intermediates, specifically an increase in early stage (fructose

1,6 bisphosphate, dihydroxyacetone phosphate, 3-phosphoglycerate) and a decrease in later stage intermediates (phosphoenolpyruvate and pyruvate) (37-40). Unfortunately, most studies that have investigated the activity of specific glycolytic enzymes in response to MGO have used concentrations (2.5-5 mM) that would likely cause non-specific modifications (37-40). Therefore, further studies investigating the effects of site-specific MGO modifications, which are shown to occur under normal or pathophysiological conditions, on the activity of glycolytic enzymes would provide valuable information and reveal currently unclear mechanistic action displayed by MGO. A recent study showed that treatment of GLO2 knockout cells with 50 μM of MGO was able to decrease metabolic output by modification of the glycolytic enzymes by the glyoxalase intermediate S-D-lactoylglutathione, which produces lact(o)yllysine (41). Interestingly, lact(o)yllysine and CEL are isomeric, with essentially the same moiety in opposite directions and may have similar signalling consequences. Furthermore, both modifications produce identical mass shifts (+72) and are difficult to differentiate by standard proteomics techniques. Therefore, it cannot be ruled out that some of the lact(o)yllysine modifications observed in the previous study were actually CEL, and vice versa for CEL modifications identified in this study. Nevertheless, both can be produced either directly (CEL) or indirectly (lact(o)yllysine) by MGO and therefore are associated with dicarbonyl stress.

Other cellular processes over-represented with MGO modifications included the spliceosome and ribosome. The spliceosome has previously been shown to be enriched with MGO modifications, which was associated with a decrease in the abundance of proteins in this pathway (14). The author's showed, using the Cancer Cell Line Encyclopedia that GLO1 mRNA expression positively correlated with the expression of spliceosome proteins (PPIL1 and CDC5L), suggesting increased GLO1 expression protects spliceosome proteins in tumour cells (14). The spliceosome protein family serine and arginine rich splicing factors, including SRSF2 which was modified with MGO in this study, are master regulators of pre-mRNA splicing. Dysregulation of this process can cause genomic instability and impede the normal expression pattern of proteins, resulting in aberrant biological function (42). Loss of SRSF2 in mouse embryo fibroblast causes cell cycle arrest in G2/M and double strand break formation due in at least part to hyperphosphorylation and hyperacetylation of p53 (43). Furthermore, mutations in SRSF2 and SF3B1, which also contained MGO modification are observed in 5-75% of patients with various myeloid neoplasms, particularly chronic myelomonocytic leukemia and refractory anaemia with

ring sideroblasts (44). Therefore, protection of spliceosome pathway proteins may confer another role of GLO1 in tumour cells.

Data herein reveals glycolysis/ gluconeogenesis, spliceosome and ribosome as major pathways enriched with MGO modifications. Although we were able to identify many MGO modified proteins it is unlikely we are seeing a complete picture. Further efforts to enrich those proteins which are modified by MGO are required, particularly to help identify low abundant proteins that may harbour modifications. Nevertheless, we were still able to gain insight into the potential impact MGO may have on cellular function. Furthermore, site-specific identification of MGO modification sites suggests it may have a role in regulating glycolytic output by altering the activity of glycolytic enzymes.

References

1. Walsh, C.T., Garneau-Tsodikova, S., and Gatto, G.J., Jr. (2005) Protein posttranslational modifications: the chemistry of proteome diversifications. *Angewandte Chemie*, **44**, 7342-7372.
2. Zheng, Q., Maksimovic, I., Upad, A., and David, Y. (2020) Non-enzymatic covalent modifications: a new link between metabolism and epigenetics. *Protein Cell*, **11**, 401-416.
3. Harmel, R., and Fiedler, D. (2018) Features and regulation of non-enzymatic post-translational modifications. *Nature Chemical Biology*, **14**, 244-252.
4. Phillips, S.A., and Thornalley, P.J. (1993) The formation of methylglyoxal from triose phosphates: investigation using a specific assay for methylglyoxal. *European Journal of Biochemistry*, **212**, 101-105.
5. Schalkwijk, C.G., and Stehouwer, C.D.A. (2020) Methylglyoxal, a Highly Reactive Dicarbonyl Compound, in Diabetes, Its Vascular Complications, and Other Age-Related Diseases. *Physiological Reviews*, **100**, 407-461.
6. Bellier, J., Nokin, M.J., Caprasse, M., Tiamiou, A., Blomme, A., Scheijen, J.L., Koopmansch, B., MacKay, G.M., Chiavarina, B., Costanza, B., Rademaker, G., Durieux, F., Agirman, F., Maloujahmoum, N., Cusumano, P.G., Lovinfosse, P., Leung, H.Y., Lambert, F., Bours, V., Schalkwijk, C.G., Hustinx, R., Peulen, O., Castronovo, V., and Bellahcene, A. (2020) Methylglyoxal Scavengers Resensitize KRAS-Mutated Colorectal Tumors to Cetuximab. *Cell Reports*, **30**, 1400-1416 e1406.
7. Rabbani, N., and Thornalley, P.J. (2015) Dicarbonyl stress in cell and tissue dysfunction contributing to ageing and disease. *Biochemical and Biophysical Research Communications*, **458**, 221-226.
8. Thornalley, P.J., Battah, S., Ahmed, N., Karachalias, N., Agalou, S., Babaei-Jadidi, R., and Dawnay, A. (2003) Quantitative screening of advanced glycation endproducts in cellular and extracellular proteins by tandem mass spectrometry. *Biochemical Journal*, **375**, 581-592.
9. Rabbani, N., and Thornalley, P.J. (2014) Dicarbonyl proteome and genome damage in metabolic and vascular disease. *Biochemical Society Transactions*, **42**, 425-432.
10. Rabbani, N., Shaheen, F., Anwar, A., Masania, J., and Thornalley, P.J. (2014) Assay of methylglyoxal-derived protein and nucleotide AGEs. *Biochemical Society Transactions*, **42**, 511-517.
11. Rabbani, N., and Thornalley, P.J. (2012) Glycation research in amino acids: a place to call home. *Amino Acids*, **42**, 1087-1096.
12. Irshad, Z., Xue, M., Ashour, A., Larkin, J.R., Thornalley, P.J., and Rabbani, N. (2019) Activation of the unfolded protein response in high glucose treated endothelial cells is mediated by methylglyoxal. *Scientific Reports*, **9**, 7889.
13. Ashour, A., Xue, M., Al-Motawa, M., Thornalley, P.J., and Rabbani, N. (2020) Glycolytic overload-driven dysfunction of periodontal ligament fibroblasts in high glucose concentration, corrected by glyoxalase 1 inducer. *BMJ Open Diabetes Research & Care*, **8**.
14. Alhujaily, M., Abbas, H., Xue, M., de la Fuente, A., Rabbani, N., and Thornalley, P.J. (2021) Studies of Glyoxalase 1-Linked Multidrug Resistance Reveal Glycolysis-Derived Reactive Metabolite, Methylglyoxal, Is a Common Contributor in Cancer Chemotherapy Targeting the Spliceosome. *Frontiers in Oncology*, **11**.
15. Keilhauer, E.C., Geyer, P.E., and Mann, M. (2016) HCD Fragmentation of Glycated Peptides. *Journal of Proteome Research*, **15**, 2881-2890.
16. Galligan, J.J., Wepy, J.A., Streeter, M.D., Kingsley, P.J., Mitchener, M.M., Wauchope, O.R., Beavers, W.N., Rose, K.L., Wang, T., Spiegel, D.A., and Marnett, L.J. (2018) Methylglyoxal-derived posttranslational arginine modifications are abundant histone marks. *Proceedings of the National Academy of Sciences of the United States of America*, **115**, 9228-9233.
17. Donnellan, L., Young, C., Simpson, B.S., Dhillon, V.S., Costabile, M., Hoffmann, P., Fenech, M., and Deo, P. (2022) Methylglyoxal Impairs Sister Chromatid Separation in Lymphocytes. *International Journal of Molecular Sciences*, **23**.
18. Donnellan, L., Simpson, B., Dhillon, V.S., Costabile, M., Fenech, M., and Deo, P. (2021) Methylglyoxal induces chromosomal instability and mitotic dysfunction in lymphocytes. *Mutagenesis*, **36**, 339-348.
19. Wisniewski, J.R., and Gaugaz, F.Z. (2015) Fast and sensitive total protein and Peptide assays for proteomic analysis. *Analytical Chemistry*, **87**, 4110-4116.

20. Perez-Riverol, Y., Csordas, A., Bai, J., Bernal-Llinares, M., Hewapathirana, S., Kundu, D.J., Inuganti, A., Griss, J., Mayer, G., Eisenacher, M., Perez, E., Uszkoreit, J., Pfeuffer, J., Sachsenberg, T., Yilmaz, S., Tiwary, S., Cox, J., Audain, E., Walzer, M., Jarnuczak, A.F., Ternent, T., Brazma, A., and Vizcaino, J.A. (2019) The PRIDE database and related tools and resources in 2019: improving support for quantification data. *Nucleic Acids Research*, **47**, D442-D450.
21. Huang da, W., Sherman, B.T., and Lempicki, R.A. (2009) Systematic and integrative analysis of large gene lists using DAVID bioinformatics resources. *Nature Protocols*, **4**, 44-57.
22. Szklarczyk, D., Gable, A.L., Lyon, D., Junge, A., Wyder, S., Huerta-Cepas, J., Simonovic, M., Doncheva, N.T., Morris, J.H., Bork, P., Jensen, L.J., and Mering, C.V. (2019) STRING v11: protein-protein association networks with increased coverage, supporting functional discovery in genome-wide experimental datasets. *Nucleic Acids Research*, **47**, D607-D613.
23. Shannon, P., Markiel, A., Ozier, O., Baliga, N.S., Wang, J.T., Ramage, D., Amin, N., Schwikowski, B., and Ideker, T. (2003) Cytoscape: a software environment for integrated models of biomolecular interaction networks. *Genome Research*, **13**, 2498-2504.
24. Sibbersen, C., and Johannsen, M. (2020) Dicarbonyl derived post-translational modifications: chemistry bridging biology and aging-related disease. *Essays in Biochemistry*, **64**, 97-110.
25. Di Sanzo, S., Spengler, K., Leheis, A., Kirkpatrick, J.M., Randler, T.L., Baldensperger, T., Dau, T., Henning, C., Parca, L., Marx, C., Wang, Z.Q., Glomb, M.A., Ori, A., and Heller, R. (2021) Mapping protein carboxymethylation sites provides insights into their role in proteostasis and cell proliferation. *Nature Communications*, **12**, 6743.
26. Sibbersen, C., Schou Oxvig, A.M., Bisgaard Olesen, S., Nielsen, C.B., Galligan, J.J., Jorgensen, K.A., Palmfeldt, J., and Johannsen, M. (2018) Profiling of Methylglyoxal Blood Metabolism and Advanced Glycation End-Product Proteome Using a Chemical Probe. *ACS Chemical Biology*, **13**, 3294-3305.
27. Ahmed, N., Dobler, D., Dean, M., and Thornalley, P.J. (2005) Peptide mapping identifies hotspot site of modification in human serum albumin by methylglyoxal involved in ligand binding and esterase activity. *Journal of Biological Chemistry*, **280**, 5724-5732.
28. Samodova, D., Hosfield, C.M., Cramer, C.N., Giuli, M.V., Cappellini, E., Franciosa, G., Rosenblatt, M.M., Kelstrup, C.D., and Olsen, J.V. (2020) ProAlanase is an Effective Alternative to Trypsin for Proteomics Applications and Disulfide Bond Mapping. *Molecular and Cellular Proteomics*, **19**, 2139-2156.
29. Priego-Capote, F., Scherl, A., Muller, M., Waridel, P., Lisacek, F., and Sanchez, J.C. (2010) Glycation isotopic labeling with 13C-reducing sugars for quantitative analysis of glycated proteins in human plasma. *Molecular & Cellular Proteomics*, **9**, 579-592.
30. Bai, X., Wang, Z., Huang, C., Wang, Z., and Chi, L. (2012) Investigation of non-enzymatic glycosylation of human serum albumin using ion trap-time of flight mass spectrometry. *Molecules*, **17**, 8782-8794.
31. Giansanti, P., Tsiatsiani, L., Low, T.Y., and Heck, A.J. (2016) Six alternative proteases for mass spectrometry-based proteomics beyond trypsin. *Nature Protocols*, **11**, 993-1006.
32. Tittmann, K. (2014) Sweet siblings with different faces: the mechanisms of FBP and F6P aldolase, transaldolase, transketolase and phosphoketolase revisited in light of recent structural data. *Bioorganic Chemistry*, **57**, 263-280.
33. Dalby, A., Dauter, Z., and Littlechild, J.A. (1999) Crystal structure of human muscle aldolase complexed with fructose 1, 6-bisphosphate: mechanistic implications. *Protein Science*, **8**, 291-297.
34. Banerjee, S., and Chakraborti, A.S. (2013) In vitro study on structural alteration of myoglobin by methylglyoxal. *The Protein Journal*, **32**, 216-222.
35. Marino, L., Ramis, R., Casasnovas, R., Ortega-Castro, J., Vilanova, B., Frau, J., and Adrover, M. (2020) Unravelling the effect of N(epsilon)-(carboxyethyl)lysine on the conformation, dynamics and aggregation propensity of alpha-synuclein. *Chemical Science*, **11**, 3332-3344.
36. Huang, H., Tang, S., Ji, M., Tang, Z., Shimada, M., Liu, X., Qi, S., Locasale, J.W., Roeder, R.G., Zhao, Y., and Li, X. (2018) p300-Mediated Lysine 2-Hydroxyisobutyrylation Regulates Glycolysis. *Molecular Cell*, **70**, 663-678 e666.
37. Leoncini, G., Maresca, M., and Bonsignore, A. (1980) The effect of methylglyoxal on the glycolytic enzymes. *FEBS Letters*, **117**, 17-18.

38. Morgan, P.E., Dean, R.T., and Davies, M.J. (2002) Inactivation of cellular enzymes by carbonyls and protein-bound glycation/glycoxidation products. *Archives of Biochemistry and Biophysics*, **403**, 259-269.
39. Gomes, R.A., Vicente Miranda, H., Silva, M.S., Graca, G., Coelho, A.V., Ferreira, A.E., Cordeiro, C., and Freire, A.P. (2006) Yeast protein glycation in vivo by methylglyoxal. Molecular modification of glycolytic enzymes and heat shock proteins. *The FEBS Journal*, **273**, 5273-5287.
40. Leoncini, G., Maresca, M., and Buzzi, E. (1989) Inhibition of the glycolytic pathway by methylglyoxal in human platelets. *Cell Biochemistry and Function: Cellular biochemistry and its modulation by active agents or disease*, **7**, 65-70.
41. Gaffney, D.O., Jennings, E.Q., Anderson, C.C., Marentette, J.O., Shi, T., Schou Oxvig, A.M., Streeter, M.D., Johannsen, M., Spiegel, D.A., Chapman, E., Roede, J.R., and Galligan, J.J. (2020) Non-enzymatic Lysine Lactoylation of Glycolytic Enzymes. *Cell Chemical Biology*, **27**, 206-213 e206.
42. Zheng, X., Peng, Q., Wang, L., Zhang, X., Huang, L., Wang, J., and Qin, Z. (2020) Serine/arginine-rich splicing factors: the bridge linking alternative splicing and cancer. *International Journal of Biological Sciences*, **16**, 2442-2453.
43. Xiao, R., Sun, Y., Ding, J.H., Lin, S., Rose, D.W., Rosenfeld, M.G., Fu, X.D., and Li, X. (2007) Splicing regulator SC35 is essential for genomic stability and cell proliferation during mammalian organogenesis. *Molecular and Cellular Biology*, **27**, 5393-5402.
44. Yoshida, K., Sanada, M., Shiraishi, Y., Nowak, D., Nagata, Y., Yamamoto, R., Sato, Y., Sato-Otsubo, A., Kon, A., Nagasaki, M., Chalkidis, G., Suzuki, Y., Shiosaka, M., Kawahata, R., Yamaguchi, T., Otsu, M., Obara, N., Sakata-Yanagimoto, M., Ishiyama, K., Mori, H., Nolte, F., Hofmann, W.K., Miyawaki, S., Sugano, S., Haferlach, C., Koeffler, H.P., Shih, L.Y., Haferlach, T., Chiba, S., Nakauchi, H., Miyano, S., and Ogawa, S. (2011) Frequent pathway mutations of splicing machinery in myelodysplasia. *Nature*, **478**, 64-69.

6 Chapter 6. Conclusion and future directions

The research presented in this thesis aimed to investigate the following questions regarding the genotoxic potential of MGO.

1. Does MGO induce DNA damage as measured by the CBMNcyt assay?
2. Is MGO induced DNA damage a result of protein or DNA modification?
3. Does folic acid deficiency increase susceptibility to MGO induced DNA damage?
4. What are the underlying mechanisms for MGO induced DNA damage in lymphocytes?

This final chapter collates the findings of the preceding chapters and discusses their relevance to the field of glycation research and utility for promoting further investigation of MGO genotoxicity.

6.1 MGO induced DNA damage

MGO was first reported to have genotoxic properties more than three decades ago, in which supraphysiological concentrations (> 1 mM) of MGO were shown to induce the formation of chromosomal aberrations, sister chromatid exchanges and MNi (1). Since then, only a limited number of studies have further investigated the genotoxic activity of MGO (1-3). Majority of studies investigating the genotoxicity of MGO have assumed any genotoxic activity has stemmed from the formation of DNA double stranded breaks caused by its ability to modify deoxyguanosine residues forming a variety of MGO-DNA adducts (3). However, in several of these studies, the methods used to measure DNA damage included those which selectively assessed DNA double strand break events, as opposed to other mechanisms such as whole chromosome loss. Therefore, we utilized the gold standard assay for assessing DNA damage, the CBMNcyt assay, which is a comprehensive assay that measures DNA damage originating from various mechanisms such as DNA double-stranded breaks, telomeric end-fusion, chromosome amplification, chromosome loss and non-disjunction events (4). Similar to previous studies, we found that MGO was genotoxic and increased the frequency of DNA damage markers, in particular MNi (5). However, in contrast to several previous studies, we observed that DNA damage was more closely associated with the formation of protein glycation, rather than DNA glycation

(5,6). Furthermore, we showed that over a 48- hour period, the formation of MNi was correlated with the formation of the MGO lysine adduct, CEL (6). The lack of association between DNA glycation and DNA damage in our study led us to investigate whether MNi formed contained whole chromosomes, indicative of whole chromosome loss events, or chromatid fragments caused by DNA double stranded break events. Interestingly, we found that in the presence of MGO approximately 88% of the MNi contained whole chromosomes (5). Therefore, although a small number of MNi may have contained chromatid fragments, majority were the result of whole chromosome loss events which is a novel mechanism whereby MGO appears to induce genomic instability. As a by-product of glucose metabolism, MGO has been shown to be elevated in individuals with T2D by ~2-10 times (7,8). Notably, individuals with T2D have also been shown to contain higher levels of DNA damage, as measured by the lymphocyte or buccal CBMNcyt assay (9-12). Furthermore, two recent meta-analyses showed the meta-mean ratio for micronucleus frequency in lymphocytes in individuals with diabetes mellitus is 1.99 ($P < 0.01$; T2D) and 1.74 ($P < 0.001$; T2D and T1D) when compared with control groups (13,14). Therefore, the increased concentration of MGO in these individuals may contribute to their elevated frequency of DNA damage markers. Further studies could investigate the association between MGO concentrations and frequency of DNA damage markers in individuals with T2D. Identifying MGO as a potential contributor to micronuclei formation in individuals with T2D may allow for the development of targeted therapies to reduce occurrence of DNA damage.

6.2 Folic acid deficiency increases susceptibility to MGO induced DNA damage

It is well known phenomena that deficiency in numerous micronutrients can lead to genomic instability (15). A recent study showed that only folic acid deficient cells were sensitive to glucose-induced DNA damage (16). Furthermore, long term use of metformin, a common treatment for individuals with T2D has been associated with lower levels of B-vitamins, including folate (B9) suggesting these individuals may be more prone to B-vitamin deficiencies (17). Therefore, having shown MGO can induce DNA damage in aim 1, we investigated whether deficiency in folic acid would increase susceptibility to MGO

and/ or glucose (the metabolic precursor to MGO) induced DNA damage. Indeed, we found increased susceptibility to DNA damage induced by both metabolites under folic acid deficient conditions (18). An interesting observation from this study was that deficiency in folic acid, regardless of glucose concentration increased several dicarbonyl stress biomarkers such as media concentration of MGO and MG-H1 and cellular MGO (18). These results suggest folic acid may have a direct or indirect role in regulating concentration of MGO. Future studies should aim to unravel this result using metabolic tracing studies and untargeted metabolomics to help identify the origin of MGO under folic acid deficient conditions. This is important because if folic acid does play a role in regulating the concentration of MGO, those deficient in folic acid may be susceptible to elevated concentrations of MGO, regardless of blood glucose levels. Nevertheless, the results from this aim suggest individuals with T2D and those with elevated levels of MGO need to be controlled to limit DNA damage. Future studies may also benefit from investigating the association between plasma MGO and folic acid on DNA damage in individuals with T2D.

6.3 MGO impairs sister chromatid separation

In our first aim, we found that MGO-induced MNi were mostly the result of whole chromosome loss events, and that this increase in DNA damage was more closely associated with protein glycation, rather than DNA glycation (5). Indeed, by measuring the frequency of protein glycation and MNi over time we found a correlation between the specific MGO adduct, CEL and MNi ($r = 0.693$; $p = 0.038$) (6). To investigate underlying mechanisms, we used untargeted proteomics to identify both up- and down-regulated proteins following MGO exposure, and those containing either CEL, MG-H1 or CEA modifications. Interestingly, we found both increased abundance and modification of numerous proteins involved in separation of sister chromatid. Furthermore, using cytogenetic analysis, we found that treatment with MGO caused phenotypic changes previously shown to be associated with impaired sister chromatid separation. Most notably, we found that the Separase inhibitor, Securin had a 1.61-fold increase in protein abundance following treatment with MGO. Moreover, half of the proteins as part of the cohesin complex were shown to contain MGO modifications. From this study, we identified several mechanisms whereby MGO may prevent sister chromatid separation, resulting in the DNA damage

biomarkers observed in our previous studies. However, it is important to note that other mitotic proteins, including those involved in centrosome duplication were also shown to be modified and therefore may also contribute to the observed DNA damage.

Under normal conditions, the Spindle Assembly Checkpoint (SAC) is a major cell-cycle checkpoint which regulates the segregation of chromosomes during mitosis (19). The SAC monitors kinetochore-microtubule attachments, tension between kinetochores and sister chromatid and chromosome bi-orientation, and as long as improperly oriented chromosomes are identified, mitosis is halted (19). However, it has been shown that under folic acid conditions the SAC becomes impaired and premature mitotic exits is observed, despite improperly oriented chromosomes (20). Therefore, under conditions of both folic acid deficiency and elevated MGO, increased DNA damage may be a result of impaired SAC, allowing cells with improperly oriented chromosomes to prematurely exit mitosis, causing chromosome missegregation events.

6.4 Future Directions

Studies from this thesis have generated results, leading to the development of new hypotheses that should greatly assist the design of future experimental work by researchers in the field.

- Is the concentration of MGO in T2D associated with the frequency of DNA damage?
- How does folic acid deficiency increase the concentration of MGO?
- Does modification of cohesin complex proteins impair separase dependent or independent cleavage?
- How does MGO increase protein abundance of the separase inhibitor, Securin?

6.5 Conclusion

In conclusion, we show that MGO increases the frequency of various DNA damage biomarkers associated with impaired sister chromatid separation. Furthermore, we show that DNA damage induced by MGO is elevated under folic acid deficient conditions. We also showed in aim 4 that MGO modifications may not be random and target specific residues. Therefore, future studies investigating

the role of MGO on DNA damage should include proteomic studies to identify those sites. These results may help unravel underlying mechanisms associated with DNA damage observed in T2D. Moreover, many of the observed DNA damage events are similar to those associated with tumorigenesis and suggest MGO may also contribute to this process.

References

1. Migliore, L., Barale, R., Bosco, E., Giorgelli, F., Minunni, M., Scarpato, R., and Loprieno, N. (1990) Genotoxicity of methylglyoxal: cytogenetic damage in human lymphocytes in vitro and in intesting cells of mice. *Carcinogenesis*, **11**, 1503-1507.
2. Bronzetti, G., Corsi, C., Chiaro, D.D., Boccardo, P., Vellosi, R., Rossi, F., Paolini, M., and Forti, G.C. (1987) Methylglyoxal: genotoxicity studies and its effect in vivo on the hepatic microsomal mono-oxygenase system of the mouse. *Mutagenesis*, **2**, 275-277.
3. Thornalley, P.J., Waris, S., Fleming, T., Santarius, T., Larkin, S.J., Winklhofer-Roob, B.M., Stratton, M.R., and Rabbani, N. (2010) Imidazopurinones are markers of physiological genomic damage linked to DNA instability and glyoxalase 1-associated tumour multidrug resistance. *Nucleic Acids Research*, **38**, 5432-5442.
4. Fenech, M. (2007) Cytokinesis-block micronucleus cytome assay. *Nature Protocols*, **2**, 1084-1104.
5. Donnellan, L., Simpson, B., Dhillon, V.S., Costabile, M., Fenech, M., and Deo, P. (2021) Methylglyoxal induces chromosomal instability and mitotic dysfunction in lymphocytes. *Mutagenesis*, **36**, 339-348.
6. Donnellan, L., Young, C., Simpson, B.S., Dhillon, V.S., Costabile, M., Hoffmann, P., Fenech, M., and Deo, P. (2022) Methylglyoxal Impairs Sister Chromatid Separation in Lymphocytes. *International Journal of Molecular Sciences*, **23**.
7. McLellan, A.C., Thornalley, P.J., Benn, J., and Sonksen, P.H. (1994) Glyoxalase system in clinical diabetes mellitus and correlation with diabetic complications. *Journal of Clinical Science*, **87**, 21-29.
8. Scheijen, J.L., and Schalkwijk, C.G. (2014) Quantification of glyoxal, methylglyoxal and 3-deoxyglucosone in blood and plasma by ultra performance liquid chromatography tandem mass spectrometry: evaluation of blood specimen. *Clinical Chemistry and Laboratory Medicine*, **52**, 85-91.
9. Shaik, N.A., Shaik, J.P., Ali, S., Imran, A., and Rao, D.K. (2010) Increased frequency of micronuclei in diabetes mellitus patients using pioglitazone and glimepiride in combination. *Food and Chemical Toxicology*, **48**, 3432-3435.
10. Shettigar, S.K., Shailaja, C., and Kulkarni, R.K. (2012) Elevated micronuclei frequency in type 2 diabetes with high glycosylated hemoglobin. *Diabetes Research and Clinical Practice*, **95**, 246-250.
11. Lazalde-Ramos, B.P., Zamora-Perez, A.L., Sosa-Macias, M., Guerrero-Velazquez, C., and Zuniga-Gonzalez, G.M. (2012) DNA and oxidative damages decrease after ingestion of folic acid in patients with type 2 diabetes. *Archives of Medical Research*, **43**, 476-481.
12. Corbi, S.C., Bastos, A.S., Orrico, S.R., Secolin, R., Dos Santos, R.A., Takahashi, C.S., and Scarel-Caminaga, R.M. (2014) Elevated micronucleus frequency in patients with type 2 diabetes, dyslipidemia and periodontitis. *Mutagenesis*, **29**, 433-439.
13. Kirsch-Volders, M., Bolognesi, C., Ceppi, M., Bruzzone, M., and Fenech, M. (2020) Micronuclei, inflammation and auto-immune disease. *Mutation Research*, **786**, 108335.
14. Deo, P., Fenech, M., and Dhillon, V.S. (2021) Association between glycation biomarkers, hyperglycemia, and micronucleus frequency: A meta -analysis. *Mutation Research/Reviews in Mutation Research*, **787**.
15. Bull, C., and Fenech, M. (2008) Genome-health nutrigenomics and nutrigenetics: nutritional requirements or 'nutriomes' for chromosomal stability and telomere maintenance at the individual level. *Proceedings of the Nutrition Society*, **67**, 146-156.
16. Guo, X., Dai, X., Ni, J., Cao, N., Yang, G., Xue, J., and Wang, X. (2019) High concentration of sugars is genotoxic to folate-deficient cells. *Mutation Research*, **814**, 15-22.
17. Wale Tesega, W., Genet, S., Natesan, G., Tarekegn, G., Girma, F., Chalchisa, D., Belay, Y., Geto, Z., and Asmamaw Dejenie, T. (2021) Assessment of Serum Vitamin B12 and Folate Levels and Macrocytosis in Patients with Type 2 Diabetes Mellitus on Metformin Attending Tikur Anbessa Specialized Hospital, Addis Ababa, Ethiopia: A Cross-Sectional Study. *Diabetes, Metabolic Syndrome and Obesity*, **14**, 2011-2018.
18. Donnellan, L., Simpson, B.S., Dhillon, V.S., Costabile, M., Fenech, M., and Deo, P. (2022) Folic acid deficiency increases sensitivity to DNA damage by glucose and methylglyoxal. *Mutagenesis*, **37**, 24-33.

19. Musacchio, A. (2015) The Molecular Biology of Spindle Assembly Checkpoint Signaling Dynamics. *Current Biology*, **25**, R1002-1018.
20. Guo, X., Ni, J., Zhu, Y., Zhou, T., Ma, X., Xue, J., and Wang, X. (2017) Folate deficiency induces mitotic aberrations and chromosomal instability by compromising the spindle assembly checkpoint in cultured human colon cells. *Mutagenesis*, **32**, 547-560.

7 Appendix

7.1 Appendix A. Statement of Authorship Aim 1

University of South Australia

Statement of Authorship

Title of Paper	Methylglyoxal induces chromosomal instability and mitotic dysfunction in lymphocytes
Publication Status	☑ Published ☐ Accepted for Publication ☐ Submitted for Publication ☐ Unpublished and Unsubmitted work written in manuscript style
Publication Details Relevant reference details	Donnellan, L., Simpson, B., Dhillon, V.S., Costabile, M., Fenech, M., and Deo, P. (2021) Methylglyoxal induces chromosomal instability and mitotic dysfunction in lymphocytes. Mutagenesis, 36, 339-348.
PRINCIPAL AUTHOR	
Name of Principal Author (Candidate)	Leigh Donnellan
Contribution to the Paper Brief description of your work in this publication	Experimental work, data analysis, initial manuscript writing and corrections
Overall Percentage (%)	75
Certification	
Signature *Signatures will be redacted by the Library at the time of publication*	[redacted] Date 25/08/2022
CO-AUTHOR CONTRIBUTIONS	
By signing the Statement of Authorship, each author certifies that: I. the candidate's stated contribution to the publication is accurate (as detailed above); II. permission is granted for the candidate in include the publication in the thesis; and III. the sum of all co-author contribution is equal to 100% less the candidate's stated contribution.	
Name of Co-Author 1	Bradley S. Simpson
% Contribution to the Paper	5
Signature *Signatures will be redacted by the Library at the time of publication*	[redacted] 25/5/2022 Date
Name of Co-Author 2	Varinderpal S. Dhillon

The University of South Australia
www.unisa.edu.au
CRICOS Provider No. 00121B

Last updated: 31 March 2022

University of South Australia

% Contribution to the Paper	5	
Signature *Signatures will be redacted by the Library at the time of publication*	[redacted]	Date 25/05/2022
Name of Co-Author 3	Maurizio Costabile	
% Contribution to the Paper	5	
Signature *Signatures will be redacted by the Library at the time of publication*	[redacted]	Date 25/05/2022
Name of Co-Author 4	Michael Fenech	
% Contribution to the Paper	5	
Signature *Signatures will be redacted by the Library at the time of publication*	[redacted]	Date 25/05/2022
Name of Co-Author 5	Permal Deo	
% Contribution to the Paper	5	
Signature *Signatures will be redacted by the Library at the time of publication*	[redacted]	Date 25/05/2022
Name of Co-Author 6		
% Contribution to the Paper		
Signature *Signatures will be redacted by the Library at the time of publication*		Date
Name of Co-Author 7		
% Contribution to the Paper		
Signature *Signatures will be redacted by the Library at the time of publication*		Date
Name of Co-Author 8		
% Contribution to the Paper		

7.2 Appendix B. Statement of Authorship Aim 2

University of South Australia

Statement of Authorship

Title of Paper	Folic acid deficiency increases sensitivity to DNA damage by glucose and methylglyoxal
Publication Status	☑ Published ☐ Accepted for Publication ☐ Submitted for Publication ☐ Unpublished and Unsubmitted work written in manuscript style
Publication Details Relevant reference details	Donnellan, L., Simpson, B.S., Dhillon, V.S., Costabile, M., Fenech, M., and Deo, P. (2022) Folic acid deficiency increases sensitivity to DNA damage by glucose and methylglyoxal. Mutagenesis, 37, 24-33.

PRINCIPAL AUTHOR

Name of Principal Author (Candidate)	Leigh Donnellan	
Contribution to the Paper Brief description of your work in this publication	Experimental work, data analysis, initial manuscript writing and corrections	
Overall Percentage (%)	75	
Certification		
Signature *Signatures will be redacted by the Library at the time of publication*	[redacted]	Date 25/05/2022

CO-AUTHOR CONTRIBUTIONS

By signing the Statement of Authorship, each author certifies that:

I. the candidate's stated contribution to the publication is accurate (as detailed above);

II. permission is granted for the candidate in include the publication in the thesis; and

III. the sum of all co-author contribution is equal to 100% less the candidate's stated contribution.

Name of Co-Author 1	Bradley S. Simpson	
% Contribution to the Paper	5	
Signature *Signatures will be redacted by the Library at the time of publication*	[redacted]	25/5/2022 Date
Name of Co-Author 2	Varinderpal S. Dhillon	

The University of South Australia
www.unisa.edu.au
CRICOS Provider No. 00121B

Last updated: 31 March 2022

University of South Australia

% Contribution to the Paper	5	
Signature *Signatures will be redacted by the Library at the time of publication*	[redacted]	Date 25/05/2022
Name of Co-Author 3	Maurizio Costabile	
% Contribution to the Paper	5	
Signature *Signatures will be redacted by the Library at the time of publication*	[redacted]	Date 25/05/2022
Name of Co-Author 4	Michael Fenech	
% Contribution to the Paper	5	
Signature *Signatures will be redacted by the Library at the time of publication*	[redacted]	Date 25/05/2022
Name of Co-Author 5	Permal Deo	
% Contribution to the Paper	5	
Signature *Signatures will be redacted by the Library at the time of publication*	[redacted]	Date 25/05/2022
Name of Co-Author 6		
% Contribution to the Paper		
Signature *Signatures will be redacted by the Library at the time of publication*		Date
Name of Co-Author 7		
% Contribution to the Paper		
Signature *Signatures will be redacted by the Library at the time of publication*		Date
Name of Co-Author 8		
% Contribution to the Paper		

7.3 Appendix C. Statement of Authorship Aim 3

University of South Australia

Statement of Authorship

Title of Paper	Methylglyoxal Impairs Sister Chromatid Separation in Lymphocytes
Publication Status	☑ Published ☐ Accepted for Publication ☐ Submitted for Publication ☐ Unpublished and Unsubmitted work written in manuscript style
Publication Details Relevant reference details	Donnellan, L., Young, C., Simpson, B.S., Dhillon, V.S., Costabile, M., Hoffmann, P., Fenech, M., and Deo, P. (2022) Methylglyoxal Impairs Sister Chromatid Separation in Lymphocytes. International Journal of Molecular Sciences, 23.
PRINCIPAL AUTHOR	
Name of Principal Author (Candidate)	Leigh Donnellan
Contribution to the Paper Brief description of your work in this publication	Experimental work, data analysis, initial manuscript writing and corrections
Overall Percentage (%)	71
Certification	
Signature *Signatures will be redacted by the Library at the time of publication*	[redacted] Date 25/05/2022
CO-AUTHOR CONTRIBUTIONS	
By signing the Statement of Authorship, each author certifies that: I. the candidate's stated contribution to the publication is accurate (as detailed above); II. permission is granted for the candidate in include the publication in the thesis; and III. the sum of all co-author contribution is equal to 100% less the candidate's stated contribution.	
Name of Co-Author 1	Clifford Young
% Contribution to the Paper	5
Signature *Signatures will be redacted by the Library at the time of publication*	[redacted] Date 01/06/2022
Name of Co-Author 2	Bradley S. Simpson

The University of South Australia
www.unisa.edu.au
CRICOS Provider No. 00121B

Last updated: 31 March 2022

University of South Australia

% Contribution to the Paper	4
Signature *Signatures will be redacted by the Library at the time of publication*	[redacted] Date 25/5/2022
Name of Co-Author 3	Varinderpal S. Dhillon
% Contribution to the Paper	4
Signature *Signatures will be redacted by the Library at the time of publication*	[redacted] Date 25/05/2022
Name of Co-Author 4	Maurizio Costabile
% Contribution to the Paper	4
Signature *Signatures will be redacted by the Library at the time of publication*	[redacted] Date 25/05/2022
Name of Co-Author 5	Peter Hoffmann
% Contribution to the Paper	4
Signature *Signatures will be redacted by the Library at the time of publication*	[redacted] Date 01/06/2022
Name of Co-Author 6	Michael Fenech
% Contribution to the Paper	4
Signature *Signatures will be redacted by the Library at the time of publication*	[redacted] Date 25/05/2022
Name of Co-Author 7	Permal Deo
% Contribution to the Paper	4
Signature *Signatures will be redacted by the Library at the time of publication*	[redacted] Date 25/05/2022
Name of Co-Author 8	
% Contribution to the Paper	

7.4 Appendix D. Statement of Authorship Aim 4

University of South Australia

Statement of Authorship

Title of Paper	Proteomic Analysis of Methylglyoxal Modifications Reveals Susceptibility of Glycolytic Enzymes to Dicarbonyl Stress
Publication Status	☑ Published ☐ Accepted for Publication ☐ Submitted for Publication ☐ Unpublished and Unsubmitted work written in manuscript style
Publication Details Relevant reference details	Donnellan, L., Young, C., Simpson, B.S., Acland, M., Dhillon, V.S., Costabile, M., Fenech, M., Hoffmann, P., and Deo, P. (2022) Proteomic Analysis of Methylglyoxal Modifications Reveals Susceptibility of Glycolytic Enzymes to Dicarbonyl Stress. International Journal of Molecular Sciences, 23, 368

PRINCIPAL AUTHOR

Name of Principal Author (Candidate)	Leigh Donnellan	
Contribution to the Paper Brief description of your work in this publication	Experimental work, data analysis, initial manuscript writing and corrections	
Overall Percentage (%)	67	
Certification		
Signature *Signatures will be redacted by the Library at the time of publication*	[redacted]	Date 25/05/2022

CO-AUTHOR CONTRIBUTIONS

By signing the Statement of Authorship, each author certifies that:

I. the candidate's stated contribution to the publication is accurate (as detailed above);

II. permission is granted for the candidate in include the publication in the thesis; and

III. the sum of all co-author contribution is equal to 100% less the candidate's stated contribution.

Name of Co-Author 1	Clifford Young	
% Contribution to the Paper	5	
Signature *Signatures will be redacted by the Library at the time of publication*	[redacted]	Date 01/06/2022
Name of Co-Author 2	Bradley S. Simpson	

The University of South Australia
www.unisa.edu.au
CRICOS Provider No. 00121B

Last updated: 31 March 2022

University of South Australia

% Contribution to the Paper	4	
Signature *Signatures will be redacted by the Library at the time of publication*	[redacted]	Date 25/5/2022
Name of Co-Author 3	Mitchell Acland	
% Contribution to the Paper	4	
Signature *Signatures will be redacted by the Library at the time of publication*	[redacted]	Date 1/6/2022
Name of Co-Author 4	Varinderpal S. Dhillon	
% Contribution to the Paper	4	
Signature *Signatures will be redacted by the Library at the time of publication*	[redacted]	Date 25/05/22
Name of Co-Author 5	Maurizio Costabile	
% Contribution to the Paper	4	
Signature *Signatures will be redacted by the Library at the time of publication*	[redacted]	Date 25/05/2022
Name of Co-Author 6	Michael Fenech	
% Contribution to the Paper	4	
Signature *Signatures will be redacted by the Library at the time of publication*	[redacted]	Date 25/05/2022
Name of Co-Author 7	Peter Hoffmann	
% Contribution to the Paper	4	
Signature *Signatures will be redacted by the Library at the time of publication*	[redacted]	Date 01/06/2022
Name of Co-Author 8	Permal Deo	
% Contribution to the Paper	4	

University of South Australia

Signature *Signatures will be redacted by the Library at the time of publication*	[redacted]	Date 25/05/2022

7.5 Appendix E. Copyright License for Chapter 2

OXFORD UNIVERSITY PRESS LICENSE
TERMS AND CONDITIONS
Aug 17, 2022

This Agreement between University of South Australia -- Leigh Donnellan ("You") and Oxford University Press ("Oxford University Press") consists of your license details and the terms and conditions provided by Oxford University Press and Copyright Clearance Center.

License Number	5314530064594
License date	May 22, 2022
Licensed content publisher	Oxford University Press
Licensed content publication	Mutagenesis
Licensed content title	Methylglyoxal induces chromosomal instability and mitotic dysfunction in lymphocytes
Licensed content author	Donnellan, Leigh; Simpson, Bradley
Licensed content date	Jul 23, 2021
Type of Use	Thesis/Dissertation
Institution name	
Title of your work	Methylglyoxal induces DNA damage
Publisher of your work	University of SOuth Australia
Expected publication date	Sep 2022
Permissions cost	0.00 USD
Value added tax	0.00 USD
Total	0.00 USD
Title	Methylglyoxal induces DNA damage
Institution name	University of SOuth Australia
Expected presentation date	Sep 2022

Order reference number	1112
	University of South Australia 9 Buttercup Grove Morphett Vale
Requestor Location	
	Adelaide, 5162 Australia Attn: University of South Australia
Publisher Tax ID	GB125506730
Total	0.00 USD

Terms and Conditions

STANDARD TERMS AND CONDITIONS FOR REPRODUCTION OF MATERIAL FROM AN OXFORD UNIVERSITY PRESS JOURNAL

1. Use of the material is restricted to the type of use specified in your order details.

2. This permission covers the use of the material in the English language in the following territory: world. If you have requested additional permission to translate this material, the terms and conditions of this reuse will be set out in clause 12.

3. This permission is limited to the particular use authorized in (1) above and does not allow you to sanction its use elsewhere in any other format other than specified above, nor does it apply to quotations, images, artistic works etc that have been reproduced from other sources which may be part of the material to be used.

4. No alteration, omission or addition is made to the material without our written consent. Permission must be re-cleared with Oxford University Press if/when you decide to reprint.

5. The following credit line appears wherever the material is used: author, title, journal, year, volume, issue number, pagination, by permission of Oxford University Press or the sponsoring society if the journal is a society journal. Where a journal is being published on behalf of a learned society, the details of that society must be included in the credit line.

6. For the reproduction of a full article from an Oxford University Press journal for whatever purpose, the corresponding author of the material concerned should be informed of the proposed use. Contact details for the corresponding authors of all Oxford University Press journal contact can be found alongside either the abstract or full text of the article concerned, accessible from www.oxfordjournals.org Should there be a problem clearing these rights, please contact journals.permissions@oup.com

7. If the credit line or acknowledgement in our publication indicates that any of the figures, images or photos was reproduced, drawn or modified from an earlier

source it will be necessary for you to clear this permission with the original publisher as well. If this permission has not been obtained, please note that this material cannot be included in your publication/photocopies.

8. While you may exercise the rights licensed immediately upon issuance of the license at the end of the licensing process for the transaction, provided that you have disclosed complete and accurate details of your proposed use, no license is finally effective unless and until full payment is received from you (either by Oxford University Press or by Copyright Clearance Center (CCC)) as provided in CCC's Billing and Payment terms and conditions. If full payment is not received on a timely basis, then any license preliminarily granted shall be deemed automatically revoked and shall be void as if never granted. Further, in the event that you breach any of these terms and conditions or any of CCC's Billing and Payment terms and conditions, the license is automatically revoked and shall be void as if never granted. Use of materials as described in a revoked license, as well as any use of the materials beyond the scope of an unrevoked license, may constitute copyright infringement and Oxford University Press reserves the right to take any and all action to protect its copyright in the materials.

9. This license is personal to you and may not be sublicensed, assigned or transferred by you to any other person without Oxford University Press's written permission.

10. Oxford University Press reserves all rights not specifically granted in the combination of (i) the license details provided by you and accepted in the course of this licensing transaction, (ii) these terms and conditions and (iii) CCC's Billing and Payment terms and conditions.

11. You hereby indemnify and agree to hold harmless Oxford University Press and CCC, and their respective officers, directors, employs and agents, from and against any and all claims arising out of your use of the licensed material other than as specifically authorized pursuant to this license.

12. Other Terms and Conditions:

v1.4

Questions? customercare@copyright.com or +1-855-239-3415 (toll free in the US) or +1-978-646-2777.

7.6 Appendix F. Copyright License for Chapter 3

OXFORD UNIVERSITY PRESS LICENSE
TERMS AND CONDITIONS
Aug 17, 2022

This Agreement between University of South Australia -- Leigh Donnellan ("You") and Oxford University Press ("Oxford University Press") consists of your license details and the terms and conditions provided by Oxford University Press and Copyright Clearance Center.

License Number	5314521508609
License date	May 22, 2022
Licensed content publisher	Oxford University Press
Licensed content publication	Mutagenesis
Licensed content title	Folic acid deficiency increases sensitivity to DNA damage by glucose and methylglyoxal
Licensed content author	Donnellan, Leigh; Simpson, Bradley S
Licensed content date	Jan 25, 2022
Type of Use	Thesis/Dissertation
Institution name	
Title of your work	Methylglyoxal induces DNA damage
Publisher of your work	University of SOuth Australia
Expected publication date	Sep 2022
Permissions cost	0.00 AUD
Value added tax	0.00 AUD
Total	0.00 AUD
Title	Methylglyoxal induces DNA damage
Institution name	University of SOuth Australia
Expected presentation date	Sep 2022

Order reference number	1111
	University of South Australia 9 Buttercup Grove Morphett Vale
Requestor Location	
	Adelaide, 5162 Australia Attn: University of South Australia
Publisher Tax ID	GB125506730
Total	0.00 AUD

Terms and Conditions

STANDARD TERMS AND CONDITIONS FOR REPRODUCTION OF MATERIAL FROM AN OXFORD UNIVERSITY PRESS JOURNAL

1. Use of the material is restricted to the type of use specified in your order details.

2. This permission covers the use of the material in the English language in the following territory: world. If you have requested additional permission to translate this material, the terms and conditions of this reuse will be set out in clause 12.

3. This permission is limited to the particular use authorized in (1) above and does not allow you to sanction its use elsewhere in any other format other than specified above, nor does it apply to quotations, images, artistic works etc that have been reproduced from other sources which may be part of the material to be used.

4. No alteration, omission or addition is made to the material without our written consent. Permission must be re-cleared with Oxford University Press if/when you decide to reprint.

5. The following credit line appears wherever the material is used: author, title, journal, year, volume, issue number, pagination, by permission of Oxford University Press or the sponsoring society if the journal is a society journal. Where a journal is being published on behalf of a learned society, the details of that society must be included in the credit line.

6. For the reproduction of a full article from an Oxford University Press journal for whatever purpose, the corresponding author of the material concerned should be informed of the proposed use. Contact details for the corresponding authors of all Oxford University Press journal contact can be found alongside either the abstract or full text of the article concerned, accessible from www.oxfordjournals.org Should there be a problem clearing these rights, please contact journals.permissions@oup.com

7. If the credit line or acknowledgement in our publication indicates that any of the figures, images or photos was reproduced, drawn or modified from an earlier

source it will be necessary for you to clear this permission with the original publisher as well. If this permission has not been obtained, please note that this material cannot be included in your publication/photocopies.

8. While you may exercise the rights licensed immediately upon issuance of the license at the end of the licensing process for the transaction, provided that you have disclosed complete and accurate details of your proposed use, no license is finally effective unless and until full payment is received from you (either by Oxford University Press or by Copyright Clearance Center (CCC)) as provided in CCC's Billing and Payment terms and conditions. If full payment is not received on a timely basis, then any license preliminarily granted shall be deemed automatically revoked and shall be void as if never granted. Further, in the event that you breach any of these terms and conditions or any of CCC's Billing and Payment terms and conditions, the license is automatically revoked and shall be void as if never granted. Use of materials as described in a revoked license, as well as any use of the materials beyond the scope of an unrevoked license, may constitute copyright infringement and Oxford University Press reserves the right to take any and all action to protect its copyright in the materials.

9. This license is personal to you and may not be sublicensed, assigned or transferred by you to any other person without Oxford University Press's written permission.

10. Oxford University Press reserves all rights not specifically granted in the combination of (i) the license details provided by you and accepted in the course of this licensing transaction, (ii) these terms and conditions and (iii) CCC's Billing and Payment terms and conditions.

11. You hereby indemnify and agree to hold harmless Oxford University Press and CCC, and their respective officers, directors, employs and agents, from and against any and all claims arising out of your use of the licensed material other than as specifically authorized pursuant to this license.

12. Other Terms and Conditions:

v1.4

Questions? customercare@copyright.com or +1-855-239-3415 (toll free in the US) or +1-978-646-2777.